



universität
wien

MASTERARBEIT

Titel der Masterarbeit

**„Change of woody vegetation and land cover using
high resolution images on the Dogon Plateau and
Seno Plains (Mali)“**

Verfasser

Raphael Spiekermann BSc

angestrebter akademischer Grad

Master of Science (MSc)

Wien, 2013

Studienkennzahl lt. Studienblatt:

A 066 855

Studienrichtung lt. Studienblatt:

Geographie

Betreuerin / Betreuer:

Univ.-Prof. Mag. Dr. Cyrus Samimi

Acknowledgements

It is with immense gratitude that I would like to thank my Professor Dr. Cyrus Samimi for his support and guidance throughout the Master degree, but in particular during this time of intense research dedicated towards my thesis. Thank you for always being available to assist with technical and theoretical problems and for offering your profound knowledge of remote sensing and environmental science whenever necessary.

I am equally indebted to my colleague Martin Brandt, who continuously shared his technical know-how and enthusiasm for the research topic, and without whom I never would have travelled to Mali to study the processes responsible for environmental change in the Sahel. Thank you for your openness and flexibility, which enabled me to conduct my research in a very explorative and free manner. I would also like to acknowledge Clemens Romankiewicz, who travelled with us to Mali and, despite being a human geographer, never failed to offer insights into local phenomena and processes, gained by years spent living and working in Sevaré and his constant lateral thinking.

Acknowledgements are also due to the *Deutsches Zentrum für Luft- und Raumfahrt (DLR)* for providing the RapidEye images for the purpose of this study from the *RapidEye Science Archive (RESA)* at no cost. My special thanks also goes out to *GRID-IT* for providing ERDAS IMAGINE Objective, the software used to extract woody vegetation from the images.

I owe my deepest gratitude to my family and friends, especially my wife Elizabeth Spiekermann, who accompanied me during this extensive time with keen interest and understanding as well as moral support. Finally, I would like to thank my parents for their encouragement and unfaltering support throughout my study.

Abstract

The Sahel region has been acclaimed as one of the “hot spots” of global environmental change in the last decades. The degradation of the environmental conditions was accelerated by prolonged droughts in the region during the 1970s and 1980s and an overall decrease in annual precipitation. The resulting loss of woody vegetation cover was often considered as irreversible desertification. Recent findings, based on small-scaled analyses of satellite images, show an increase of vegetation greenness over most parts of the Sahel since the mid-1980s. However, due to a lack of detailed regional studies, it remains largely unclear if this is a return to pre-drought conditions or a transformation of land cover to a new equilibrium state.

This study uses remote sensing techniques, supplemented by ground truth data to compare the pre-drought woody vegetation and land cover with the current situation for a study area approximately 3600 km² large.

High resolution panchromatic Corona imagery of 1967 and multispectral RapidEye imagery of 2011 form the basis of this regional scaled study, which includes parts of the Dogon Plateau and the Seno Plains in the Sahel of Mali. The feature extraction and classification operations included in ERDAS IMAGINE Objective are used in an object-oriented approach in combination with spectral properties to analyse the datasets and map woody vegetation. Almost six million polygons representing single, as well as groups of trees and shrubs are extracted for the years 1967 and 2011. Results indicate number of trees per hectare as well as woody vegetation coverage in percent for both 1967 and 2011. Additionally, the land cover change during the past half century is assessed at a resolution of 20 m, followed by an analysis of current and past woody vegetation densities in relation to land cover classes.

Results show a significant increase of sparsely vegetated land, in particular in the Seno Plains, a reduction of dense bush fallow as well as an increase of trees on farmer's primary fields. Furthermore, degraded land makes up a worrying proportion of 9.9% of the total area of the Dogon Plateau in 2011.

The results show that neither the desertification paradigm nor the greening paradigm can be generalized in the Sahel. Rather spatial variations of changes exist; the explanations for these are equally manifold.

Zusammenfassung

Die Sahel Region ist als eine "Hot-Spot-Region" der globalen Umweltveränderungen in den letzten Jahrzehnten anerkannt. Die Degradierung der Umwelt wurde durch schwere Dürren während den 1970er und 1980er Jahren in Kombination mit einer Abnahme der jährlichen Niederschlagssummen verstärkt. Die daraus resultierende Abnahme der Baum- und Strauchschicht wurde oft als irreversible Desertifikation betrachtet. Neue Erkenntnisse, die auf kleinmaßstäbigen Analysen von Satellitenbildern basieren, zeigen eine großflächige Zunahme der Vegetation über viele Teile der Sahelzone seit Mitte der 1980er-Jahre. Aufgrund eines Mangels an detaillierten regionalen Studien, bleibt es weitgehend unklar, ob dies eine Rückkehr zu einem Zustand vor den Dürren bedeutet oder vielmehr eine Transformation der Landbedeckung zu einem neuen Gleichgewichtszustand stattfindet.

Diese Studie verwendet Techniken der Fernerkundung, welche durch Felddaten ergänzt und validiert werden, um Gehölz- und Landbedeckung vor den Dürren mit dem aktuellen Zustand in einem 3600 km² großen Untersuchungsgebiet zu vergleichen.

Hochauflösende panchromatische Corona Bilder von 1967 und multispektrale RapidEye Satellitenbilder von 2011 bilden die Basis dieser regionalen Studie, die in Gebieten des Dogon Plateaus und der Seno Plains in der Sahelzone von Mali durchgeführt wurde. Die in ERDAS IMAGINE Objective integrierten Feature Extraction und Classification Funktionen wurden in einem objekt-orientierten Ansatz eingesetzt und mit spektralen Eigenschaften kombiniert, um die zwei Datensätze zu analysieren und Gehölze zu kartieren. Fast sechs Millionen Polygone, die sowohl Individuen, als auch Gruppen von Bäumen und Sträuchern repräsentieren, wurden für die Jahre 1967 und 2011 extrahiert. Ergebnisse enthalten die Gehölzdichte sowie die Gehölzabdeckung in Prozent für 1967 und 2011. Zusätzlich wurde die Veränderung der Landbedeckung der letzten fünfzig Jahre mit einer Auflösung von 20 m evaluiert, gefolgt von einer Analyse der aktuellen und vergangenen Gehölzdichte in Bezug zu den Landbedeckungsklassen.

Die Ergebnisse zeigen, insbesondere in den Seno Plains, eine signifikante Zunahme von spärlich bewachsenen Flächen, eine Reduzierung von dichtem Busch sowie eine Zunahme von Bäumen auf primären Feldern. Degradierten Flächen bilden einen Anteil von 9,9% der Gesamtfläche des Dogon Plateau in 2011.

Die Ergebnisse zeigen, dass weder das Paradigma der Desertifikation noch des „Greening—in der Sahel verallgemeinert werden kann. Vielmehr existieren zahlreiche räumliche Unterschiede; Erklärungen für diese sind gleichermaßen vielfältig.

Table of Contents

Acknowledgements.....	1
Abstract.....	2
Zusammenfassung	3
List of Figures	6
List of Tables	10
1. Introduction	12
1.1 Objectives and Hypotheses.....	14
1.2 The Desertification Debate	16
1.3 Human Impact.....	22
1.3.1 Detecting Human Influences with Remote Sensing.....	22
1.3.2 Agroforestry and Farmer-managed Natural Regeneration.....	24
2. Study Area.....	27
2.1 Climate.....	30
2.1.1 The Sahelian Climate.....	30
2.1.2 The Climate of the Study Area	33
2.2 Vegetation and Land Use	34
2.3 Soil.....	37
3. Methods.....	39
3.1 Datasets and Data Problems.....	39
3.2 Image Data and Pre-processing	40
3.2.1 Corona Imagery	41
3.2.2 RapidEye Imagery	46
3.2.3 Field Data	48
3.3 Land Cover Classification.....	49
3.3.1 Corona 1967	50
3.3.2 RapidEye 2011	52

3.4	Land Cover Change	60
3.5	Woody Vegetation Assessment.....	61
3.5.1	Theoretical Background	61
3.5.2	Corona 1967	69
3.5.3	RapidEye 2011	71
3.5.4	Woody Vegetation Density and Cover	72
3.5.5	Woody Vegetation Density and Cover Change	75
4.	Results.....	76
4.1	Land Cover.....	76
4.1.1	Land Cover 1967	76
4.1.2	Land Cover 2011	78
4.1.3	Land Cover Change 1967 - 2011	80
4.1.4	Case Study: Diamnati	83
4.1.5	Case Study: Diambara	88
4.2	Woody Vegetation Density and Cover	92
4.2.1	Woody Vegetation Density and Cover 1967 and 2011	92
4.2.2	Woody Vegetation Density and Cover Change	99
4.2.3	Case Study: Diamnati	107
4.2.4	Case Study: Diambara	113
4.3	Vegetation Composition	120
5	Discussion	123
6	Conclusion	132
7	Outlook	135
8	References	136

Curriculum Vitae

List of Figures

Fig.1.1: Research phases of the thesis.	15
Fig.1.2: Gully system in fossil sand dunes west of Gama, Seno Plains. Source: Spiekermann 2011.	17
Fig.1.3: An example for use of high resolution images to compare woody vegetation cover visually for any given site. Source: Above: Corona 1967; Below: RapidEye 2011.	19
Fig.1.4: NDVI trends in study area 1982-2010 showing “hotspots” (1-4), which represent selected sites, visited during the field trip in 2011. 1) & 3): Negative NDVI trends; 2) and 4) Positive NDVI trends. Source: Martin Brandt.	20
Fig.1.5: Overall trends in vegetation greenness throughout the period 1982-2003 based on monthly AVHRR NDVI time series. Percentages express changes in average NDVI between 1982 and 2003. Source: Herrmann <i>et al.</i> 2005.	20
Fig.1.6: Linear correlations of monthly NDVI with 3-month cumulative rainfall based on GPCP estimates for the period 1982-2003 (above) and 1982-2007 (below). Source: Herrmann <i>et al.</i> 2005 (above), Huber <i>et al.</i> 2011 (below).....	22
Fig.1.7: Overall trends in the residual NDVI throughout the period 1982-2003 (above) and 1982-2007 (below) based on regression of vegetation greenness (AVHRR NDVI) on 3-monthly cumulative rainfall (GPCP estimate). Source: Herrmann <i>et al.</i> 2005 (above), Huber <i>et al.</i> 2011 (below).	23
Fig. 2.1: Map of the study area in Mali. Source: © Bing maps: Microsoft Corporation and its data suppliers 2010. Cartography: Raphael Spiekermann.....	28
Fig. 2.2: A) View of Kowa, southwest of Sevaré on the Dogon Plateau, with surrounding fields; B) Onion plantations line the Yamé River, Dogon Plateau; C) Bandiagara Escarpment (La Falaise); D) View of the Seno Plains from the Bandiagara Escarpment.....	29
Fig. 2.3: Overview of the Sahel region as defined by climatic parameters. Source: Millennium Ecosystem Assessment.	30
Fig. 2.4: Linear correlation between monthly NDVI and 3-month sums of rainfall for the months July to October – a suggested definition for the Sahel; The red box shows approximate location of the study area. Source: Huber <i>et al.</i> 2011.	31
Fig. 2.5: Above: Overall spatio-temporal trends of rainfall based on annual sums (average change in mm) from 1982-2007. Source: Huber <i>et al.</i> 2011. Below: Overall trends in monthly	

rainfall (average change in %) for the period 1982-2003 based on GPCP estimates. Source: Herrmann <i>et al.</i> 2005.....	32
Fig. 2.6: Annual precipitation (1901-2009) for Bandiagara. Source: M. Brandt.....	33
Fig. 2.7: Average annual temperature (1901-2009) for the West Sahel. Source: M. Brandt.....	34
Fig. 2.8: Intensive use of bark and wood of <i>Balanites aegyptiaca</i> , Seno Plains. Souce: R. Spiekermann.....	35
Fig. 2.9: Soil sample location: Cropping field southeast of Diamnati, Dogon Plateau. Source: R. Spiekermann.....	37
Fig. 3.1: Section of a Corona image December 1967 providing detailed information on the landscape. Source: Corona 1967.....	42
Fig. 3.2: Control points used for georeferencing the 12 Corona images. Source: © GoogleEarth® Cnes/Spot image 2012.....	44
Fig. 3.3: Study area 1967: Result of the Corona image processing and data base for all further analyses for the year 1967.....	45
Fig. 3.4: Study area 2011: RapidEye images and data base for all further analyses for the year 2011.....	47
Fig. 3.5: Post-processing model of Corona unsupervised classification.....	52
Fig. 3.6: Photos of the four major land cover classes with corresponding cut-outs of the RapidEye images: DV1-DV2: Densely vegetated SV1-SV2: Sparsely vegetated; R1-R2: Rock; D1-D2: Degraded areas; Source: Photos: R. Spiekermann; Satellite images: RapidEye 2011.....	54
Fig. 3.7: Decision rules for the supervised classification. Source: ERDAS Inc. 1999.....	57
Fig. 3.8: Separability graph of Dogon Plateau RapidEye 07.12.2011 supervised land cover classification.....	59
Fig. 3.9: Feature space image with bands 5 (near-infrared) and 3 (red) showing separability of training areas of Dogon Plateau RapidEye 07.12.2011 supervised land cover classification.....	60
Fig. 3.10: Process flow in ERDAS IMAGINE Objective. Source: (ERDAS Inc. 2008).....	64
Fig. 3.11: IMAGINE Objective: Swipe showing Corona image part before (right-hand side) and result of the Single Feature Probability after (left-hand side).....	65

Fig. 3.12: IMAGINE Objective: Swipe showing Corona image part before (right-hand side) and result of the Raster Object Creator after (left-hand side).	66
Fig. 3.13: IMAGINE Objective: Example of RVC results in a sparsely vegetated area.....	68
Fig. 3.14: IMAGINE Objective: Example of the final results of the woody vegetation feature extraction for a section of the sparsely vegetated Corona image part.....	68
Fig. 3.15: Example of contrast in Corona image before and after clipping of bush fallow areas enabling improved detection of woody vegetation.	71
Fig. 3.16: Model in ArcGIS 10 used to calculate woody vegetation density and cover maps.	75
Fig. 4.1: Land cover classification 1967.	77
Fig. 4.2: Land cover classification 2011.	79
Fig. 4.3: Land cover change 1967-2011.....	82
Fig. 4.4: Diamnati, Dogon Plateau: Data base 1967 and 2011.....	84
Fig. 4.5: Diamnati, Dogon Plateau: Land cover classification 1967 and 2011.....	85
Fig. 4.6: Photographs of land cover types in the Diamnati case study area: A1, A2: Densely vegetated cropland; B1, B2: Sparsely vegetated cropland and fallow; C1, C2: Degraded land; D1, D2: Examples of the "Riverbed" class.	86
Fig. 4.7: Diamnati, Dogon Plateau: Land cover change 1967-2011.....	87
Fig. 4.8: Diambara, Seno Plains: Data base 1967 and 2011.	89
Fig. 4.9: Diambara, Seno Plains: Land cover classification 1967 and 2011.....	90
Fig. 4.10: Diambara, Seno Plains: Land cover change 1967-2011.....	91
Fig. 4.11: Woody vegetation density map of study area 1967.	93
Fig. 4.12: Woody vegetation density map of study area 2011.	94
Fig. 4.13: Woody vegetation cover map of study area 1967.....	97
Fig. 4.14: Woody vegetation cover map of study area 2011.....	98
Fig. 4.15: Woody vegetation density change 1967 – 2011.	101
Fig. 4.16: Woody vegetation cover change 1967 – 2011.....	103
Fig. 4.17: Retaining walls designed to capture soil and hinder progression of degraded areas west of Diamnati, Dogon Plateau.	108
Fig. 4.18: Woody vegetation feature extraction results in Diamnati 1967 and 2011.....	109

Fig. 4.19: Tree density in Diamnati 1967 and 2011.	110
Fig. 4.20: Change to woody vegetation density in Diamnati 1967 – 2011.....	111
Fig. 4.21: Woody vegetation cover in Diamnati 1967 and 2011.....	112
Fig. 4.22: Woody vegetation cover change in Diamnati 1967 – 2011.	113
Fig. 4.23: Woody vegetation feature extraction results in Diambara 1967 and 2011.	115
Fig. 4.24: Tree density in Diambara 1967 and 2011.....	116
Fig. 4.25: Change to woody vegetation density in Diambara 1967 – 2011.	117
Fig. 4.26: Woody vegetation cover in Diambara 1967 and 2011.	118
Fig. 4.27: Woody vegetation cover change in Diambara 1967 – 2011.....	119
Fig. 4.28: Average proportion of vegetation species according to land use (cropland and bush fallow).....	122
Fig. 5.1: Feature extraction results for an area on the Dogon Plateau: Advantages and disadvantages of Corona and RapidEye imagery for feature extraction.....	124
Fig. 5.2: Comparison of GPS-tagged photography (1-2) with very high resolution images (1a-2a) and RapidEye images (2a-2b). Source: Photos 1-2: R. Spiekermann; 1a-2a: © Bing maps: Microsoft Corporation and its data suppliers 2010; 1b-2b: RapidEye 2011.....	125
Fig. 5.3: Diambara: Land cover change 1967-2011 and woody vegetation 2011 with photo locations.....	129
Fig. 5.4: Photos of cropland (C1 – C11 in map of Fig. 5.3).....	130
Fig. 5.5: Photos of fallow land (F1 – F12 in map of Fig. 5.3).....	131

List of Tables

Table 2.1: Selected examples of multi-purpose trees in the Sahel with site requirements and uses. Source: Maydell 1990.	36
Table 2.2: Soil analysis results of 2 mixed samples from fields on the eastern outskirts of Diamnati.....	38
Table 3.1: Coarse resolution multi-temporal datasets used to assess vegetation dynamics in the Sahel.....	39
Table 3.2: High resolution datasets capable of assessing land cover and woody vegetation change in the Sahel.....	40
Table 3.3: Specifications of satellite images used for the study.....	41
Table 3.4: Seno Plains RE 26.11.2011: Land cover classes and training areas.	56
Table 3.5: Contingency matrix of Seno Plains RapidEye 26.12.2011 supervised land cover classification.....	56
Table 3.6: Dogon Plateau RE 26.11.2011: Land cover classes and training areas.....	58
Table 3.7: Contingency matrix of Dogon Plateau RapidEye 26.12.2011 supervised land cover classification.....	58
Table 3.8: Dogon Plateau RE 07.11.2011: Land cover classes and training areas.....	59
Table 3.9: Reclassification of land cover maps for change analysis.	60
Table 3.10: Data base of woody vegetation feature extraction and the corresponding number of training samples (TS) and background samples (BS).....	63
Table 3.11: Feature model process nodes of Corona image parts.	70
Table 3.12: Feature model process nodes of RapidEye image parts.....	72
Table 3.13: Results (number of features per image part) of woody vegetation assessment.	73
Table 4.1: Land cover classification 1967 results (total area (ha) and percent).	78
Table 4.2: Land cover classification 2011 results (total area (ha) and percent).	80
Table 4.3: Land cover change 1967 – 2011 in hectare and percent. DV: Densely vegetated; SV: Sparsely vegetated; R: Rock; W: Water; RB: Riverbed; I: Infrastructure.....	81
Table 4.4: Summary of feature extraction results for each Corona and RapidEye image part. ..	95

Table 4.5: Detailed statistics of woody vegetation feature extraction results, classified acc. year and plateau/plain.....	99
Table 4.6: Summary of woody vegetation density change 1967 – 2011.....	100
Table 4.7: Summary of woody vegetation cover change 1967 – 2011.....	102
Table 4.8: Woody vegetation density and cover on sparsely vegetated (SV) and densely vegetated (DV) areas on the Seno Plains and Dogon Plateau 1967 and 2011.....	105
Table 4.9: Woody vegetation and cover change 1967 – 2011 for the sparsely vegetated (SV) and densely vegetated (DV) areas of 2011.	106
Table 4.10: Vegetation survey results: Land use: Cropland (CL), Bush (B), Fallow (F); number of trees, vegetation species; dominant species (BAL: <i>Balanites aegyptiaca</i> , COG: <i>Combretum Glutinosum</i> , BOA: <i>Borassus aethiopum</i> , BOS: <i>Boscia senegalensis</i> , GUI: <i>Guiera senegalensis</i> , ACA: <i>Acacia albida</i> , ACN: <i>Acacia nilotica</i> , BI: <i>Sclerocýarya birrea</i> , COM: <i>Combretum micranthum</i> , AI: <i>Azadirachta indica</i>).....	120

1. Introduction

The African Sahel region has been acclaimed as a “hot spot of global environmental change” (Hickler *et al.* 2005p. 1) in the last decades, with the UN (UNEP) in 2005 predicting up to 50 million “environmental refugees” till the year 2010 (UNCOD 1978), reflecting the disastrous effects of apparent widespread desertification and environmental degradation. The apparent degradation of the environmental conditions was accelerated by prolonged droughts in the region during the late 1960s to early 1980s. The droughts, combined with weak economies, ineffective political institutions and civil strife were in part responsible for the loss of human life (an estimated 100,000 drought-related deaths according to Kandji *et al.* (2006)), as well as leading to a “tide of mass migration” (Kandji *et al.* 2006 p. 11). This sparked not only concern at global scale by politicians and development organizations, but also an increasing scientific interest in the causation and extent of the observed environmental change in the Sahel.

The prosperity in the African Sahel largely depends on the well-being of the woody vegetation cover, which forms the basis for life in the semi-arid climate zone. In a semi-arid to arid climate, with nine months of no rainfall, several deep-rooted trees are the only form of vegetation that remain green throughout the year, fulfilling multiple functions, particularly in rural areas where trees are used as foliage for livestock, a source of energy and medicinal uses among other functions (Maydell 1990). Although variability in rainfall and the occurrence of droughts in semi-arid and arid environments may be seen as normal phenomena (Hermann & Hutchinson 2005), the vulnerability of the rural Sahelian population is high, considering the strong dependency on the climate, especially with rapid population growth linked with increasing pressures on natural resources in the past 50 years.

Recent findings by Hermann & Hutchinson (2005), Olsson *et al.* (2005) and Huber *et al.* (2011) among others, based on analyses of satellite images, show an increase of vegetation greenness, i.e. biomass, over most parts of the Sahel since the mid-1980s, challenging previous scientific reports of widespread irreversible desertification in the Sahel and fears of an encroachment of the Sahara desert (Lamprey 1975). These developments lead to a questioning of the causes and even the existence of irreparable desertification. A revitalized desertification debate thus began, a critical hint of scepticism towards previous assertions setting the tone, in light of findings showing an increased greenness in the Sahel. Multiple studies (mainly making use of remote sensing) followed (Hermann & Hutchinson 2005, Tucker *et al.* 2005, Huber *et al.* 2011, Hickler *et al.* 2005, Olsson *et al.* 2005 and Giannini *et al.* 2008) and have contributed to a more in-depth knowledge of the physical processes taking place during the past decades in the Sahel. These environmental studies assess the dynamics of the vegetation and climate in the

Sahel, also attempting to explain the causes of environmental change. To complement the many remote-sensing studies, scientists have additionally attempted to link processes at a local level to environmental change, largely dealing with the human impact in regard to land management practises (Reij *et al.* 2005, Reij & Smaling 2008, and Brandt *et al.* in review). Concerning environmentally induced migration, on-going research questions the actual causes for migration and possible impacts of climate change in the Sahel, showing that predictions of environmental refugees is a much more complex and delicate matter than one may assume (Romankiewicz & Doevenspeck 2011 and Adamo 2008).

Particularly in regard to the re-greening of the Sahel, small-scaled remote-sensing studies covering the entire Sahel region fail to offer much detail of the actual greening process. This is due to the resolution of the data used as well as an obvious lack of field work. The commonly used NDVI dataset (GIMMS) has 8 km pixels, which thus represent a product of multiple processes at ground level, i.e. multiple processes are integrated into a single pixel (see chapter 2). For this reason, a well-founded interpretation of the trends is more than difficult, rather impossible. The following questions can therefore only be answered hypothetically: Why do spatial disparities in the greening trends exist? Which proportion of the greening can be attributed to an increase in trees, and which proportion is perhaps an increase of useless grass and shrubs on wasteland (maybe even a form of degradation)? Does the greening trend equal a return to pre-drought conditions? If not, how has the vegetation composition and land use changed since then? Brandt *et al.* (in review) and Hermann & Tappan (2013) go a step further by combining remote-sensing analyses of vegetation dynamics at various scales and include interdisciplinary field work to find explanations of trends at a local scale. These studies remain largely qualitative, mainly investigating at a case-study level.

A significant gap between the broad-scaled remote-sensing studies and the large-scaled case studies still exists although the works mentioned above are an initial response by environmental scientists to combine the strengths of high resolution remote sensing studies with field work. High-resolution multi-spectral images now make regional-scaled assessments of the vegetation cover possible. A quantification of the woody vegetation is needed to determine actual “useful” greening, as far as the long-term benefit to the local population is concerned. Furthermore, an assessment of the land cover and land-management practises can advance understanding of the continuous evolution of the Sahelian landscape. This study intends to use both remote sensing techniques as well as data collected during a field trip, where processes at a local level are assessed, to offer insight into the many processes and factors responsible for the general increase in greening that has been observed at a very coarse scale during the past three decades, and to assess whether or not the change is a return to pre-drought conditions of the 1960s.

1.1 Objectives and Hypotheses

In this context, my thesis intends to assess the change of woody vegetation density (WVD) and land cover at a regional scale in a typical Sahelian area, namely on the Dogon-Plateau and Seno-Plain in Mali. The situation of today is compared to the situation prior to the great Sahelian droughts (mid-1960s to mid-1980s).

The primary hypotheses of this thesis include the following:

- 1) Woody vegetation (i.e. individual trees and large shrubs) can be mapped and quantified using high resolution images.
- 2) Changes to the woody vegetation can be assessed by comparing woody vegetation classified with Corona high resolution photographic images of 1967 and RapidEye images of 2011.
- 3) The tree density today is similar to the pre-drought situation and is thus in part responsible for the greening trends in the Sahel observed since the mid-1980s.
- 4) The environment of the study area is returning steadily to conditions similar to the pre-drought situation.
- 5) The distance to settlements is decisive for tree density.
- 6) The land cover change, as a proxy for land use change, has contributed greatly to environmental change during the past 50 years.
- 7) The land cover is directly related to tree density.
- 8) The land use is directly related to the vegetation composition.

In order to investigate these hypotheses, high resolution imagery from the mid-1960s (Corona images 1967) is processed and analysed. The methodology includes the geo-referencing of the Corona-images and enhancement operations as preparation for further use. In order to assess the tree density, a recently developed extension of ERDAS Imagine, namely "IMAGINE Objective", is applied. This extension contains various feature extraction and classification operations and combines an object-oriented approach with spectral properties to analyse geospatial data. This software has found little use for tree detection in semi-arid areas, thus the methodological approach may be of broad interest to environmental scientists. A similar assessment of tree density is carried out for the situation today by making use of high resolution multispectral RapidEye imagery. Because RapidEye offers multispectral information at a slightly different resolution to the Corona images, the methods of woody vegetation mapping differs somewhat between the two. Furthermore, data collected from the many vegetation surveys that were conducted during the field trip to Mali (November-December, 2011) are used to offer

specific information on the vegetation composition and are also indispensable for evaluating the land cover and woody vegetation maps.

Not only the change in density of the woody vegetation is of interest, but especially the factors involved in causing change. During the field trip to Mali an observation was made that farmer-management practises and other forms of resource use seem to influence woody vegetation density. Therefore change of land use could also explain change of woody vegetation density. This leads to the question: In what way has land use changed in the study areas during the past fifty years? This hypothesis is investigated more closely by producing detailed land cover maps for the study area, as a proxy for land use. To do so, the high-resolution images mentioned above are used to produce land cover maps for 1967 and 2011. The scope of this study is therefore fairly elaborate. Fig. 1.1 graphs the various phases of the thesis.

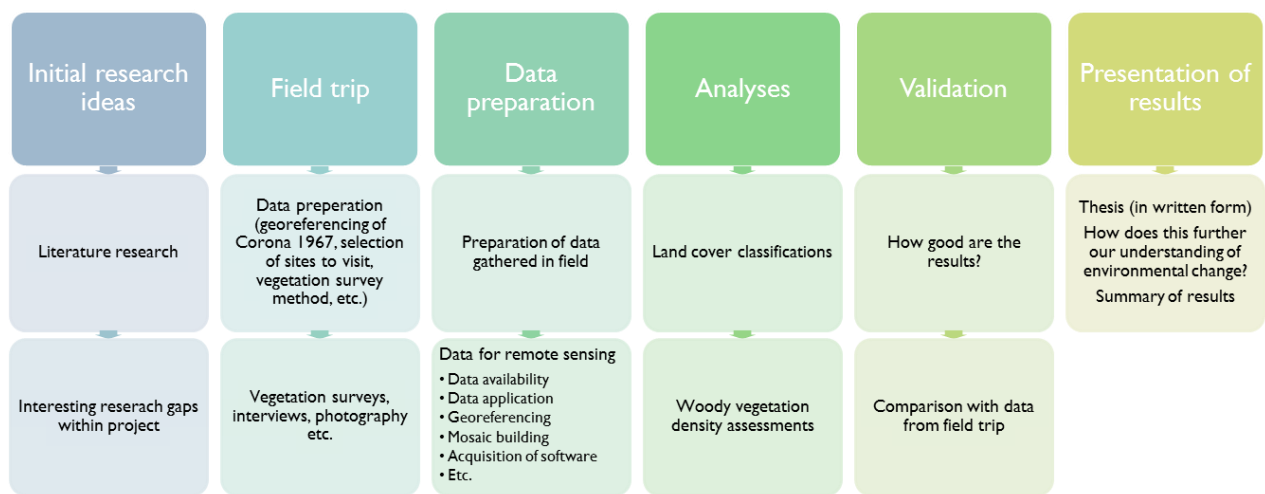


Fig. 1.1: Research phases of the thesis.

This thesis is integrated into the Project *“micle”* (Migration, Climate and Environmental Changes in the Sahel), which investigates the complex relationships between (climate-related) environmental changes and migration. Funded by the German Federal Ministry of Education and Research (BMBF) - Framework Programme Research for Sustainable Development (FONA), an inter- and trans-disciplinary research approach is applied, involving the Institute for Social-Ecological Research (ISOE), the University Bayreuth and the University of Vienna. The thesis builds on previous and on-going research by Martin Brandt, in particular time series analyses of satellite imagery (e.g. trend maps of NDVI), which were used among other things to select case study sites within the study area, which were then visited during a field trip (see Fig. 1.4). Initial results of the field trip are illustrated by Brandt *et al.* (in review).

1.2 The Desertification Debate

The desertification debate has been on-going for many years, revolving around the definition of desertification, methods for assessing and measuring the process and sceptics questioning its existence (Hermann & Hutchinson 2005). Perspectives on the topic of desertification and its effects are almost as numerous as the number of scientists, politicians, lobbyists and so forth concerned with the issue. Generally speaking, two sides to this debate can be identified. The first adamantly support the desertification hypothesis, which sprung up in the 1980s and held the overuse of resources and human mismanagement responsible for what was referred to as an irreversible decline in vegetation conditions and density (Hermann *et al.* 2005). The desertification sceptics on the other hand, backing what may be called the adaptation hypothesis, made their perspective known in various publications towards the end of the 20th century (e.g. Nicholson *et al.* 1998, Olsson *et al.* 2005). These challengers of the irreversible desertification hypothesis regard the drought as the primary cause for the temporary reduction of the vegetation cover, with the human impact viewed as secondary (Hermann *et al.* 2005).

It seems obvious that the degrading landscape in the Sahel during and following the droughts is the product of an interaction of several processes, which differ spatially depending on the spatial variability of precipitation, land use management practises, soil, morphology, etc. The prolonged droughts of the second half of the 20th century with low average rainfall levels led to increased levels of stress on the vegetation and in many cases dehydration of many plants (in particular young plants with no fully-established root system reaching to groundwater levels). A decline of vegetation density and a loss of vegetation diversity followed. The pressures of the drought also had a major impact on the human population, leading to an intensive use of trees and overgrazing by stock. In many areas of the Sahel the situation became so dire that famine was a common occurrence as the supply of the annual harvests simply could not meet the demands of the population and external aid also failed to stabilize the situation.

An example for drought-related degradation, as observed during the field trip in Mali (see Brandt *et al.*, in review), is presented by the fossil dunes near the village of Gama, just south of the Bandiagara escarpment on the Seno Plains (see Fig. 3.3 and 3.4 for location). Compared to the pre-drought situation, this area is deprived of trees with no future recovery in sight. During the drought the trees could not reach to groundwater levels and the sandy dunes were unable to hold moisture for extended periods of time, making this area especially prone to degradation. The tree cover therefore steadily declined during the droughts. With no vegetation and the related deep-rooting systems available for stabilization purposes, the entire dune area increased in susceptibility to soil erosion. Because of the lack of vegetation, neither interception nor temporary storage of rainfall could take place, thus accelerating the soil erosion process.

Very soon the rills had grown to channels and today wide-spread gully systems are observed, steadily increasing in size with every rainy season and reducing the area of cropland used by local farmers (Fig. 1.2). This perhaps irreversible process is however very local and dependent on the characteristics of the local landscape, and thus shows that reasons for change differ from one place to the next. A few kilometres further east, many young trees can be seen growing steadily in the fields.



Fig. 1.2: Gully system in fossil sand dunes west of Gama, Seno Plains. Source: Spiekermann 2011.

As was mentioned above, a general increase of greenness throughout the semi-arid Sahel and Sudan zones of West Africa has been observed since the mid-1980s. This chapter intends to review literature on the remote-sensing studies concerned with the greening Sahel in order to draw out the benefits and limits of such studies, thereby showing which questions remain unanswered.

Remote sensing studies at a fairly coarse scale, mostly using the normalized difference vegetation index (NDVI) as a proxy for vegetation, form the basis of these positive greening observations. In light of the debate discussed in the previous chapter, it came as somewhat of a surprise that the hypothetically irreversible desertification of the Sahel may not be so permanent after all. Scientists began to ask whether the Sahelian vegetation could indeed be so adaptable to rainfall variability in time and space. Thus several further questions may be posed.

The first very basic question would for one be: What is greening? This may appear to be a very simple inquiry, but because 8-kilometre pixels (GIMMS dataset) are at the root of these studies, an obvious lack of detail and knowledge of the processes on the ground exist. A greening does not automatically correspond with benefits for the population but rather depends on what is greening – an increase of grass and useless shrubbery is one thing, an increase of tree density another. A further question would be whether the greenness is a mere recovery from the

droughts or whether there are significant differences to the pre-drought situation as far as the vegetation composition is concerned. Which driving factors are behind the changing greenness? As we will see, studies show major spatial differences within the Sahel and yet little is known about why these disparities exist. We will now take a look at some of the leading studies related to the assessment of the situation and changes of vegetation greenness in the Sahel.

A closer look at two similar remote sensing studies on the greening Sahel may shed light on the challenges of assessing environmental change at such a coarse scale. This chapter reviews two recent and well-known studies on the greening Sahel, in particular that of Hermann *et al.* (2005) and Huber *et al.* (2011). First of all, a look at the actual greening will be taken, followed by an analysis of possible driving factors. Hermann *et al.* (2005) correlate rainfall with NDVI to explore explanations for the greening and continue with an attempt to disentangle climatic and non-climatic impacts on vegetation.

Although it is an interesting exercise to pick out examples of land cover and tree density change, as in Fig. 1.3, to do so for the entire Sahel is an impossible task. To quantitatively assess vegetation dynamics, satellite images are used at a much coarser scale. As mentioned above, Hermann *et al.* (2005) and other authors base their analyses on the Advanced Very High Resolution Radiometer (AVHRR) Global Inventory Modelling and Mapping Studies (GIMMS) NDVI time series (Tucker *et al.* 2005). The dataset contains 15 day maximum NDVI values at a spatial resolution of 8 km and are available for a 25 year period from 1981 to 2006. For each 8 km pixel the change in NDVI over time is calculated by computing trend lines by means of a simple linear function, which shows the average annual change of NDVI. For regional scaled studies, other datasets such as SPOT VGT-S data with a spatial resolution of 1 km and temporal resolution of ten days may be more useful and accurate, as is exemplified by Fig.1.4 for the study area in Mali.

Although there are fluctuations in the NDVI from season to season and from year to year, the general trend is positive. Using this method for calculating changing greenness, each 8 km pixel of the Sahel is processed in a similar way by Hermann *et al.* (2005), the results of which are displayed in Fig. 1.5. The map shows the overall trend of monthly maximum NDVI for each pixel, expressed in percentage relative to the value of the linear trendline at the starting point of the time series, for the period 1982-2003. As can be seen, most parts of the Sahel are positive with some areas showing an increase of up to 50%.

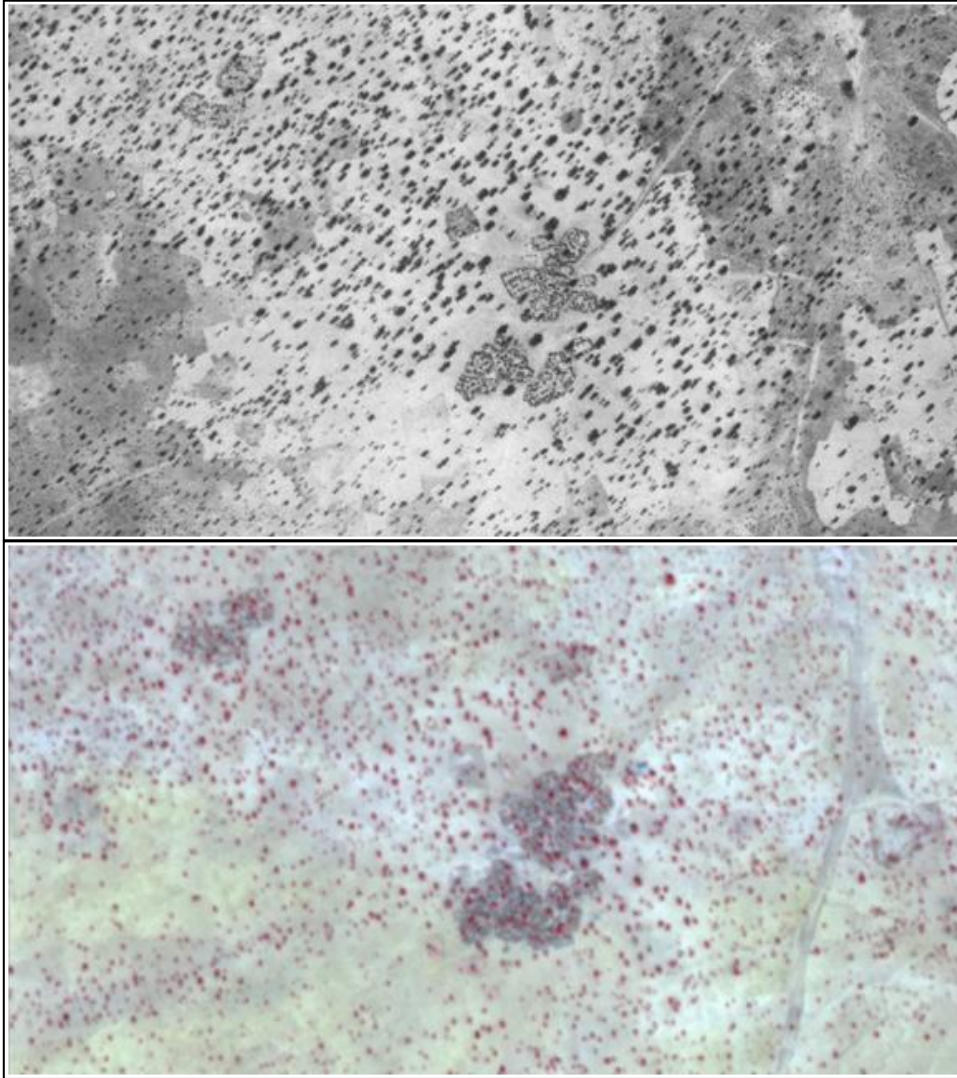


Fig. 1.3: An example for use of high resolution images to compare woody vegetation cover visually for any given site. Source: Above: Corona 1967; Below: RapidEye 2011.

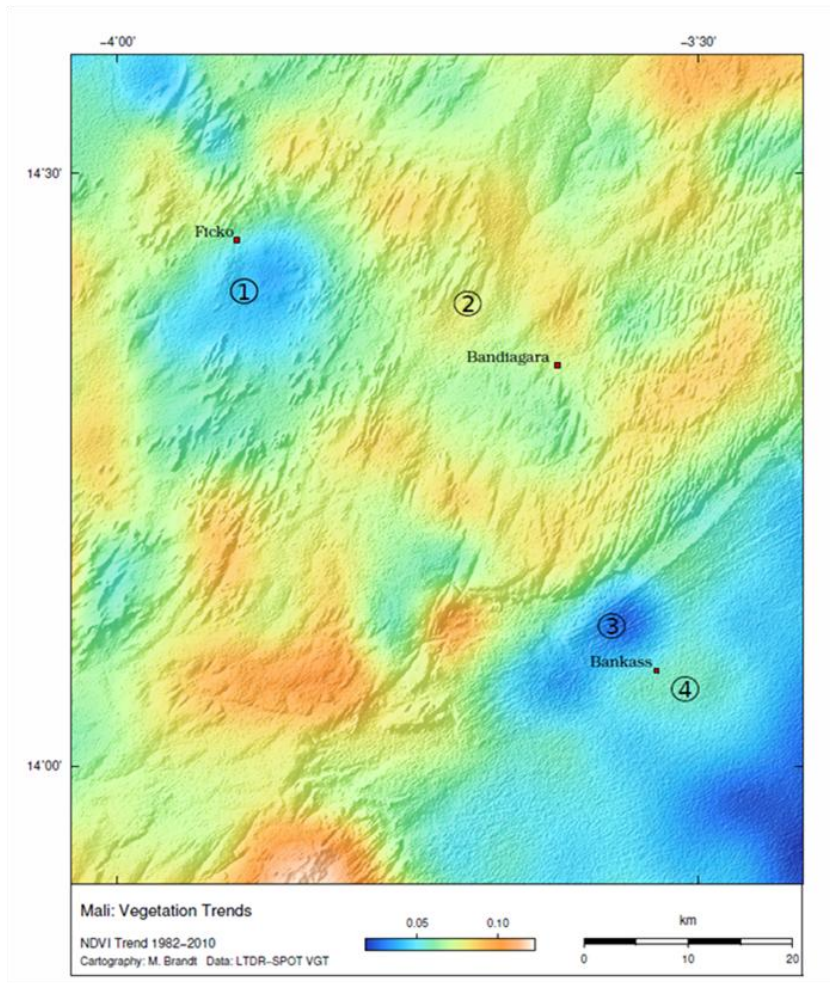


Fig. 1.4: NDVI trends in study area 1982-2010 showing “hotspots” (1-4), which represent selected sites, visited during the field trip in 2011. 1) & 3): Negative NDVI trends; 2) and 4) Positive NDVI trends. Source: Martin Brandt.

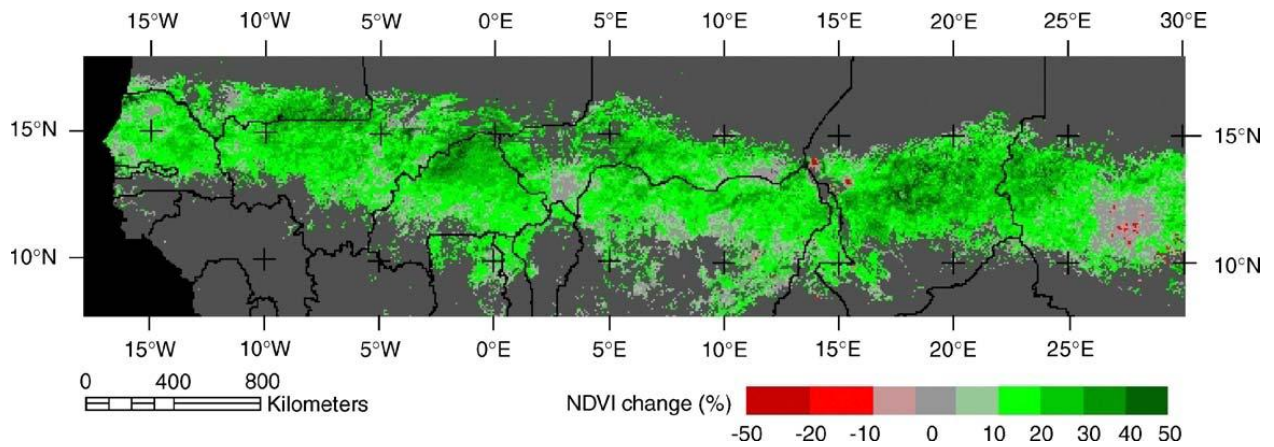


Fig. 1.5: Overall trends in vegetation greenness throughout the period 1982-2003 based on monthly AVHRR NDVI time series. Percentages express changes in average NDVI between 1982 and 2003. Source: Hermann *et al.* 2005.

The dataset of the Global Precipitation Climatology Project (GPCP) merges data from over 6,000 rain gauge stations and satellite observations since 1979 to produce monthly gridded satellite precipitation estimates at 2.5° spatial resolution and is often used as input for correlation analyses with the outputs of the greening trends to investigate drivers of environmental change.

Hermann *et al.* (2005) and Huber *et al.* (2011) found the strongest correlation between NDVI and 3-monthly cumulative rainfall. The results of the analysis are displayed in Fig. 1.6 below and show highly significant correlation coefficients throughout the Sahel. The increase of greenness is accompanied by a general increase of rainfall since 1982 for most parts in the Sahel. It follows that precipitation is most likely the most important driver of an increase of vegetation greenness. Both maps by Hermann *et al.* (2005) and Huber *et al.* (2011) reflect the same general pattern across the Sahel with a marked zonality from north to south. The correlation coefficients of Huber *et al.* (2011) are stronger in many areas, particularly in the central eastern Sahel, where coefficients between 0.9 and 1.0 cover a large proportion of the region, reflecting the slightly different methods used (extended length of the period of analysis and the statistical threshold used to display significant results) (Huber *et al.* 2011).

The results of these trend analyses thus provide an excellent overview of the developments in the Sahel (e.g. that rainfall is the dominant causative factor for vegetation greenness); however the interpretation of the actual processes at ground level remains highly challenging without on-site studies. With this in mind, as well as the suggestion by Herrmann *et al.* (2005) that the residuals most likely represent a human signal, a look at some on-site studies will be taken in the following chapter.

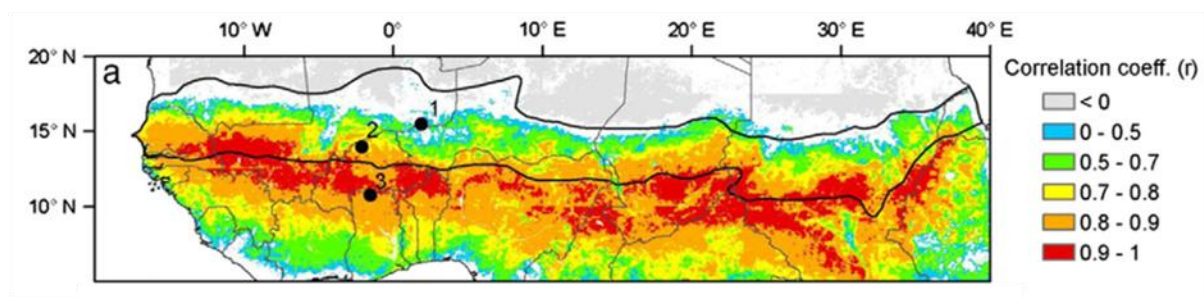
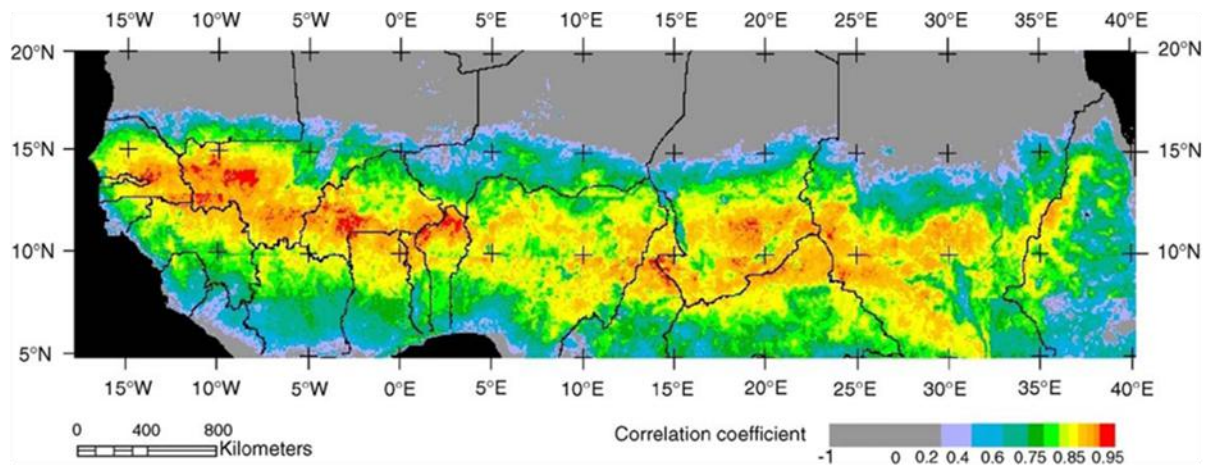


Fig. 1.6: Linear correlations of monthly NDVI with 3-month cumulative rainfall based on GPCP estimates for the period 1982-2003 (above) and 1982-2007 (below). Source: Herrmann *et al.* 2005 (above), Huber *et al.* 2011 (below).

1.3 Human Impact

Both remote sensing and field work can help assess the human impact on greening in the Sahel. First of all, we want to look at attempts by remote sensing studies to extract the human impact on the vegetation layer, followed by examples at a local scale.

1.3.1 Detecting Human Influences with Remote Sensing

Following the analysis of the relationship between rainfall and NDVI, a linear regression analysis is carried out by Herrmann *et al.* (2005) with NDVI as the dependent variable and three month cumulative rainfall as the independent variable. The regression equations for each pixel may then be used to calculate the predicted values of maximum NDVI for each month and each pixel from the observed monthly rainfall values (Herrmann *et al.* 2005). The difference between observed NDVI and predicted NDVI (residuals) thus represent the effects on the NDVI, which cannot be explained by rainfall. In other words, the effects of rainfall are supposedly removed

from the NDVI time series. Hermann *et al.* (2005) computed trends for these residuals, which reflect the trends in vegetation greenness that are not explained by rainfall dynamics and hypothesized that these trends represent the human impact on vegetation greenness. The map of the Sahel, illustrating the trends of the residuals, is shown in Fig. 1.7 below. As a comparison, the results of Huber *et al.* (2011) are also displayed.

Three main findings are exposed by the spatial pattern of NDVI residuals, as seen in Fig. 1.7. First of all, a large proportion of the area lacks significant trends, meaning the NDVI/ vegetation greenness trends relate to what would be expected by the monthly rainfall trends. Furthermore, a very large extent of the region (in particular widespread areas of Chad, Burkina Faso, Mali and Mauritania) reveals significant positive trends, i.e. areas where vegetation has been greening more than would be expected given the actual rainfall trends. Conversely, negative areas, located primarily in northern Nigeria and Sudan, comprise a much smaller area and reflect regions where the vegetation greenness is less than would be expected given the increase in rainfall in those areas.

The differences of the results presented by Huber *et al.* (2011) are somewhat different to those of Hermann *et al.* (2005) and unveil some of the difficulties of working with satellite imagery and precipitation data at such a coarse scale. Using slightly different methods can lead to very different results, even if the general trend remains comparable in this case.

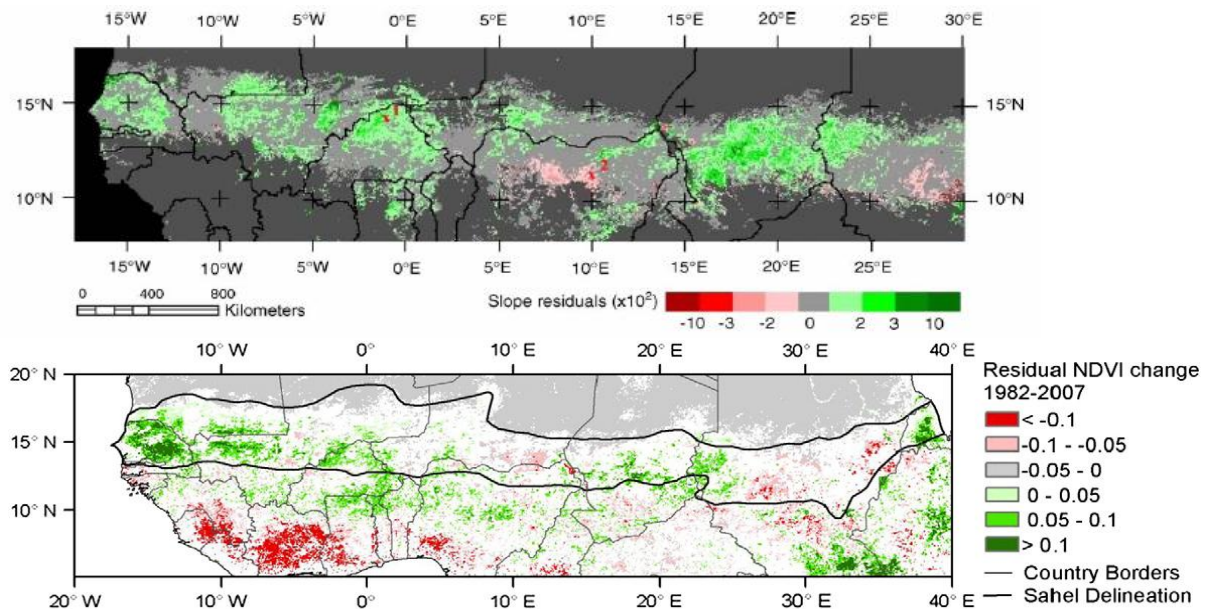


Fig. 1.7: Overall trends in the residual NDVI throughout the period 1982-2003 (above) and 1982-2007 (below) based on regression of vegetation greenness (AVHRR NDVI) on 3-monthly cumulative rainfall (GPCP estimate). Source: Hermann *et al.* 2005 (above), Huber *et al.* 2011 (below).

Furthermore, the interpretation of these results is a very difficult matter. The negative trends of the NDVI residuals cannot be explained by human-induced land degradation or bush fires (as examples) until detailed studies at local level are carried out. There are some obvious problems when using datasets with majorly different scales such as these. The spatial differences are much greater in reality, and thus represent a clear source of error. Brandt *et al.* (in review) demonstrate the problem of interpreting coarse resolution trend analyses as many processes are combined in a single pixel.

The human impact on the landscape and vegetation in the Sahel can, as anywhere, be both negative, with a degrading effect, or positive and sustainable with e.g. a rehabilitating effect. The influences of humankind cannot be undermined and often represent the main driver of change. Examples of a negative effect would be land degradation via overgrazing, deforestation and changed land management practices because of both external and internal pressures such as the environmental and economic crisis of the 1970s and 80s combined with population pressure on natural resources (Hickler *et al.* 2005). This human induced form of land degradation is often referred to as “desertification” in arid, semi-arid and sub-humid zones of the globe. The term implies a spreading of desert-like conditions. It is however important to bear in mind that the Sahel may physiognomically have the appearance of an arid desert in times of prolonged droughts. This can be seen as a normal phenomenon resulting from fluctuations of rainfall at a decadal time scale (see Tucker & Nicholson 1999). As long as the climate of the Sahel does not change considerably, the desert-like conditions of the Sahel will remain temporary during times of drought. Desertification should therefore not be confused with a long-term transformation of the landscape to a desert. As long as average annual rainfall in the Sahel remains above that of deserts such as the Sahara, wide-spread desertification is not a process to be attributed to the semi-arid Sahel and Sudan zones of West Africa.

1.3.2 Agroforestry and Farmer-managed Natural Regeneration

Agroforestry is a major form of land use in the rural Sahel. Agroforestry is a form of combining agricultural activities with forest management on farmland. When this method is practised in a sustainable and effective manner, it may have a positive impact on the environment. According to Reij *et al.* (2005), Reij (2009) and Reij (2011), farmer-managed natural regeneration (FMNR), in combination with improved soil and water conservation techniques, has contributed significantly to the re-greening of the Sahel since the droughts.

Farmer-managed natural regeneration (FMNR) adopts traditional centuries-old methods of woodland management to produce continuous harvests of trees for various uses including for fuel, building materials, food and fodder for livestock without the need for frequent, costly replanting (Rinaudo 2005a). The trees are trimmed and pruned to maximize harvests while at

the same time promoting optimal growing conditions, thus a sustainable form of management. A rather new feature uses these techniques in agricultural cropland and to manage trees as part of a farm enterprise. For many decades, farmers had felled trees on their fields to make way for agricultural crops and grazing areas for cattle, sheep and goats. Especially since the droughts, farmers have realized the importance of trees and the need to integrate woodland management as an important part of their farm enterprise. FMNR is based on the existence of re-sprouting tree stumps. Rinaudo (2005a p. 7) describes why it took so long for NGOs and funded projects to discover the most simple and yet effective form of forest regeneration, which has led to the unleashing of the “underground forest”:

“Each year multiple shoots sprouted, however, they were not given the opportunity to grow to their full height because of the standard slash and burn practice. Consequently, low-lying shrubs was all that was visible. As a result, forestry agents did not recognise that these shrubs were actually felled trees with the capacity to regenerate. The fact that the true nature of this vegetation was not realised led to the coining of the term ‘the underground forest’.”

FMNR follows a four-step process:

- 1 Selecting the stumps to regenerate based on the usefulness of the species.
- 2 Selecting stems to prune and protect on each stump – usually the tallest and straightest
- 3 Removing unwanted stems and side branches
- 4 Removing new stems and regularly pruning surplus side branches (as often as one day)

Another form of regeneration is by planting pits and half-moons (so-called ‘zai pits’) roughly 30 cm wide and 20 cm deep in rows until an entire barren area of hard-packed earth is covered with these holes (Dodd 2009). This process is carried out in spring before the rainy season. The pits are filled with compost, leaves or other organic matter in which the rainfall can be stored for much longer periods of time. The mounds and pits also attract termites and thus increase soil fertility, turning the area into productive farmland and making it possible for trees and crops to grow. This method has proven to be successful in many areas of the Sahel because of its simplicity and also the increased yields seen by the farmers, thus growing in attraction and spreading very quickly. The documentary film *“The man who stopped the desert”* by Dodd (2009) provides an in-depth account of the success zai-pits may have.

Reij *et al.* (2005) discuss the impact of several soil and water conservation projects initiated in the 1980s by governments, donor agencies and NGOs seeking to rehabilitate the productive capacity of farmland through better control of rainfall and runoff and soil fertility management and reforestation. These projects on the Central Plateau of Burkina Faso proved to be highly successful and lead to increases in crop yields and more trees on fields than 15 years previously. At the same time the vegetation on the non-cultivated areas continued to degrade.

This shows the important role of human intervention to transform barren areas into productive farmland (Reij *et al.* 2005).

Success stories of agriculture and land management are provided in detail by Reij & Smaling (2008) and a few of these will be exemplified here. In the densely populated Maradi and Zinder Regions of Niger around five million hectares of land have greened using the simple methods described above (Reij 2011).

“Over the last two decades, farmers in Niger have grown 200 million new trees on their cultivated fields. Where farmers had only 2 or 3 trees per hectare 20 years ago, they now have 40, 60 or even over 100. (...) They thus achieved almost 20 times more than all tree planting projects in Niger over the same period combined.” (Reij 2011 p. 22).

Benefits of re-greening include the following (Reij 2011):

- Fodder is no longer a major constraint to livestock; farmers are able to increase number of livestock.
- Poverty reduction: a 10% increase in agricultural production reduces rural poverty by 6-9%.
- Increased resilience to drought: In drought years poor families can also rely on trees for nourishment.
- Reduction of conflicts between herders and farmers: sufficient resources for everyone.
- Changes in micro-climate: Reduction in soil-temperatures.
- Crops are protected by wind and sand by vegetation lining fields; Farmers must only plant crops once instead of trying 3-4 times as they did 20 years ago.
- Greater awareness of farmers: Some species improve soil fertility more than others.
- Time spent by women to collect firewood has reduced significantly.

FMNR is a very effective form of re-greening and Reij (personal contact 2012) believes *“human management is a more determining factor for re-greening than rainfall”*. The break-through is that farmers have taken matters into their own hands and are accepting responsibility of caring for their land and improving living conditions by means of re-greening.

These success stories are obviously not spatially comprehensive throughout the Sahel and much of what is written above is not necessarily true for the study area of this thesis, which will therefore be introduced in more detail in the following chapter.

2. Study Area

The study area is located in the Mopti Region in the Northeast of Mali, 600 km northeast of the capital Bamako, as is shown in the overview of Fig. 2.1. It is approximately 3661 km² large, featuring the major town of Sevaré in the north-west and also includes the towns of Bandiagara on the Dogon Plateau and Bankass on the Seno Plains to the South. In 2009, the Mopti region was reported to have two million inhabitants with an average population density of 25 inhabitants per km² (INSTAT 2009).

The study area can generally be divided in the Dogon Plateau (2705 km²) in the north and the Seno Plains (956 km²) to the south (as seen in Fig. 3.3 and Fig. 3.4). The steep Bandiagara escarpment (known as “Falaise de Bandiagara”) divides the plateau from the sandy plains (see Fig. 2.2-C). The Dogon Plateau is characterised by a more complex and rough morphology, with rocky outcrops dominating the appearance of the landscape at an altitude between 450 and 700 m. Various rivers, mostly tributaries of the Niger River, cut across the plateau. The Yamé River is the largest of these seasonal rivers and flows eastwards through Bandiagara. The cultivated areas and grazing land, as well as areas of dense natural vegetation, are spread between the rocky outcrops in the valleys of the plateau. Apart from the major towns mentioned above, which rely primarily on tourism and trade as the main contributors to the economy, agriculture and animal husbandry represent the main sources of income and/or means of subsistence farming in rural areas. The main crops are millet, peanuts and sorghum. Onion plantations are often found close to major streams and rivers and recent construction of hydro-dams have enabled irrigation systems to be expanded, which has led to an increase of such onion plantations (See Fig. 2.2-B). The lateritic, sandy soils on the plateau mean cultivation is in some areas more difficult than on the sandy fields of the Seno Plains. The rocky sandstones often restrict the expansion of cropland areas so that many such spaces are dominated by dense natural vegetation, which in turn serves as a provider of fuel wood as an energy source. Upon closer inspection a typical pattern may be observed. The villages are often built in close-knit formations of clay huts with narrow passage ways connecting the various houses, storage rooms and community facilities. A water-well is usually located in close proximity to the village, providing ground water all year round. The villages commonly accentuate having plenty of large trees within the village borders to offer shade during the hot hours of the day. The quality of fields is typically directly proportional to the distance from the village (see Croll & Parkin 1992). Manure provided by livestock is spread on the fields surrounding the village, many large old trees (mainly *Acacia albida* and *Balanites aegyptiaca* and the popular *Adansonia digitata*) offer plenty of shade and the fields are ploughed regularly, mainly by hand. Cropland at greater distances from the villages are usually lain fallow for three to four years at a time before crops are once

again sown for a similar period of time. During the period of use, the trees on these outlying fields are especially protected and encouraged to grow. During fallow years the trees are often found to be used more intensively, e.g. for cooking purposes or to protect smaller trees with branches.

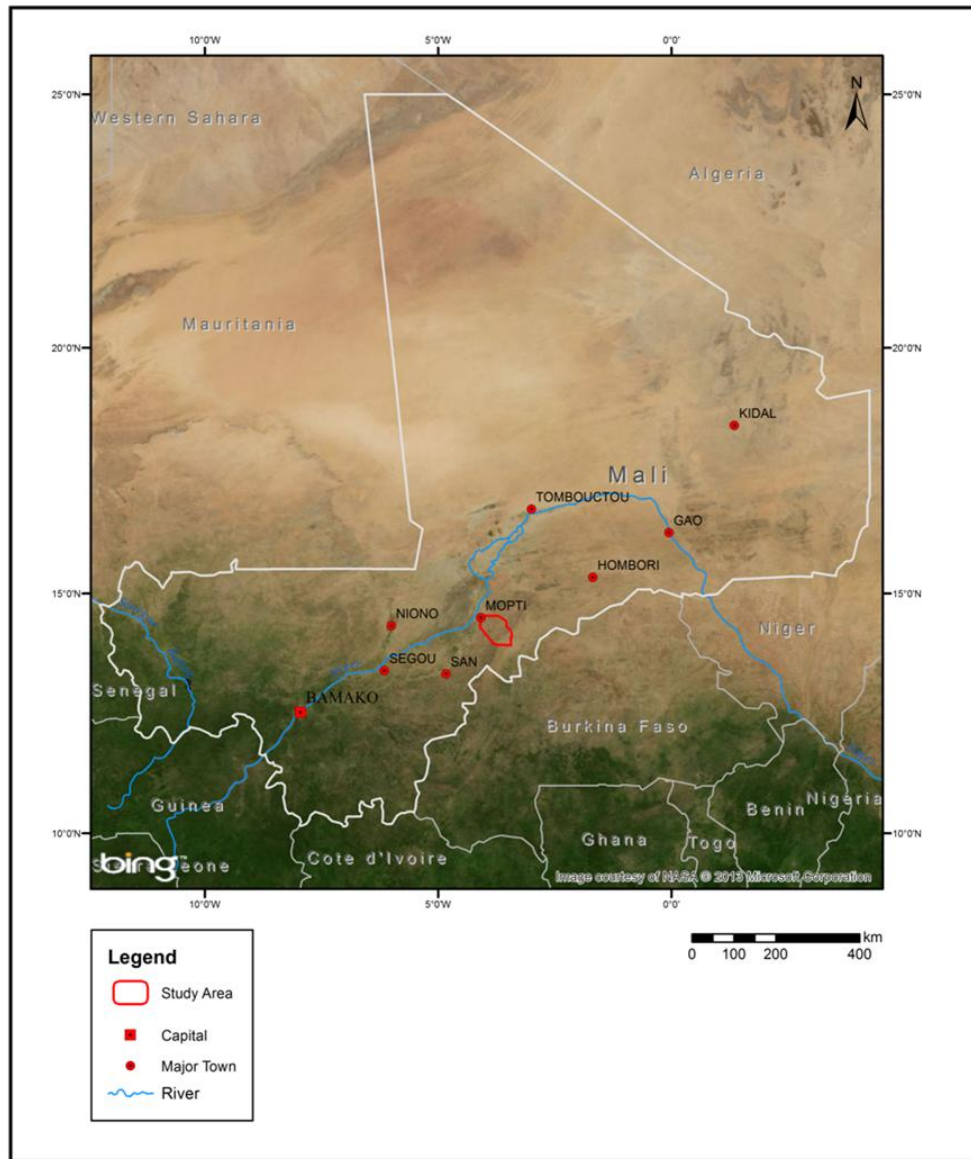


Fig. 2.1: Map of the study area in Mali. Source: © Bing maps: Microsoft Corporation and its data suppliers 2010. Cartography: Raphael Spiekermann.

The Seno Plains lie roughly 200 m lower than the plateau at an altitude of 200-300 m. The aeolian fossil dunes that lie parallel to the Bandiagara escarpment protrude up to 50 m higher than the surrounding plain and were formed during the Late Pleistocene (Nicholson & Flohn 1980). The population density has increased during the past decades, which has had a

significant impact on the land cover (see chapter 4). Almost all areas of the Seno Plains are used for agricultural purposes today. Soils are, for the most part, deep sandy-loam, and the relatively smooth topography of the plains means the arable land is most suited for cropping. As will be shown below, the dense natural vegetation of former times has largely been cleared and a stark reduction of vegetation species has accompanied this change.

As can be seen in Fig. 2.2, the Seno Plains differ in many ways from the landscape of the

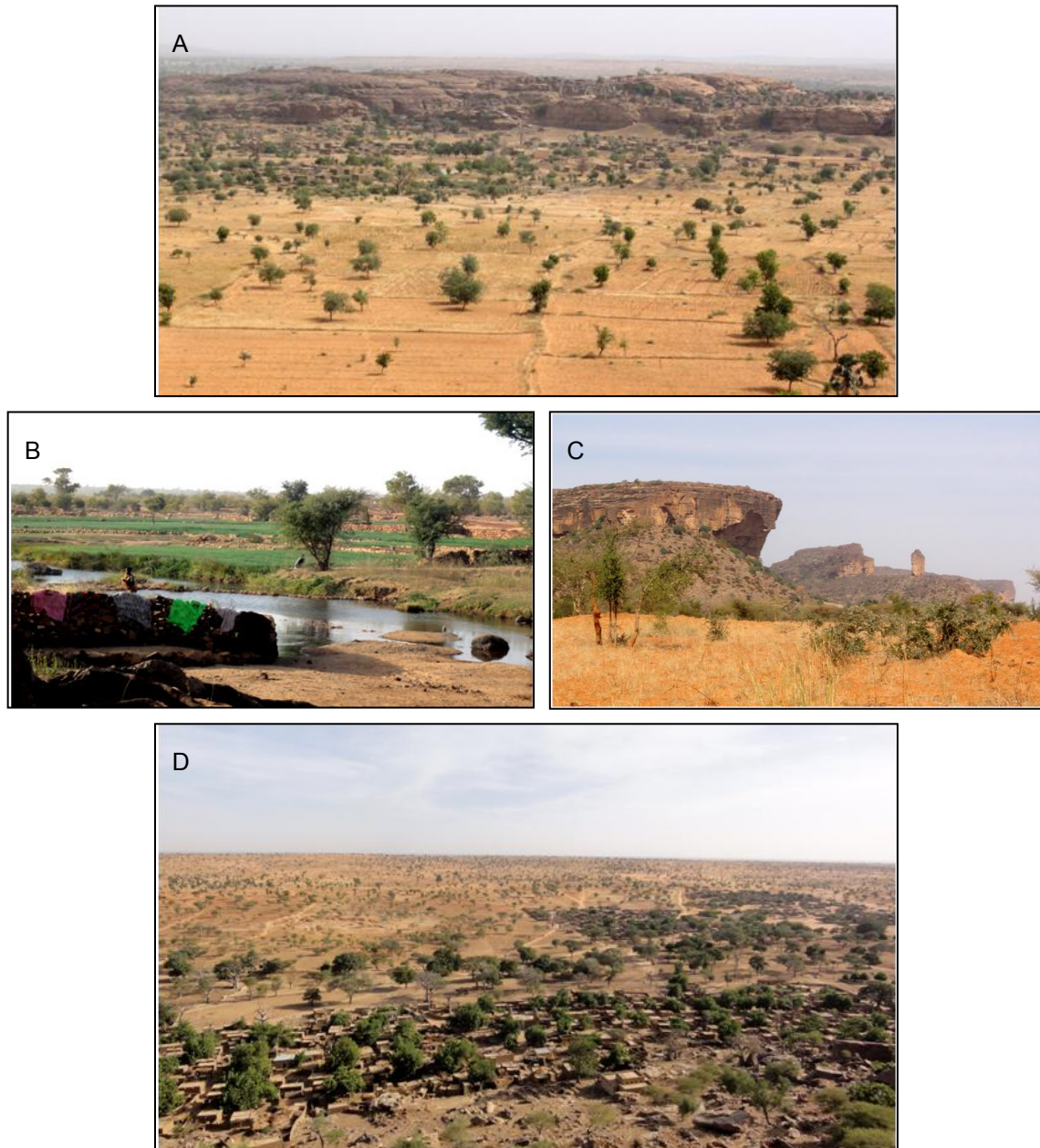


Fig. 2.2: A) View of Kowa, southwest of Sevaré on the Dogon Plateau, with surrounding fields; B) Onion plantations line the Yamé River, Dogon Plateau; C) Bandiagara Escarpment (La Falaise); D) View of the Seno Plains from the Bandiagara Escarpment.

Dogon Plateau, the morphology being the primary reason for this. The land use, vegetation cover and population density are all impacted by the complex and rough morphology of the plateau. For this reason, the analyses used in this thesis treat the plateau separately from the plains. Below a more detailed account of various environmental attributes of the study area are given, as well as a broader overview of the environment of the Sahel.

2.1 Climate

2.1.1 The Sahelian Climate

A challenging issue of environmental change research in the Sahel is defining the boundaries of the Sahel region. The ‘Sahel’ (Arabic for shore) is defined by Hermann *et al.* (2005 p. 394) as “a transition zone between the arid Sahara in the north and the (sub-) humid tropical savannas in the south, and is marked by a steep north-south gradient in mean annual rainfall”. Similarly Giannini *et al.* (2008 p. 119) uses climatic zones to the north and south to define the spatial extent of the Sahel, describing it as an area, which “stretches from the Atlantic coast of Senegal and Mauritania to the Red Sea coast of Sudan and Eritrea. It forms the southern margin of the Sahara desert, or alternatively, the northern margin of the region influenced by the northern summer African monsoon.” It thus seems that the Sahel is a very general term for the transition zone between the Sahara desert and the tropical savannas with fuzzy, fluid boundaries (which vary from year to year) and that are defined primarily by climatic factors. Often mean annual rainfall thresholds are used to set boundaries. The Millennium Ecosystem Assessment describes the Sahel region as the area between the mean 250 mm and the 900 mm isohyete, as can be seen in Fig.2.3.

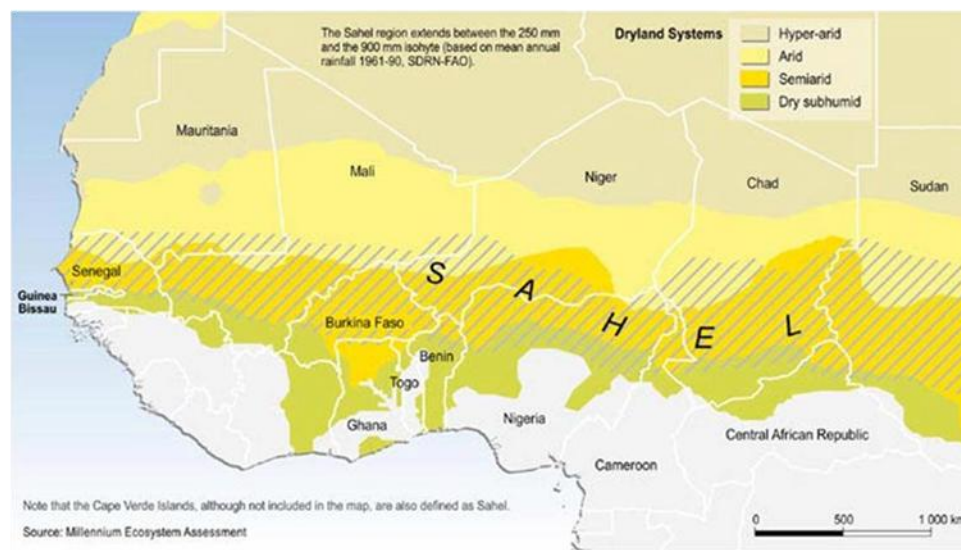


Fig. 2.3: Overview of the Sahel region as defined by climatic parameters. Source: Millennium Ecosystem Assessment.

As an alternative to average annual precipitation, Hermann *et al.* (2005) as well as Tucker *et al.* (1991) derived a definition from a 20-year-annual NDVI with boundaries set at a minimum NDVI of 0.15 and a maximum of 0.4, which “corresponds to the region with the steepest north-south gradient in vegetation greenness” (Hermann *et al.* 2005 p. 397). It is interesting to see that both rainfall and the NDVI as a proxy for vegetation are used independently of each other to define the boundaries of the Sahel. Furthermore, both rainfall and precipitation have a strong north-south gradient up to a certain point. As will be shown below, the Sahel is characterized by the strong dependency of the vegetation on the rainy season, with precipitation being the primary natural determining factor for vegetation greenness. I would therefore propose that a natural form of deriving boundaries for the Sahel would simply be the area where a significant relationship between long-term trends of NDVI and rainfall exists. Fig. 2.4 displays the results of a correlation between monthly NDVI and 3-month sums of rainfall for the months July to October by Huber *et al.* (2011). The strength of the correlations falls away both to the north as well as to the south. This can be explained by the non-existence of vegetation in the Sahara desert to the north (as well as no significant rainfall amounts) and in the tropical south other determining factors are more important than rainfall.

As mentioned earlier, the climate of the Sahel is very dynamic and is very much responsible for the unique environment of the Sahel. The Sahelian ecosystem is very much governed and controlled by the unpredictable climate, especially the variations of precipitation at all time scales (Hermann *et al.* 2005). The lack of regular precipitation, limited to a three to four month rainy season, mean all forms of life must adjust to the harsh reality of the climate. The climate is thus the main reason for the uniqueness of the Sahelian ecosystem, at the same time increasing its vulnerability to change, given the dependency on the little annual precipitation. The climate of the Sahel can be characterized by its strong seasonality with a long dry season and a shorter humid season (July to October). The seasonal differences are influenced by major fluctuations of rainfall at interannual and –decadal time scales (Hermann *et al.* 2005).

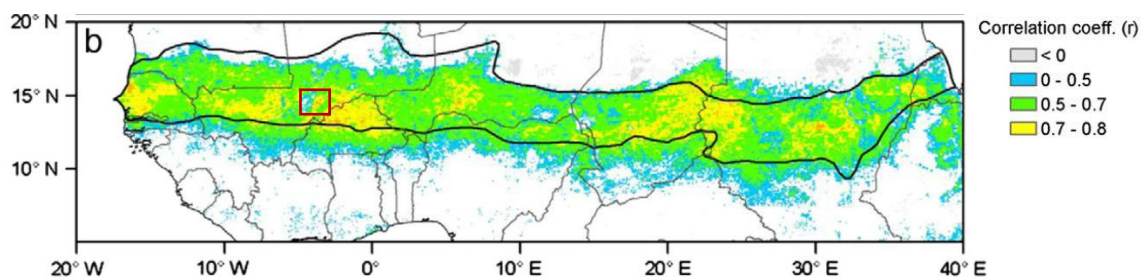
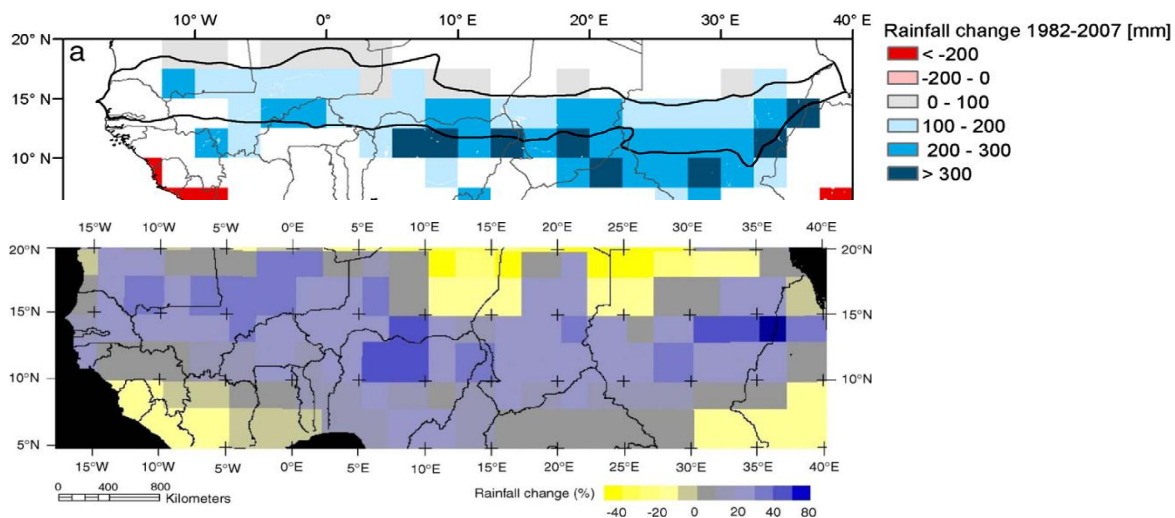


Fig. 2.4: Linear correlation between monthly NDVI and 3-month sums of rainfall for the months July to October – a suggested definition for the Sahel; The red box shows approximate location of the study area. Source: Huber *et al.* 2011.

The seasonal variations are caused by the Sahel's relative position to major global and regional circulation features and the seasonal variation of tropical weather patterns. The striking deviations of rainfall amounts at interannual and –decadal time scales is more difficult to explain because of the increased complexity with so many factors involved. However several probable causes can be identified: For one, sea surface temperature anomalies in the Pacific have shown to be a causative factor as well as an indirect influence of the El Niño Southern Oscillation cycles (Hunt 2000). Major land cover change and the impact of this on land–atmosphere interactions are also hypothesized to influence rainfall variability (Giannini *et al.* 2008).

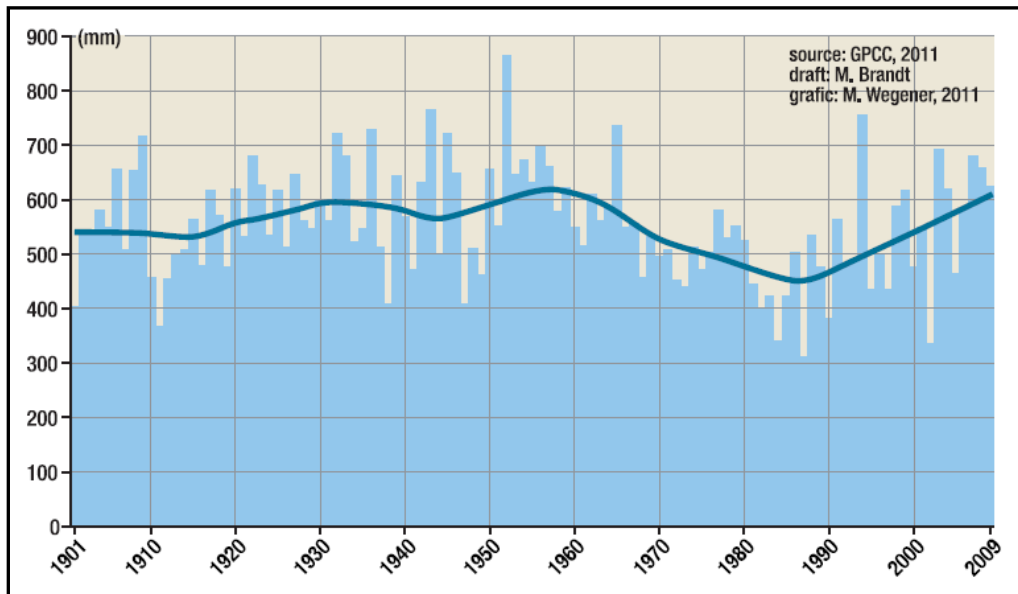
Significant spatial differences of rainfall amounts in the Sahel overlay the variability in time. Fig. 2.5 displays two maps by Huber *et al.* (2011) and Hermann *et al.* (2005) showing the overall trends in monthly rainfall in the Sahel from 1982-2007 and 1982-2003 respectively. The graphs, although based on the same dataset, show two rather different results, though the general pattern shows a broad increase of rainfall throughout the Sahel with up to 300 mm in northern Nigeria, which corresponds to an overall increase of around 60%. The dissimilarities of the two maps allow the results of the trend analyses to be questioned. Huber *et al.* (2011) suggest that differing trend analysis methods and time coverage are responsible for conflicting results. Further studies, in particular at regional scales, are required to achieve greater understanding of significant variability of rainfall amounts in the Sahel in space and time.



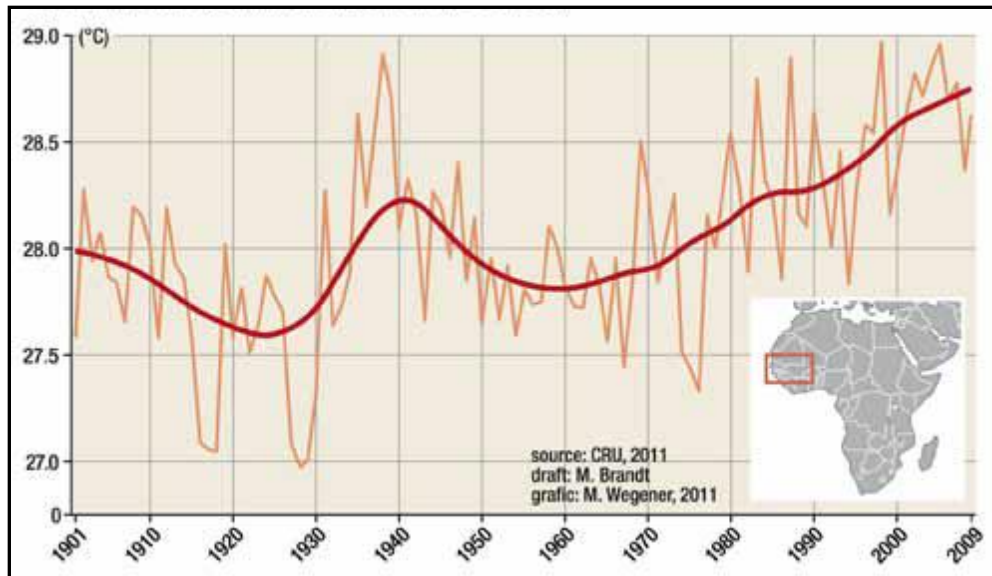
2.4: Above: Overall spatio-temporal trends of rainfall based on annual sums (average change in mm) from 1982-2007. Source: Huber *et al.* 2011. Below: Overall trends in monthly rainfall (average change in %) for the period 1982-2003 based on GPCP estimates. Source: Hermann *et al.* 2005.

2.1.2 The Climate of the Study Area

The study area is located well within the boundaries of the Sahel and can thus be attributed with its typical arid to semi-arid climate. The Mopti region is covered in part by the North Sudanian zone (550-750 mm of average annual rainfall) and also by the Southern Sahel zone (350-550 mm average annual rainfall) (Yossi & Diakité 2008). In general, the study area receives an average of 500-600 mm of annual precipitation, which mainly falls during the months of June to October. Fig. 2.6 also shows the interannual and –decadal variability of rainfall with a noticeable increase since the mid-1980s. One may argue that the rainfall amounts are back to pre-drought conditions, however the interannual variability seems to have increased significantly. The positive trend of the past thirty years seen in Fig. 2.6 also corresponds roughly to increase of 200 to 300 mm or 30-40% respectively shown in the maps of Fig. 2.5. The same trend is also displayed in the graph in Fig. 2.6 for the study area. Floods are also fairly common during rainy months and 50,000 inhabitants were affected by flooding in Mali in 2007 (Samimi *et al.* 2012), including many inhabitants of the study area. Similarly, the entire Western Sahel has seen a considerable rise of average annual temperature, as displayed by Fig. 2.7 showing the mean annual temperature for the Western Sahel from 1901 to 2009. Reports from locals within the study area suggest that the effects of increased temperatures are noticeable at a local level (Romankiewicz & Doevenspeck 2011), however farmers note that the distribution of rainfall throughout the season is of far greater importance (Brandt *et al.* in review). Little research is concerned with rainfall variability and its impact at monthly and daily time scales. The reason for this is simply the lack of long term daily and monthly precipitation records in Sahelian countries.



2.5: Annual precipitation (1901-2009) for Bandiagara. Source: M. Brandt.



2.6: Average annual temperature (1901-2009) for the West Sahel. Source: M. Brandt.

2.2 Vegetation and Land Use

The land use within the study area is dominated by a combination of agroforestry and livestock management. In the study area, the Dogon ethnic group is traditionally known for its mixed crop cultivation within the bounds of an agroforestry system. Often, the Dogon work closely with nomadic Fulbe farmers, another major ethnicity of the region. The Dogon have a long tradition of working the fields and farmers generally know which soil types are favourable, which trees are desirable on fields and when to sow their fields in accordance with seasonal weather changes. Similarly the Fulbe are renowned for their animal husbandry skills. Mostly nomadic Fulbe farmers of cattle and goats graze on grasslands in the wet season and within areas of dense vegetation where the stock may also feed on trees and shrubs as they pass through. As the dry season gains severity, the herds are driven to the Niger Delta, where the animals graze for the remaining dry season. Small herds remain on the plateau and feed off the green woody vegetation, again underlining the importance of the woody vegetation within the agroforestry system.

Agroforestry systems encourage scattered growth of useful trees selected by the farmer on arable farmland used for cultivation purposes. Agroforestry techniques offer many advantages compared to cleared farmland, as described by Kandji *et al.* (2006 p.35):

“The effects of different agroforestry techniques in enhancing the resilience of agricultural systems against adverse impacts of rainfall variability, shifting weather patterns, reduced water

availability, soil erosion as well as pests, diseases and weeds have been well documented. A successful and well-managed integration of trees on farms and in agricultural landscapes results in diversified and sustainable crop production, in addition to providing a wide range of environmental benefits. Some of the mechanisms through which agroforestry practices may improve the resilience of agroecosystems in the occurrence of extreme climate are improved microclimate and reduced evapotranspiration.”

Most of the predominant tree species in the Sahel have deep root-systems and are capable of reaching the water table, which commonly lies 40 m below surface during the dry season (Huber *et al.* 2011). Thus Sahelian trees are much less sensitive to intra- and interannual variations in rainfall. The trees provide the basis for life in the rural Sahel as they represent the only form of vegetation that can survive prolonged periods of droughts and perform multiple functions for the Sahelian population including enriching soils to ensure a productive harvest. Table 2.1 lists a few of the main species found in the study area and their corresponding site requirements and uses. A great example of a multipurpose tree is the *Acacia albida*, as it not only has a role in



2.7: Intensive use of bark and wood of *Balanites aegyptiaca*, Seno Plains. Source: R. Spiekermann.

tribal customs and traditional law, but also in site improvement (by shedding nutrient-rich leaves at the beginning of the vegetation period), forage production for livestock and the wood is soft and easy to work with for the production of cooking utensils and so forth (Maydell 1990). The *Balanites aegyptiaca* is one of the many trees with medicinal uses, the fruits are also popular. The bark and roots are used as laxatives; the bark may also be consumed against stomach-ache, epilepsy, yellow fever and syphilis just to mention a few (see Table 2.1 for further uses). In general, farmers know their trees well enough to use them effectively without causing long-term damage to these hardy species. Fig. 2.8 shows a *Balanites aegyptiaca* on the Seno Plains, exemplifying typical usage.

Table 2.1: Selected examples of multi-purpose trees in the Sahel with site requirements and uses. Source: Maydell 1990.

Botanical name	Site requirements	Uses
<i>Acacia albida</i>	Very adaptable, growth under 300 mm and up to 1800 mm, survives dry periods of up to several years, as well as several weeks of inundation; tolerates wide range of temperatures; Mainly species of alluvial plains. No particular soil structure or nutrient requirements, but needs a relatively high water table.	Multipurpose tree: role in tribal customs and traditional law; site improvement by shedding nutrient-rich leaves at the beginning of the vegetation period, supplemented by a concentration of animal dung under the canopy as livestock assemble under tree crown; Forage production; wood is soft and easy to work; bark contains tannin, wood ashes used for soap, seeds are sometimes eaten, also medicinal uses.
<i>Acacia senegal</i>	Drought resistant, annual rainfalls between 100 - 800 mm, mainly 200 - 400 mm with dry period of 8-11 months. Tolerates very high daily temperatures, dry winds and sandstorms but no frost. Prefers sandy soils, fossil dunes very suitable, also slightly loamy sands; altitudes vary between 100 - 1700 m a.s.l.	Produces 90% of commercial gum arabic (very high quality). Natural hydrocolloid with solutions up to 50% gum content. Medicinal uses: to treat gastritic disorders, haemorrhage, ophthalmia, colds, diarrhoea, aphrodisiac. Further uses: nectar for bees, forage for livestock (esp. pods).
<i>Balanites aegyptiaca</i>	Drought resistant and not damaged by grass fires, grows of very different soils with annual rainfalls between 200 and 800 mm. Grows well in valleys and on river banks, in depressions, on the foot and slope of rocky hills, up to 1500 m a.s.l.	Wood is widely used for saws and planestool handles, bowls, posts, mortars and pestles and many household and agricultural implements as it is insect-resistant, hard, tough and heavy. Excellent fuelwood, and highly esteemed for charcoal. Thorny branches commonly used for fencing. Young leaves, sprouts, green thorns and fruits are eaten by all livestock and wildlife. Lopping is widely practised and trees regenerate readily after lopping or heavy browsing. The fruit is edible, the cellulosic shell of the fruit is a source of fuel, the kernel supplements food products. All parts of the plant yield sapogeninsdiosgenin and yamogenin, both used in partial synthesis of steroid drugs. Many medical uses: bark and roots as laxatives or tranquilizers, bark against stomach-aches, sterility, mental diseases, epilepsy, yellow fever, syphilis, and as vermifuge. Fruit and leaves, esp. kernel oil applied for rheumatism, bark extracts for toothaches.

The Seno Plains also has a very particular vegetation pattern. Trees are interspersed on fields almost at random, as it is uncommon for farmers to plant trees; rather trees favoured by farmers are left to grow and protected. These include *Acacia albida*, *Balanites aegyptiaca*, *Acacia senegalesis*, and *Adansonia digitata*. The fields are used either for agricultural purposes during and directly following the rainy season or as grazing land spread out between the trees, demonstrating the integration of agriculture, forestry and livestock. Fig. 2.2-D offers an example of the typical vegetation pattern on the Seno Plains of Mali.

Although the trees of the Sahel are, for the most part, very adaptable to fluctuations of rainfall, assisted by deep root-systems, vegetation growth is strongly dependent on precipitation. Huber *et al.* (2011) explore rainfall and modelled soil moisture as a principal determinant of Sahelian vegetation dynamics, using remotely sensed NDVI as a proxy for the vegetation greenness response. Their findings show a very strong linear correlation between monthly NDVI and 3-month sums of rainfall for all months per year (Correlation coefficients (r) up to 0.9-1); although it may be argued that the NDVI here mainly reflects the impact of rainfall on grass growth. The vegetation is however even more dependent on land use and human impact than by fluctuations

of precipitation. Various projects within the study area show the positive impact man may have on tree growth. The area around Bankass has particularly benefited from input by projects such as SahelEco (SahelEco website - access 01.03.2013) and many protected sites with dense tree growth exemplify the capabilities of trees to survive years with little rainfall and flourish in the long-term.

2.3 Soil

The arable land on the Dogon Plateau is dominated by silty sandy soils. Non-arable land is partially suitable for agricultural production and is dominated by shallow soils on lateritic rock. These soils have a very low capacity of water storage (see Table 2.2). The plateau also has a considerable amount of areas consisting of bare rock surfaces, which are highly unsuitable for any form of agricultural production. Soils on the Seno Plain are comparatively infertile and either sandy-loam soils or very sandy dune soils. (Yossi & Diakité 2008)



Fig. 2.8: Soil sample location: Cropping field southeast of Diamnati, Dogon Plateau. Source: R. Spiekermann.

Table 2.2 presents laboratory results of two mixed samples collected during the field trip from a field just east of the village of Diamnati on the Dogon Plateau. This field is of superior quality and well tended to, as several large *Acacia albida* and the mounds caused by ploughing prove (see Fig. 2.9). Millet is the main cereal that is sown here and the samples were taken in December 2011 following the harvest in dry conditions. The grain fraction shows the large proportion of sand with an average of 82% and only a small fraction of silt. This has obvious consequences for the water storage with a maximum water capacity of 9.60 % of dry mass.

Table 2.2: Soil analysis results of 2 mixed samples from fields on the eastern outskirts of Diamnati.

Sample	Diamnati 1	Diamnati 2
Depth in cm	50	50
Colour in max. water capacity acc. MUNSELL	7.5 YR 4/6	7.5 YR 4/6
Clay (< 2 μ) in %	0.76	5
Silt (2 μ - 63 μ) in %	3.77	25.94
Sand (0,063 - 2mm) in %	95.47	69.06
Soil sediment-type	S	S
CaCO ₃ in % DM	0.18	0.14
pH - value 0.01 mol CaCl ₂	4.16	4.35
Organic substance in % DM	2.436	2.749
WM fresh in % DM	0.74	0.45
WM RD in % DM	0.08	0.06
WM max WC in % DM	9.76	9.43
θ_v fresh in % volume	2.47	1.55
θ_v max. WC in % volume	32.98	31.85
ρ_s in g/cm ³	2.54	2.5
ρ_w in g/cm ³	1.64	1.66
ρ_d in g/cm ³	1.62	1.64
SV in %	63.79	65.55
GPV in %	36.21	34.45
LV in %	33.74	32.9
WV in %	97.53	98.45

3. Methods

3.1 Datasets and Data Problems

This chapter intends to explore the datasets available for studies, which focus on the analysis of vegetation trends and the environment. As seen in the introduction, many environmental studies have been carried out by various research institutes world-wide. These remote-sensing studies are in part responsible for both the “desertification debate” and the “greening debate”, as they monitor vegetation trends over the entire Sahel for various periods of time since the beginning of the 1980s. Table 3.1 offers an overview of the most commonly used multi-temporal datasets that use the NDVI as a proxy for vegetation to analyse the vegetation trends. Each dataset has a specific spatial resolution and period of availability. It can be seen that there are many pros and cons related to each dataset and the right dataset needs to be selected depending on the aim and extent of the study. As mentioned above, the analysis of vegetation dynamics for the entire Sahelian zone is commonly based on the GIMMS NDVI time series (Tucker *et al.* 2005). The dataset contains 15 day maximum NDVI values at a spatial resolution of 8 km, and is available for a 25 year period from 1981 to 2006. It has many advantages over other datasets; not only because it is a pre-processed dataset with no further need of calibration or major forms of pre-processing, but also the modelling and computer calculations at a greater spatial resolution than 8 km for an area the size of the Sahel would require an ever increasing processing capacity. As will be seen below, the spatial differences of vegetation dynamics are much greater in reality, thus the coarse resolution of the datasets represents a clear source of error. However, studies such as that of Hermann *et al.* (2005) are important for monitoring purposes and raising awareness in the scientific community of changes to the environment. They thus represent an impulse for more detailed studies and exploration of explanations for change.

Table 3.1: Coarse resolution multi-temporal datasets used to assess vegetation dynamics in the Sahel.

	MODIS	SPOT VGT	LTDR	AVHRR	GIMMS
Resolution	250 m	1 km	~5 km	1 km	8 km
Period	Since 2000	Since 1998	1981 – 2000	Since 1987	1981-2006

Before detailed remote sensing studies at tree level as well as studies that include field work are carried out, explanations for change can only be hypothesized. A range of high resolution datasets available for such studies are displayed in Table 3.2. As can be seen, the attributes of

the datasets are very different. The ground resolution of older satellite images such as Landsat and older SPOT images are fairly poor compared to the most recent imagery available such as World-View2 or GeoEye-2. The prices of very high resolution images are however proportionate to the resolution. Depending on the available budget, size of the study area, processing capacity and last but not least, the study aim, the product selection marks an important process of all research projects. For the purpose of this study, the datasets described in chapter 3.2 are selected, primarily due to the period the images are available for and their (relatively) low cost, besides the fact that the images have the characteristics necessary for serving their purpose of achieving research aims.

Table 3.2: High resolution datasets capable of assessing land cover and woody vegetation change in the Sahel.

Satellite	Ground MS Resolution (m)	Period	No. bands	Cost
Corona KH-4B	1.8 (Pan.)	1963-1969	1	\$US 30/scan
Landsat	30	1978 - on-going	4-6	Free of charge
SPOT	8	1986 - on-going	4	\$US 8700/scene (60 x 60 km)
RapidEye	6.5	2009-2015	5	\$US 1.28/km ²
World-View2	1.8	2009 - on-going	8	min. \$US 32/km ²
GeoEye-2	1.4	2013 - on-going	4	\$US 25/km ²
Quickbird	2.4	2001-2008	4	min. \$US 32/km ²
IKONOS	4	1999 - on-going	4	\$US 20/km ²

3.2 Image Data and Pre-processing

This chapter will introduce the datasets used for the study as well as describe the data preparation process. In order to assess the changes of tree density, the two datasets listed in Table 3.3 are used. The Corona dataset required thorough preparation in form of georeferencing and photogrammetric processing before further analyses was possible. The RapidEye dataset also needed slight adjustments in horizontal positioning, although delivered with a reference system so that the RapidEye and Corona datasets had the same horizontal positioning, a necessity for spatial comparisons. As Table 3.3 shows, the two datasets differ in many ways. The following two chapters will take a closer look at the datasets used for the land cover and woody vegetation feature extraction of this study. At this point, it should also be noted that, depending on the context, the word “trees” within the bounds of this study may often be used to denote and include all forms of (large) woody vegetation.

Table 3.3: Specifications of satellite images used for the study.

Dataset	Corona KH-4B	Rapid Eye
Date	December 1967	December 2011
Spectral bands	Panchromatic (Grey-scales)	Multi-spectral (Blue, Green, Red, Red Edge and Near-Infrared)
Geometric resolution / resample size	1.8 m / 2.0 m	6.5 m / 5.0 m
Ortho-corrected, projected	No	Yes

3.2.1 Corona Imagery

Corona images belong to the very first U.S. photo intelligence satellites that surveyed the earth's surface and include a collection greater than 860,000 photographic images of the period 1960 – 1972. The three classified military satellite systems were code-named CORONA, ARGON, and LANYARD. The images were to provide detailed aerial coverage of foreign powers, in particular of the former Soviet Union during the Cold War, to the intelligence agencies of the United States. A telescopic camera system attached to the satellite was responsible for taking the photos prior to loading the film into a capsule. The camera was designed to jettison the exposed films within the capsule back to earth over Hawaii, equipped with a parachute so that a plane could snatch it in mid-air. In 1992, the images were evaluated by the Environment Task Force, which concluded that the images posed no threat to national security and could therefore be declassified to assist in particular with global change research. (USGS 2011)

The satellite which was responsible for photographing the study area in Mali in December of the year 1967 was named Corona KH-4B and was operational for the period September 1967 to May 1972. The Corona KH-4B was equipped with two panoramic rotator cameras with a focal length of 61 mm and a ground resolution of 1.8 m. The images used for this study were taken on 10th December 1967. This particular mission (code KH-4B 1102) was launched on 9th December 1967 at the Vandenburg Airforce Base in California. (NASA)

A section of one of the Corona images used may be viewed in Fig. 3.1. Although the image is black and white, i.e. grey-scaled, a remarkably large amount of detail may be extracted. The black circular and oval shapes indicate the location of trees or shrubbery and a village can also clearly be identified. Furthermore, the differing shades of grey of the fields refer to various uses of these areas. The lighter greyscale shades signify an area of bare soil. As the photographic image was taken in December, i.e. directly following harvest time, it may be assumed that the lighter areas represent cropland. The darker areas in the upper right of the cropped image in Fig. 3.1 are most likely fallow covered by grass and perhaps low-lying shrubs. By interpreting the

Corona images in this way, much detailed information regarding land cover and woody vegetation may be extracted from these images for the study area. Studies that make use of the historic Corona images to assess changes to land cover include Ruelland *et al.* 2010, Reij *et al.* 2005 and Tappan *et al.* 2004.

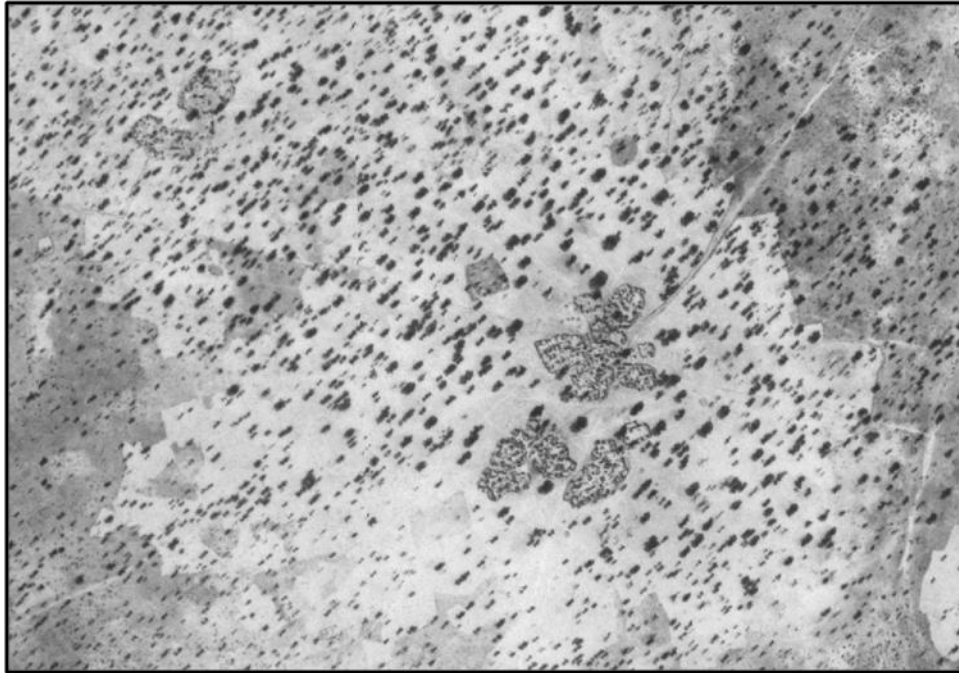


Fig. 3.1: Section of a Corona image December 1967 providing detailed information on the landscape. Source: Corona 1967.

The Corona images for the study area encompass an area of 3621 km² of the study area. These panchromatic images may be acquired for 30 U.S. dollars per scanned frame for research purposes from the U.S. Geological Survey, however lack position data or any form of orthorectification. All twelve images used for this assessment thus needed to be georeferenced - a very time-consuming process as for each image multiple control points are needed.

This is done using ERDAS IMAGINE (Raster – Panchromatic – control points – polynomial – keyboard only) and GoogleEarth®. Control points are found using simultaneous viewing mode with two screens in order to identify the exact same locations in both GoogleEarth® and on the respective Corona image within ERDAS Imagine. Points are marked in GoogleEarth® and coordinates extracted in form of the Universal Transversal Mercator coordinate system (UTM) and imported into ERDAS IMAGINE from a text file. For each Corona image (12 images) between 30 and 50 control points are required to obtain good results. Although it is understood that the position data provided by GoogleEarth® often has significant discrepancies compared with position data provided by other data sources (Becek & Ibrahim 2011), no other high

resolution images (requirement for finding accurate control points) are freely available. At this point an application for RapidEye images had not yet been made. The search for control points is particularly difficult due to the relatively homogeneous landscape and lack of permanent infrastructure and landmarks. Thus control points need to be chosen not only at intersections and at buildings, where one cannot even be sure no changes have occurred in the past fifty years, but also at edges of rocky outcrops and large trees which are judged to be old enough according to size and by an initial comparison with the relative position to other objects and secondly, with today's high resolution images.

Several geometric models are tested for the Corona images and it is proven that the rubber sheeting (linear) method provides the most accurate results. Furthermore, the nearest neighbour method is chosen as the resample method, rounding the input cell size to 2 m. It cannot be avoided that the images become somewhat distorted along the edges, and that the results of the georeferencing differ somewhat spatially, i.e. the accuracy varies slightly from one area in the image to another. The accuracy of each image is assessed visually with an overlay of RapidEye images. Additional control points are added until the respective image is judged to be as accurate as possible given the resolution and spatial extent of each image. The 12 Corona images often overlap each other so that the same control points could be used for the areas of the two images that overlap. This ensures that the images are spatially coherent. Fig.3.2 shows all the control points used in GoogleEarth® for the twelve Corona images. It should be noted that only ten of the twelve images are needed, after comparing the coverage of the RapidEye images, which were acquired at a later date.

A mosaic of the twelve Corona images is created for easier and simpler management of the data for further analyses. For this purpose, MosaicPro in ERDAS IMAGINE is applied.

The final step is to clip the images to the study region, whereby areas in the Seno Plains that extend further south than the RapidEye images are included in order to obtain a more conclusive impression of the situation of the Seno Plains in 1967 in regard to land cover and tree density. Furthermore the datasets are split in two regions according to the morphology (plateau and plain) to simplify procedures for the land cover and woody vegetation assessments. The morphology, as has been shown in the introduction, has a major impact on both land cover and tree density, which is why the morphology also influences the spectral information of the datasets. This means a different approach of mapping on the Dogon Plateau and the Seno Plains is necessary, as will be shown below.

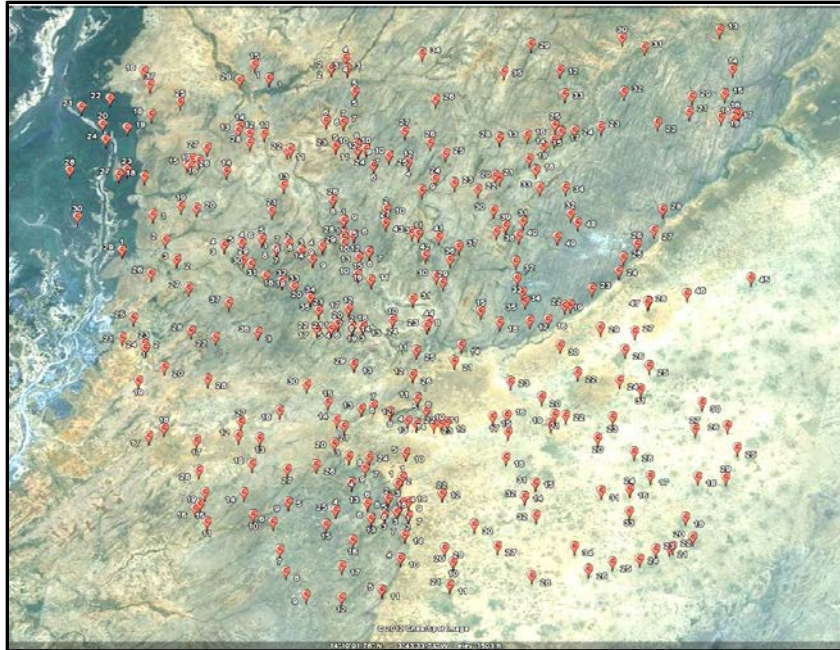


Fig. 3.2: Control points used for georeferencing the 12 Corona images. Source: © GoogleEarth® Cnes/Spot image 2012.

The Subset and Chip tool in ERDAS IMAGINE is used for this purpose and proved to be a much more reliable and stable clipping tool than that of ArcGIS or Quantum GIS. The result of georeferencing and mosaic-building is seen in Fig. 3.3. The plateau can clearly be distinguished from the plains, the border, i.e. the Bandiagara escarpment, cutting through the image very sharply. A gap in the Seno plains means that the coverage in 1967 is not entirely complete. Several major towns and the main roads are also given. The two case study sites, Diamnati and Diambara (often spelt *Tiembara*), are also displayed.

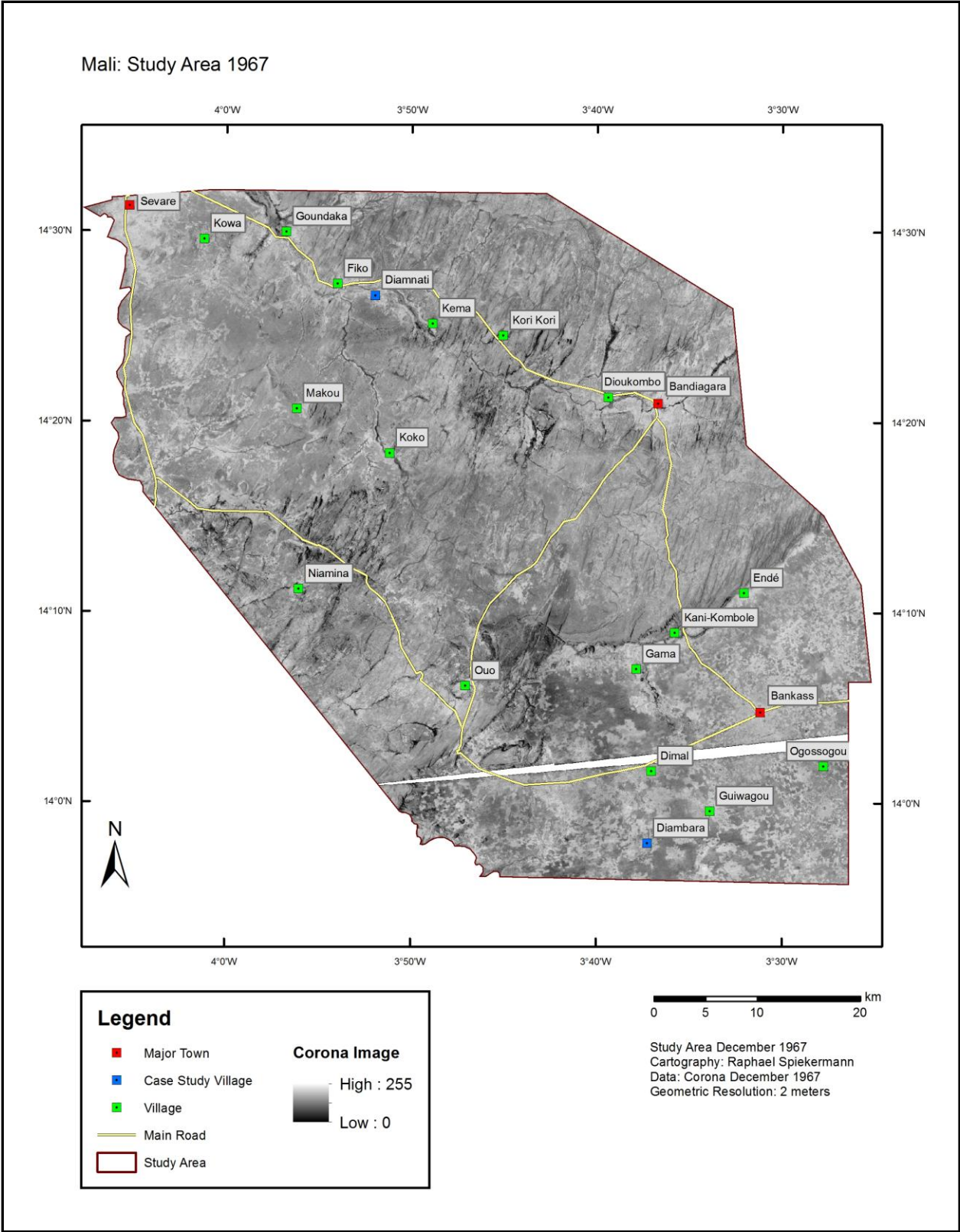


Fig. 3.3: Study area 1967: Result of the Corona image processing and data base for all further analyses for the year 1967.

3.2.2 RapidEye Imagery

RapidEye imagery form the product of a constellation of five satellites that are each equipped with a 5-band (VIS, 6.5 m multi-spectral push broom sensor (images are orthorectified and resampled to 5 m resolution). The satellites have been operational since February 2009 at a sun-synchronous orbit (altitude of 630 km) and are capable of capturing five million km² of imagery per day (swath width of 77 km) with daily revisits possible. For the purpose of the analyses carried out in this thesis, the high resolution multi-spectral images of RapidEye provide a dataset to assess the situation in the study area for today and cover a total area of 3501 km² within the study area. The question whether or not an orthorectified pixel size of 5 m would be sufficient to identify and map individual trees and woody shrubs on the ground in such a way that the results can be compared to the results of the tree mapping in the Corona images remains to be seen. The advantage of the RapidEye images obviously lies in its multi-spectral characteristics in combination with its moderate high resolution. This allows vegetation indexes, such as the normalized vegetation index (NDVI) to be used for identifying the ground cover more easily, as well as enabling object-based analyses to be carried out. Several remote-sensing studies using RapidEye images are listed on the RapidEye homepage and include object-based, automatic change-detection studies (Hese *et al.* 2010 and Nielsen *et al.* 2010) as well as land cover classifications (e.g. Förster *et al.* 2011). No studies could be found using RapidEye imagery to detect and map individual trees and other forms of woody vegetation. This is probably due to the fact that the RapidEye dataset is fairly new and other very high resolution datasets (e.g. GeoEye-1 and IKONOS products) may produce more accurate results, however are very cost-intensive compared to RapidEye products, not to speak of the hardware components needed to use such datasets for the large study area in Mali.

The RapidEye images used here were acquired from the RapidEye Science Archive (RESA) and provided by the Deutsches Zentrum für Luft- und Raumfahrt (DLR) free of charge. For the study area in Mali, two images are selected, which correspond to the dates spent in field, more importantly after harvest and while the woody vegetation remains very green. The image covering almost the entire study area is dated 26th December 2011 (made up of 13 sub-images) and is displayed in Fig. 3.4 (code-named for further reference as RE-D-26122011 for the Dogon Plateau section and RE-S-26122011 for the Seno Plains section). The second image covers only a small section in the northwest of the plateau and dates 7th December 2011 (code-named RE-D-07122011). The RapidEye images were delivered as digital numbers (DN) and then converted to reflectance values. Furthermore, an atmospheric correction is made using the FLAASH module (Fast Line-of-sight Atmospheric Analysis of Spectral Hypercubes) in ENVI.

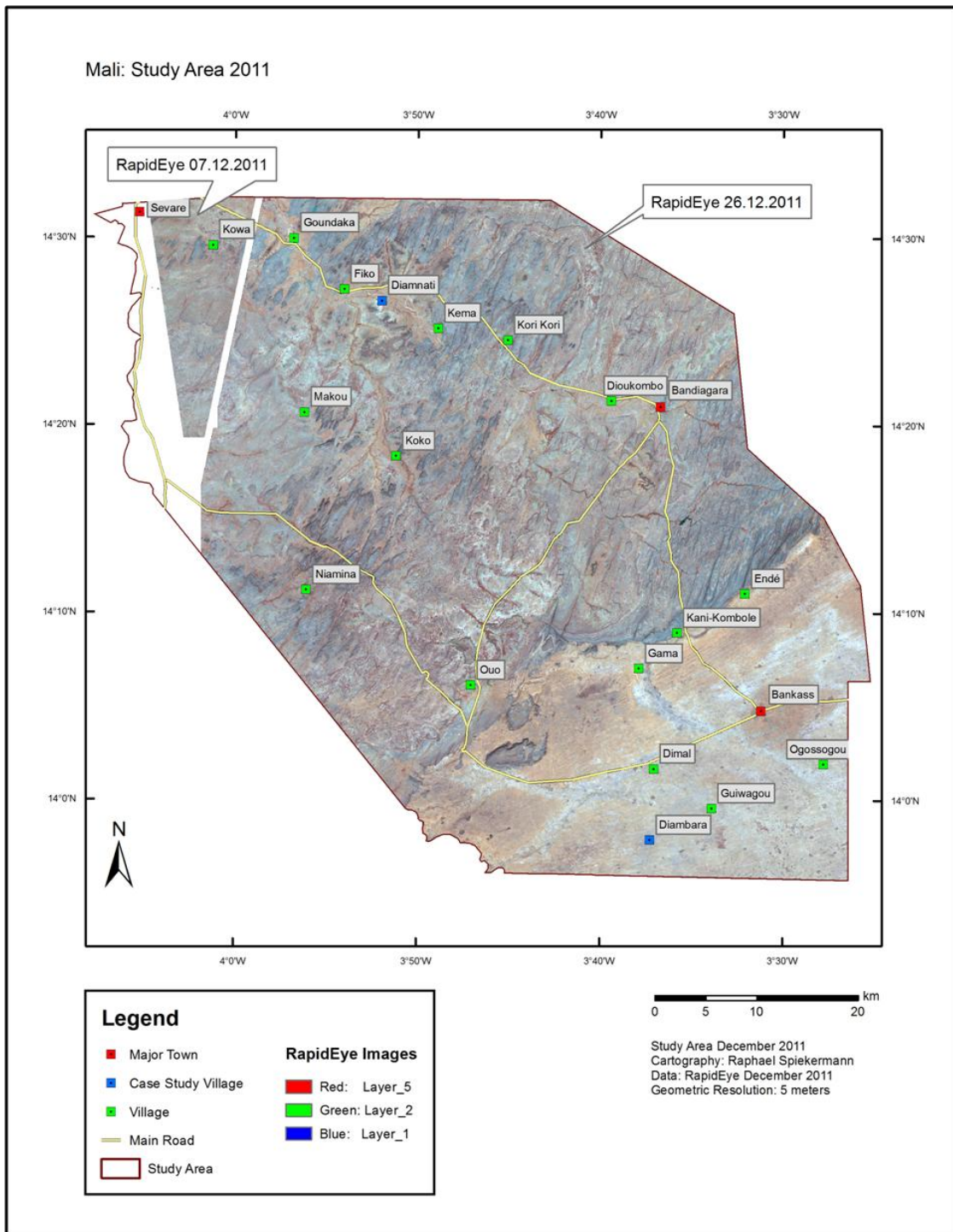


Fig. 3.4: Study area 2011: RapidEye images and data base for all further analyses for the year 2011.

Before any analyses with the respective datasets can be carried out, one must verify whether or not the two datasets, which differ greatly in resolution, quality and coverage, have a horizontal positioning accurate enough to allow spatial analyses and comparisons to be carried out. Slight adjustments needed to be made after thorough on-screen visual inspection of the images (in

particular RE-D-07122011) because spatial disparities up to 30 m were detected, which at a resolution of 5 m is regarded as too high. The result is very good for the most part with large trees and roads and other forms of infrastructure forming the basis for a visual inspection. It may be said that the maximum difference of spatial positioning is ca. 20 m, although the two datasets largely correspond with one another more accurately than that. The coverage of the datasets also differs so that the “common ground” of the two datasets more or less lead to the formation of the border of the study area, as is seen in Fig. 3.4.

3.2.3 Field Data

Time spent in the field is often essential for remote sensing studies, as many forms of knowledge and understanding of processes and phenomena seen on-screen simply cannot be found sitting at a desk. A thorough validation and interpretation of results should always have field work at its basis, otherwise the worth and benefit of such studies remains unknown. Thus a six week field trip was undertaken during the period November to December 2011 together with Martin Brandt and Clemens Romankiewicz (PhD students at University of Bayreuth).

During the field trip many sites of interest were visited. These sites were pre-selected based on environmental trends that were detected using NDVI time series such as LTDR, MODIS and SPOT VGT (Brandt *et al.* 2012). Brandt *et al.* (in review) and Brandt *et al.* 2012 offer first results of the field trip, showing the importance of working at various spatial scales in environmental remote sensing studies and the advantage of an interdisciplinary approach. At multiple sites on the Dogon Plateau and Seno Plains vegetation surveys were carried out as follows:

Each surveyed site had to be homogeneous in nature as far as the land cover and land use is concerned. A handheld GPS noted the coordinates of the starting point of the survey. All shrubs and trees were then assessed approximately 25 meters to the left and right of a straight line, usually 100 m in length. The area of each vegetation survey was thus approximately 5000 m². The end point of the survey was equally accounted for by the GPS and multiple photos of each survey site were also taken with an integrated GPS so that the coordinates and direction of each photo are known and can be integrated into a GIS for later mapping procedures. The vegetation was mapped with following attributes: land use, woody vegetation species, height, tree crown diameter, trunk circumference at chest height, tree condition, percentage of green leaves, and usage intensity. Not only could this information be useful to validate results, but may also be used for calibrating satellite images for other purposes within the project that are not necessarily directly related to this thesis.

As mentioned in chapter 1, the aim of this study is to not only map land cover change and woody vegetation density change between 1967 and today, but to discuss reasons for change.

The environmental trend maps drew our attention to a range of trends (positive, stagnant, negative) at various sites, which often could not be explained by merely viewing the landscape on-site (see Fig. 1.4). Dialogue with local farmers often provided invaluable information and clarification of events. As an example, a village chief was able to tell us that population pressures in the Seno Plains in the 1950s lead to a resettlement of families in what is now Diamnati near Fiko on the Dogon Plateau, one of the two case study sites introduced below. This led to a change of land use and land cover in the immediate surroundings of the village, which continued as the population of the village grew and thus represents an important aspect for explaining changes to the regional environment, which otherwise would remain unknown. Clemens Romankiewicz, a human geographer from the University of Bayreuth, was therefore particularly interested in the perspective of local people in regard to the environment and its change over time and conducted hundreds of interviews during various lengthy stays. The results of these interviews also provide useful information to environmental scientists (Brandt *et al.* in review). The vegetation surveys were often conducted in conjunction with the human geographer, i.e. sites were selected based on common interests (e.g. “hot spots” identified by the results of trend analyses as described above and seen in Fig. 1.4) as well as insights provided in advance by locals. Often local farmers as well as a local guide accompanied us on transect walks and could provide additional information on the use of trees and farmer management strategies. The main results of the vegetation surveys are discussed in chapter 4.4.

3.3 Land Cover Classification

In the context of remote sensing and image processing, a classification may be defined as *“the process of sorting pixels into a finite number of individual classes, or categories of data, based on their data file values”* (ERDAS Inc. 1999 p. 243). Each class has a set of unique criteria that a pixel must fulfil in order to be assigned to a particular class, which is why this process is often referred to as image segmentation. Depending on which information one intends to obtain from the original image, the classes are related to known units on the ground or else various features on the computer screen that contain more information than can be extracted by the visible spectrum of the eye (e.g. hyperspectral images).

One can generally differentiate two types of classifications – unsupervised and supervised classifications. The main difference is the method used for identifying the classes. An unsupervised classification automatically distributes the pixels to the number of classes set by the analyst, based entirely on variations of the spectral attributes. A supervised classification, on the other hand, integrates the analyst’s knowledge of the environment in the image into the

classification. However, unlike the ability of the human brain to detect patterns according to textures and colours, a computer system makes use of the statistics of the spectral attributes of the image, followed by mathematical functions. In this way, a computer system can classify an image into a finite number of classes. One can therefore see that the quality of a supervised classification depends entirely on expert knowledge of the given environment and the accuracy of the analyst's work as far as setting the criteria for the classification is concerned. In this process, known as *training*, the analyst assigns a number of pixels (training areas) to each class, thus informing the computer system of the spectral characteristics of each class. As an example, an analyst may map a handful of small areas within a region of the image he/she knows to be deciduous forest, a further number of areas for cropland and so forth, depending on the number of classes needed. Because the software uses statistical methods to assign the remaining pixels of the image to the selected classes, it is crucial to include multiple training areas for each individual class. The degree to which the classification reflects the reality of the environment is almost entirely dependent on the quantity and accuracy of the training areas. (ERDAS Inc. 1999)

Land cover maps are created for 1967 and 2011 using the panchromatic Corona images and the multispectral RapidEye images. An unsupervised classification method is used for the Corona images and a supervised classification for the RapidEye images. The methods will be explained in detail below. As the available data sets the guidelines for the possible classification methods and results, no previously developed classification scheme is applied.

3.3.1 Corona 1967

3.3.1.1 Land Cover Classes

For the Corona image of 1967 only two classes for the land cover map are produced as the information provided by the panchromatic data is minimal, regardless of the high resolution. The two classes selected are sparsely vegetated and densely vegetated land. As will be shown below, the two types of land covers can clearly be distinguished simply with variations of grey-scales. The land cover may be used as a proxy for land use. The sparsely vegetated areas in 1967 include all areas with little or no vegetation. These areas are thus usually used for agricultural purposes and include cultivated, fallow and grazing areas. The densely vegetated areas are mostly areas of dense natural vegetation, which have not been deforested for cultivation, or also areas which have been laid fallow for extended periods of time and are now covered by shrubbery and grass. Tappan *et al.* (2004) refers to these areas as "bush fallow". The third land cover class "rock", only used for the plateau, represents areas of barren rock with limited vegetation cover. This class was however adopted from the land cover classification

2011 with the assumption (verified visually on-screen) that only minor changes will have occurred to these areas, i.e. barren rock identified today will most likely not have had vegetation growth in 1967, primarily due to the continuous lack of soil.

The method used to produce the land cover maps is fairly straight-forward, yet computationally intensive. As mentioned, the Corona dataset is subdivided according to morphological characteristics into plateau and plains, simply because of the effect the morphology has on the grey-scales. In this way, a greater contrast can be achieved. The images (named Corona-Seno and Corona-Plateau) are then handled separately but a similar methodological procedure is applied.

3.3.1.2 Corona Seno Plains

The software used for the land cover classification of the Seno Plains is ERDAS IMAGINE 2011. The only option here is a standard unsupervised classification with two classes – sparsely and densely vegetated land. The clustering algorithm is an iterative self-organizing data analysis technique (ISODATA), which makes use of spectral distance to cluster the pixels and recalculates the statistics with each iteration (convergence threshold: 0.950) (ERDAS Inc. 1999). In this case the unsupervised classification is fairly unspectacular as it represents merely a binary segmentation. Only two classes are needed as the aim is to find out to what extent this area was sparsely/densely vegetated in 1967 and the single band panchromatic image does not offer much more information concerning the land cover. The only alternative would be on-screen digitizing to extract more information, but not a reasonable option for the entire study area.

The intense salt and pepper effect that resulted because of the high resolution of 2 m means that the map has to be smoothed as the general land cover is of interest at a broader scale than pixel level (e.g. the unsupervised classification assigns individual trees within sparsely vegetated areas to the “densely vegetated” class rather than including the trees as part of the surrounding “sparsely vegetated area”). To smoothen the result, a simple method in ArcGIS is implemented (see Fig. 3.5). The classification is firstly resampled to 20 m using the majority resampling technique, followed by a majority filter. Finally, the boundary clean up tool smoothenes the boundary between zones by first expanding, then shrinking the polygons. Zones with larger total areas are given higher priority to expand into smaller polygons than areas with smaller total area (descending sorting technique).



Fig. 3.5: Post-processing model of Corona unsupervised classification.

3.3.1.3 Corona Dogon Plateau

In the very same way to the Seno Plains, the Dogon Plateau is classified using an unsupervised classification. It was however noted that the areas of bare rock from 1967 are generally the same in 2011 so that the rock class of the classification created with the RapidEye 2011 images on the plateau is adopted for the Corona 1967 land cover classification. This is achieved by using a simple model in ERDAS IMAGINE and multiplying the Corona 1967 unsupervised classification by the rock class of the RapidEye 2011 classification and reclassifying into three classes.

3.3.2 RapidEye 2011

As noted above, the RapidEye dataset is subdivided into the same two areas as the Corona dataset: Dogon Plateau and Seno Plains. On the Dogon Plateau, two images are used, which are dated 07/12/2011 and 26/12/2011 (see Fig. 3.4). The image used for the Seno Plains is the southern extent of the image covering the Dogon Plateau dating 26/12/2011. Each of these is handled separately to acquire improved results, as the spectral information in each area differs significantly. Initially, an attempt was made to produce a single supervised classification using a mosaic of all the images mentioned above. The results were however far from perfect so that three supervised classifications had to be individually produced as follows. ERDAS IMAGINE is again the software used for this purpose.

3.3.2.1 Land Cover Classes

The multispectral RapidEye images offer much more information than the Corona images, which is why a greater number of classes could be selected and differentiated for the land cover classification of 2011. Because of differences regarding morphology, land use and thus also land cover, the classes chosen for the plateau and the plains differ slightly. The Seno Plains are classified into five classes. Because the landscape here is more homogenous, only four of the six classes used for the Dogon Plateau (see Table 3.8) are used for the Seno Plains. The classes “Degraded” and “Riverbed” are unique to the plateau. This is because the Seno-Plains

contain only minor areas of degraded land and distinguishing between a barren, degraded sand dune and a cultivated field with limited vegetation proved to be too difficult. The eroded lateritic soils, unique to the plateau, are however much easier to detect in the satellite images. However the class "Infrastructure", which primarily includes the main road running in a west to east direction through Bankass and the buildings in and around Bankass, is limited to the classification of the Seno Plains. As with the classification of 1967, the class "Sparsely Vegetated" includes agricultural land, i.e. cultivated and grazing areas, but also fallow land within the normal cycle of a farming system. It does not include fallow land, which has been uncultivated for several years and is now covered by dense shrubbery and bushes, i.e. bush fallow. This form of land use is included in the class "Densely Vegetated", as do all the areas of dense natural vegetation, often referred to as "bush-land" or "bush fallow" (see Tappan *et al.*, 2004). Groups of large trees within cropland areas are also included in this class. The class "Degraded" refers to areas with little or no vegetation, which most often have crusty lateritic soils. These areas were identified during the field trip and cover extensive areas within the study area. The class "Rock" is somewhat related to the "Degraded" class, in that the vegetation cover is also limited here. Most of the rocky outcrops have a fair amount of shrub and tree growth, primarily in depressions and channels in the land surface where water may gather. However many areas are free of vegetation, especially in areas exposed to strong winds, and these are represented by the land cover class "Rock", and may be distinguished from the degraded areas by the differing reflection properties. Degraded areas may be revived with extensive efforts; however rocky outcrops always remain unsuitable for cultivation. Examples of the four main land cover classes are shown in the photos in Fig. 3.6 with a corresponding cut-out from RapidEye.

The class "Riverbed" is limited to the plateau as the plateau contains a greater number of large rivers, which in December 2011 were mostly dry. These areas may be differentiated because of the reflective characteristics of deposits found in riverbeds. Again these areas are free of vegetation, but are covered mainly by sand and silt, which have been washed downstream during the rainy-season. For this reason, the class "Riverbed" is not solely limited to actual riverbeds, but includes areas where extensive fluvial deposition has occurred. An example of this form can be seen very well in Fig. 4.5 (land cover map Diamnati), where because of extensive fluvial erosion in the degraded area, the land cover in the area of deposition is similar to that of actual river beds. The final class "Water" covers only a minute area of the plateau as the rainy season is over and rivers are mainly dry. A few lakes and large rivers are an exception here.

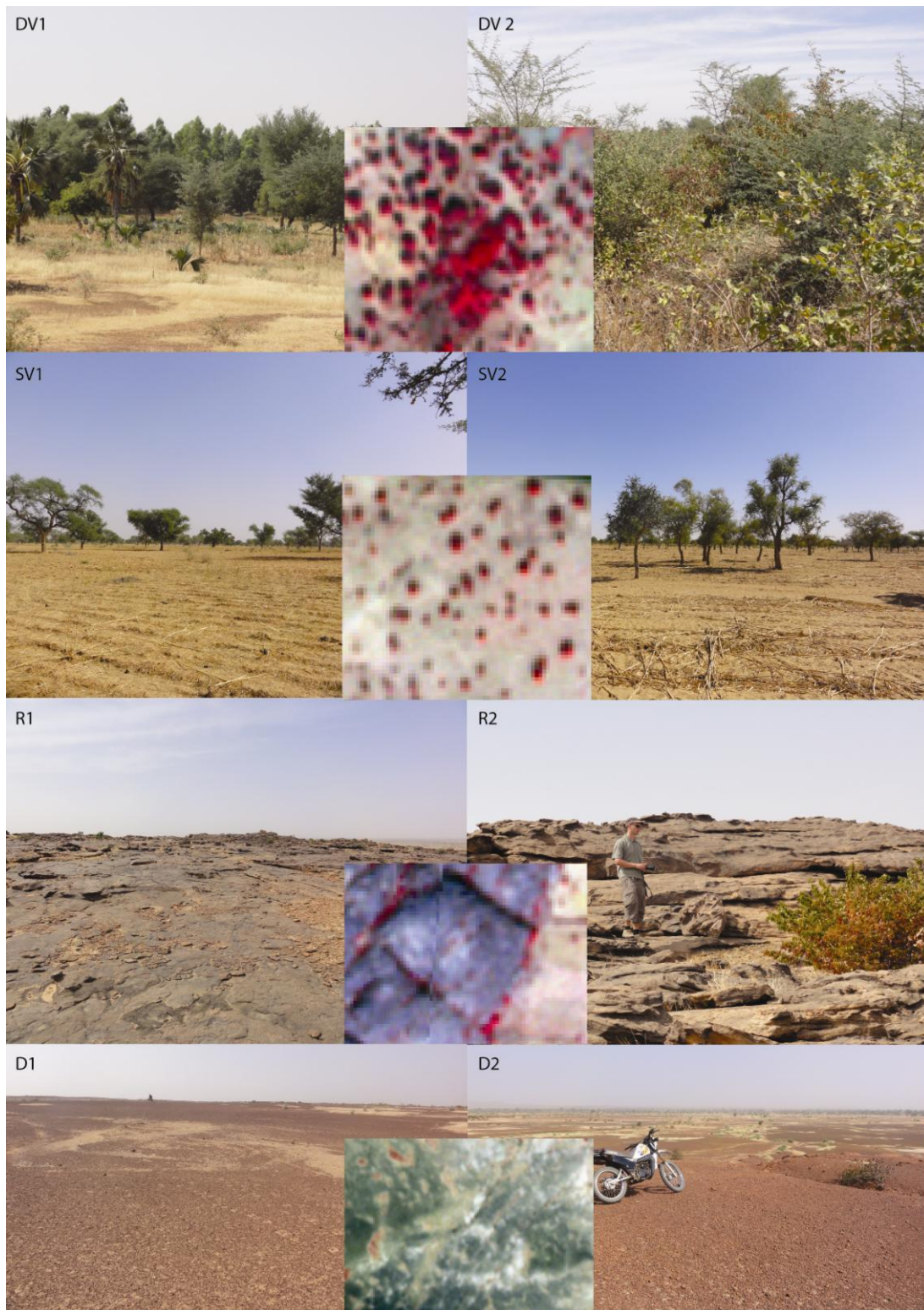


Fig. 3.6: Photos of the four major land cover classes with corresponding cut-outs of the RapidEye images: DV1-DV2: Densely vegetated SV1-SV2: Sparsely vegetated; R1-R2: Rock; D1-D2: Degraded areas; Source: Photos: R. Spiekermann; Satellite images: RapidEye 2011.

3.3.2.2 RapidEye Seno Plains

The classification for the RapidEye images uses a supervised classification in contrast to the panchromatic unsupervised classifications. In a first step, the NDVI is calculated and added as a 6th layer to the layer stack of the image to enhance the characteristics and provide additional information. Training samples are mapped on screen as it can be argued that at 5 m resolution on-screen mapping is made possible and a high degree of control by the analyst is maintained, provided the analyst has spent an extended period of time in the study area, which is the case here. This is combined with the seed pixel tool, which generates training samples from a single pixel identified as representative of a given class. Furthermore supplemental ground truth information in the form of 3000 GPS-tagged photos is used to verify the correct association of a training sample when uncertain. In addition, the surveyed areas during the field trip are digitized so that the land cover maps may be validated with the help of this ground information by means of visual comparison.

For the Seno Plains, Table 3.4 summarizes the results of the training samples for the classification. These training samples are loaded into the signature editor where a signature mean plot, error matrix and feature space images are created to evaluate the classes according to their separability and accuracy. Many adjustments to the classification are made regarding the training areas (addition/ deletion of training samples to improve the separability between classes), number of classes and classification method (e.g. maximum likelihood vs. minimum distance algorithms). In this experimental way a classification is produced, which is considered to best reflect the reality of the environment. The final classification (see Fig. 4.2) is created using the following decision rules:

- Non-parametric Rule: Parallelepiped
- Overlap Rule: Classify by Order
- Unclassified Rule: Parametric Rule
- Parametric Rule: Maximum Likelihood

The decision rules are the set of criteria which decide which class each individual pixel is assigned to (see Fig. 3.7). In this case the first decision rule is a nonparametric rule, namely the parallelepiped rule, which compares the data file values of the candidate pixel with the upper and lower limits given by the values of each band in the signature. If the pixel is not included in any of the parametric boundaries, the parametric rule is applied. The maximum likelihood rule is the parametric rule used here and represents the most commonly used statistical classification method. Under the assumption that all input bands have a normal distribution, probabilities are calculated for each pixel using the spectral information of the training samples to assign each pixel to the most probable class. If the pixel lies within the boundaries of a unique class, the

pixel is assigned directly to that class without further parametric rules. If the pixel lies within the boundaries of more than one class, the overlap rule is applied. In this case the pixel is classified by an order defined by the analyst using expert knowledge of the study area, as seen in Table 3.4. (ERDAS Inc. 1999)

The contingency matrix for the training areas is displayed in Table 3.5 and shows that the training areas were drawn very accurately so that only a minimal number of pixels within the training areas are classified into classes other than the class they were drawn as. For example, 5 of the 621 pixels drawn as “Densely Vegetated” were classified as “Sparsely Vegetated”, as these five pixels were more similar to the “Densely Vegetated” class than the “Sparsely Vegetated” class ascribed to it as the training areas were drawn. The classification is resampled to 20 m using the majority resample technique to equal the geometric resolution of the land cover classifications of 1967 and to smoothen the classification.

Table 3.4: Seno Plains RE 26.11.2011: Land cover classes and training areas.

Class	No. Training Areas	Pixel Count	Class Order
Sparsely Vegetated	25	1651	1
Densely Vegetated	23	622	2
Rock	9	142	3
Infrastructure	12	116	4
Water	3	58	5

Table 3.5: Contingency matrix of Seno Plains RapidEye 26.12.2011 supervised land cover classification.

RE-S-26122011	Reference Data					Row Total
	Sparsely Vegetated	Densely Vegetated	Rock	Infrastructure	Water	
Classified Data						
Sparsely Vegetated	1646	3	0	0	0	1649
Densely Vegetated	5	616	0	0	0	621
Rock	0	3	142	0	0	145
Infrastructure	0	0	0	116	0	116
Water	0	0	0	0	58	58
Column Total	1651	622	142	116	58	2589

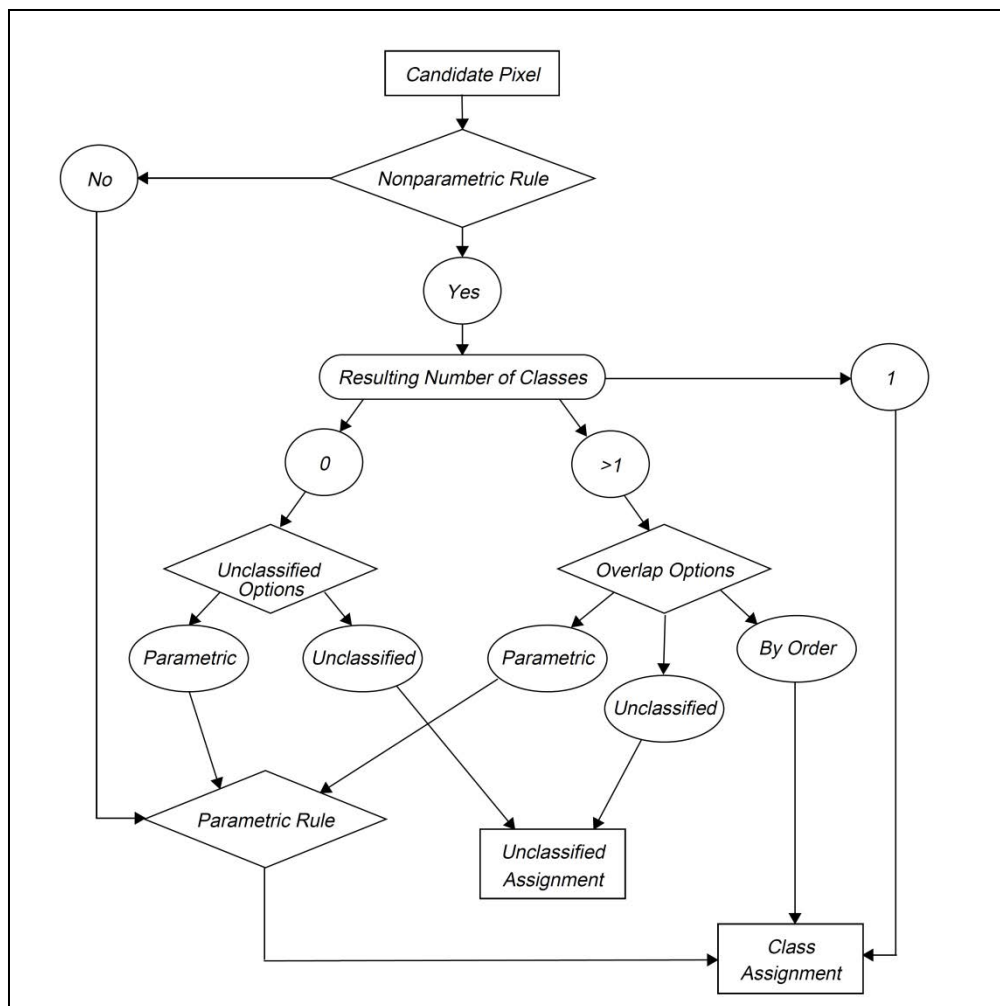


Fig.3.7: Decision rules for the supervised classification. Source: ERDAS Inc. 1999.

3.3.2.3 RapidEye Dogon Plateau

As mentioned above, the two images for the plateau (RE-D-07122011 and RE-D-26122011) are classified separately, due to the differing dates and the influence the time difference has on the spectral information.

RapidEye Dogon Plateau 26.12.2011

In a similar way to the Seno Plains, training samples are mapped on-screen for RE-D-26122011, however with slightly different classes to the Seno Plains, representing the reality of the very different situation on the ground compared to the Seno Plains. Table 3.6 offers an overview of the classes for the land cover classification of RE-D-26122011. The classes “Riverbed” and “Degraded Area” are added to the classification and the class “Infrastructure” no longer exists as classification attempts with this class proved too difficult. The same decision

rules are used as for the Seno Plains, however the use of probabilities is included, a form of weighting classes for the parametric decision rule. Again the contingency matrix of the training samples show that the on-screen mapping results are very good, i.e the separability of classes is effectively achieved (see Table 3.7).

Table 3.6: Dogon Plateau RE 26.11.2011: Land cover classes and training areas.

Class	No. Training	Pixel	Class Order
Sparsely	13	1385	1
Densely Vegetated	16	1093	3
Rock	10	344	2
Degraded	10	706	5
Riverbed	9	676	6
Water	9	2055	4

Table 3.7: Contingency matrix of Dogon Plateau RapidEye 26.12.2011 supervised land cover classification.

RE-D-26122011	Reference Data						
Classified Data	Sparsely Vegetated	Rock	Densely Vegetated	Water	Degraded	Riverbed	Row Total
Sparsely Vegetated	1384	0	0	0	6	3	1393
Rock	0	344	0	0	0	0	344
Densely Vegetated	0	0	1092	0	3	0	1095
Water	0	0	0	2055	0	0	2055
Degraded	1	0	0	0	667	14	682
Riverbed	0	0	0	0	30	659	689
Column Total	1385	344	1092	2055	706	676	6258

RapidEye Dogon Plateau 07.12.2011

The land cover classification for this comparably small section of the Dogon Plateau uses the same classes as RE-D-26122011 (see Table 3.8). However, only a parametric rule is applied, i.e. the maximum likelihood classification, including a priori probabilities or weight factors assigned by the analyst, which act as a further guide to the classification of pixels (ERDAS, Inc. 1999). Again a contingency matrix is calculated to assess what percentage of the training samples are classified as the class they were mapped as. Corrections are made (deletion and creation of new training samples) until the matrix shows suitable results. A separability graph as well as feature space images offer a further means to evaluate the separability of classes visually. The separability graph showing mean band values for each class in Fig. 3.8 and the

feature space image with bands 5 (near-infrared) and 3 (red) in Fig. 3.9 show good results. Such feature space images may also be used to edit the classes.

Table 3.8: Dogon Plateau RE 07.11.2011: Land cover classes and training areas.

Class	No. training areas	Pixel Count	Class Order	Probability
Dense Vegetation	19	956	1	1.0
Cultivated Area	18	7148	2	1.0
Barren Rock	8	1259	3	1.0
Degraded Area		139	4	0.5
Water	5	394	5	0.2
Riverbed	6	614	6	0.2

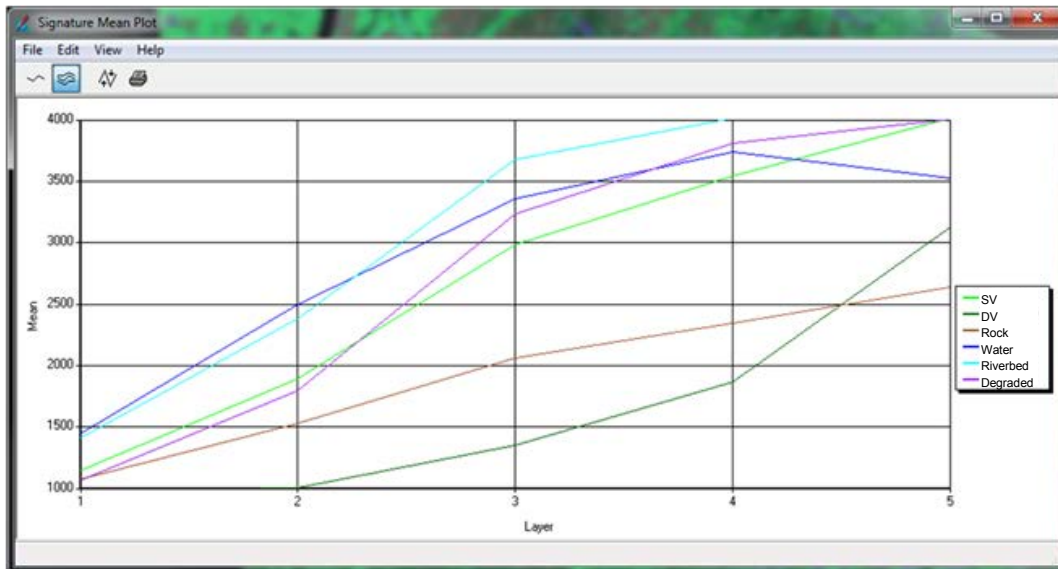


Fig.3.8: Separability graph of Dogon Plateau RapidEye 07.12.2011 supervised land cover classification.

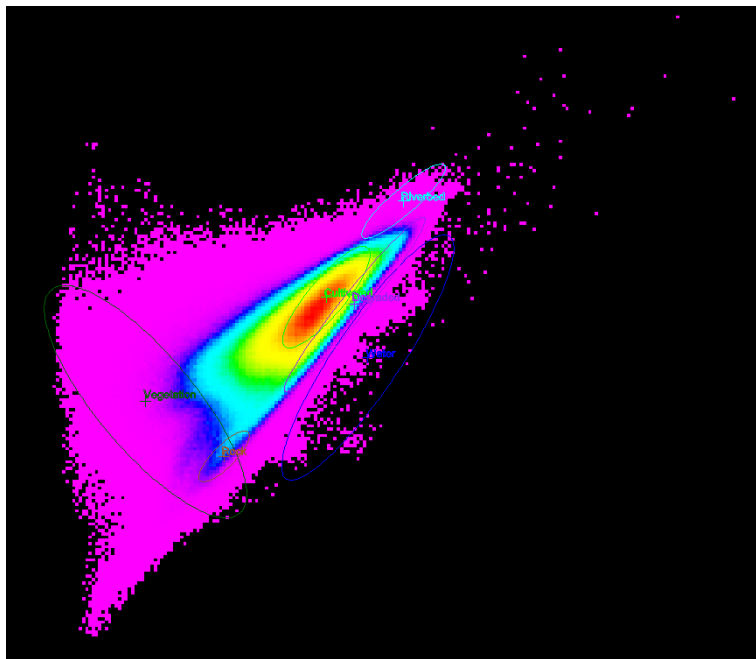


Fig. 3.9: Feature space image with bands 5 (near-infrared) and 3 (red) showing separability of training areas of Dogon Plateau RapidEye 07.12.2011 supervised land cover classification.

3.4 Land Cover Change

The land cover raster files of the plateau for 2011 are merged so that the change maps for the plateau and plains can be calculated. The Corona land cover maps are reclassified as shown in Table 3.9. A simple multiplication of the two raster files using the Model Builder in ERDAS IMAGINE returns a file with unique codes which describe the change. The results are displayed in chapter 4.

Table 3.9: Reclassification of land cover maps for change analysis.

Land Cover Class	Corona	RapidEye Plateau	RE Seno
Dense Vegetation (DV)	10	2	2
Sparse Vegetation (SV)	100	1	1
Rock (R)	1000	3	3
Water (W)		4	4
Infrastructure (I)			5
River Bed (RB)		5	
Degraded Area (D)		6	

3.5 Woody Vegetation Assessment

3.5.1 Theoretical Background

The woody vegetation assessment maps individual trees, groups of trees and large shrubs using object-oriented, automatic mapping technology with the high resolution panchromatic Corona images and the multispectral RapidEye images with the help of a relatively new tool by ERDAS Inc., namely *IMAGINE Objective*. Semi-automatic mapping of individual trees using high-resolution satellite images appears to be relatively unexplored. It is assumed that this has to do with the only recent availability of very high resolution satellite images and the associated cost of such data for regional scaled studies. Previous studies of automatic tree detection and delineation have also applied object-based analyses using high resolution photography. Scientific literature on this topic is limited primarily to the forestry sector and includes studies by Leckie *et al.* (2005), Ke & Quackenbush (2012), Erikson & Olofsson (2005) or Pouliot *et al.* (2002). Regional-scaled studies using object-oriented automated feature extraction within the bounds of environmental research are however practically non-existent. Environmental scientists until now appear to be content with traditional methods of interpreting coarse-scaled resolution data such as Landsat or MODIS to derive an estimated tree density or else lack of funding, time, experimental capabilities can explain the absence of studies. Only by mapping at tree level can an accurate account of changes to woody vegetation density be guaranteed. Much debate on the state of the environment in the Sahel continues and a reasonable assessment of the woody vegetation density today in comparison with the pre-drought situation can assist in improving knowledge of the continuous progression of the ligneous cover in the Sahel. The punctiform nature of the ligneous cover in semi-arid climate zones such as the Sahel makes an object-oriented assessment a logical approach. San Emeterio & Mering (2012) offer a study, which explores a method based on granulometric analysis of high resolution imagery to quantify the ligneous cover. This method generates reasonable results by applying software originally intended for analysis of medical-related images to detect objects in a single phase image, depending on the texture within a moving window, or as explained by Mering & Chopin (2002 p. 19), “a granulometric map is built by automatic classification of every pixel of the image according to the granulometric density inside a sliding neighbourhood.” The method of an object-oriented classification approach for tree detection and mapping with use of high resolution imagery in a semi-arid environment, such as the Sahel, has until now only been illustrated in a case study by Chepkochei (2011), which specifically explores the capabilities of ERDAS IMAGINE Objective. This methodological study advances further than the IMAGINE Objective User’s Guide by ERDAS Inc., the only other form of IMAGINE Objective-related literature found that includes the so-called “IMAGINE Objective Tree Crown Tour Guide”

(ERDAS Inc. 2008). The User's Guide proved to be of little use for the methods in this thesis, apart from providing definitions for various tools as well as important background information on IMAGINE Objective. The method used for the woody vegetation mapping below is based to a large extent on Chepkochei (2011), which uses a very high resolution multi-spectral World View-2 image to demonstrate the capabilities of IMAGINE Objective for the classification of tree crowns. The detailed description of the methodology and the various tools within IMAGINE Objective are very helpful and are adapted for the purpose of this study. However major differences include the study area size (2 x 0.25 km² compared to the 3660 km² study area used here) as well as the data (World View-2 from DIGITALGLOBE – 8 bands with 2 m resolution, compared to the 5 m resolution of RapidEye and 2 m resolution of Corona images used here). The 2 m resolution of the World View-2 images is an obvious advantage and means that the accuracy of the tree detection is greater. Furthermore, Chepkochei (2011) is able to distinguish between shadows of trees and the actual trees, thus attaining a very accurate assessment of the real tree crown size. The large-scaled study represents an ideal situation for tree crown mapping, however for regional-scaled environmental studies, very high resolution data such as that of the World View-2 is at this point of time remains simply unaffordable for low-budget University research projects. In contrast, the RapidEye images used for the assessment below are provided by the RESA program funded by the DLR free of charge for the purpose of this research.

A further reason for the land cover maps is their use for attaining woody vegetation density maps of high quality. This represents another more practical reason for the land cover analysis besides the interest of the scientific community in the role of land cover change and its impact on woody vegetation density on environmental change. As will be seen below, the detection of woody vegetation is based almost entirely on the spectral information provided by the pixels of the training samples and so-called "background training samples". First of all, the background pixels may differ greatly between an area of natural vegetation and that of cropland or of a rocky outcrop. This is true for both the Corona and the RapidEye datasets. In an area of dense natural vegetation, the areas between trees or large shrubs are often covered by grass and small shrubs and the tree density is much higher than on cropland. For the Corona imagery, this means that the background pixels in natural vegetation areas may take on similar grey-scale values to trees or shrubs, i.e. the target pixels, in a cropland area. For the multispectral RapidEye imagery, this so-called *adjacency effect* is caused by scattering in the atmosphere - land surface system - an effect which increases in a heterogeneous landscape (Liang *et al.* 2001). The pixels immediately surrounding trees and large bushes in an area of natural vegetation are thus affected by the scattering of neighbouring pixels. Therefore the contrast of pixel values is not as great as in an area of cropland. The values of trees on cropland may thus

also be similar to background pixels in a natural vegetation area. For this reason the mapping of woody vegetation not only requires a separation of the Dogon Plateau from the Seno Plains, but also needs to be carried out for the various land cover types separately. Table 3.10 offers an overview of the input data used for the woody vegetation assessment and the corresponding number of training samples and background samples used for each feature model.

Table 3.10: Data base of woody vegetation feature extraction and the corresponding number of training samples (TS) and background samples (BS).

Image	Image Part	Land Cover	Code	No. of TS	No. of BS
Corona (10.12.1967)	Seno Plains	Sparsely Vegetated	CSPSV	26	15
		Densely Vegetated	CSPDV	40	27
	Dogon Plateau	Sparsely Vegetated	CDPSV	51	14
		Densely Vegetated	CDPDV	30	15
RapidEye (26.12.2011)	Seno Plains	Sparsely Vegetated	RESPSV	91	48
		Densely Vegetated	RESPDV	34	31
	Dogon Plateau	Sparsely Vegetated	REDPSV	30	17
		Densely Vegetated	REDPDV	34	22
RapidEye (07.12.2011)	Dogon Plateau	Sparsely and Densely Vegetated	REDP07	89	23

A description of the object-oriented method for the classification of woody vegetation for each of the respective datasets listed in Table 3.10 is given below. For each “Code” (the individual image representing a particular land cover type within the “image part”) a separate “Feature Model” is created for use in IMAGINE Objective. The advantages of IMAGINE Objective over other software packages that have similar capabilities (such as ENVI and eCognition) are its user-friendliness and relative simplicity. The major disadvantage here include that no moving window is applied so that, for example, thresholds set are valid for the entire image and cannot be adjusted from one area of the image to another. The results of the classification produce vectors, which can be immediately integrated into a GIS for further processing or map design (Chepkochei 2011). Each feature model is a line of algorithms which consists of up to seven process nodes and the corresponding input data that may be adapted as needed. Fig. 3.9 offers an overview of the process flow within a feature model. As can be seen, the process of automatic feature extraction is based on pixel cue metrics, which have been modelled in IMAGINE Objective according to the human visual system for image interpretation (ERDAS Inc. 2008). The cues thus use both spectral information, i.e. pixel level cues to identify colour, texture, tone and site (e.g. elevation), as well as spatial information, i.e. object level cues, to

analyse shape, size, orientation and so forth (ERDAS Inc. 2008). The following describes this process as used for the mapping of woody vegetation in the study area.

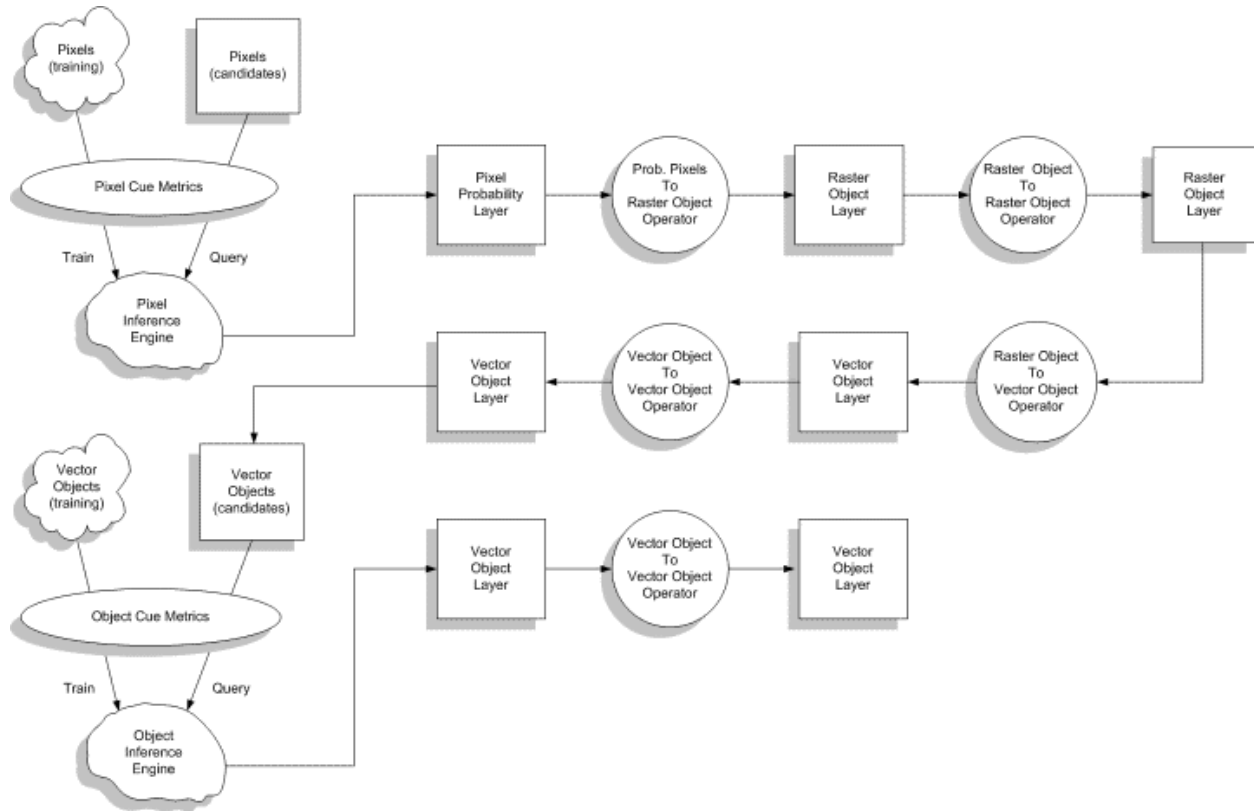


Fig. 3.10: Process flow in ERDAS IMAGINE Objective. Source: (ERDAS Inc. 2008)

3.5.1.1 Identifying training samples

The first step is to identify training samples, which represent groups of pixels mapped by the analyst that have the pixel values sought after, i.e. pixel values relating to woody vegetation. As mentioned above, background training samples may also be mapped to define unwanted pixels. Depending on the size of the study area and the type of input data, a sufficient number of training samples need to be drawn.

3.5.1.2 Raster Pixel Processor (RPP)

After exploring all options within the RPP, the *Single Feature Probability* (SFP) is clearly the most suitable pixel classifier here. The SFP is a pixel classifier that makes use of the Bayesian Network classification (statistical classification). Based on spectral similarity/dissimilarity to the spectral information offered by the statistics of the training samples/background training

samples, the candidate pixels are attributed values between 0 and 1. The output is thus a raster file with pixel values describing the likelihood of each pixel being woody vegetation (values tending towards 1.0) or a background pixel (values tending towards 0.0). The quality of the SFP pixel classifier depends in this case entirely on the statistics of the training samples (spectral information of the single band for Corona and all 5/6 bands for RapidEye). Therefore care needs to be taken when selecting pixels for the training samples and edited if results show it to be necessary, as this layer forms the basis for all other operations to follow. Fig. 3.10 shows the result of the SFP in IMAGINE Objective. The swipe shows the clipped sparsely vegetated image part of the Corona image on the right side. The black areas here are the densely vegetated areas excluded from this particular feature extraction. As mentioned above, the sparsely and densely vegetated areas are treated separately (see Table 3.10). Individual trees and shrubs can be identified on the fields. To the left of the swipe, the white pixels represent woody vegetation and have a high probability (values tending towards 1.0) and the background pixels have a low probability shown in black.

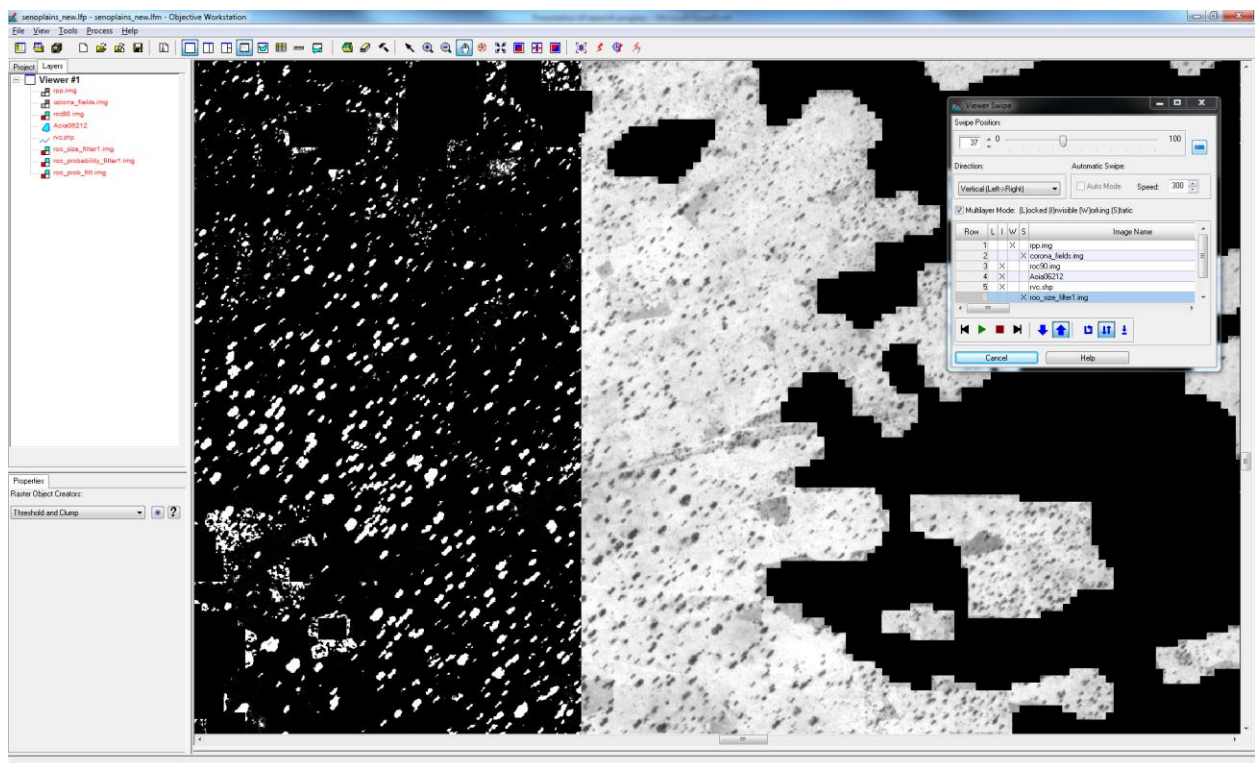


Fig. 3.11: IMAGINE Objective: Swipe showing Corona image part before (right-hand side) and result of the Single Feature Probability after (left-hand side).

3.5.1.3 Raster Object Creators (ROC)

This step groups the pixels of the RPP output layer according to their probability. All neighbouring pixels with a probability greater than or equal to the given threshold are grouped into so-called raster-objects. After testing both the *Segmentation* and *Threshold and Clump*, the latter proved to be more successful and was implemented for all nine of the images in Table 3.10 above. In a first step, the *Threshold and Clump* creates a binary file according to the probability threshold defined by the analyst. In a second step, the remaining pixels are clumped as described above. The output of this calculation is a raster object layer with an attribute table containing a unique ID for each raster object as well as the zonal mean probability. The raster objects are displayed for the same section in Fig. 3.11. The various colours reflect the unique IDs of each raster object. The zonal mean probability, i.e. the average probability of a given raster object, is calculated from the RPP output. (ERDAS, Inc. 2008)

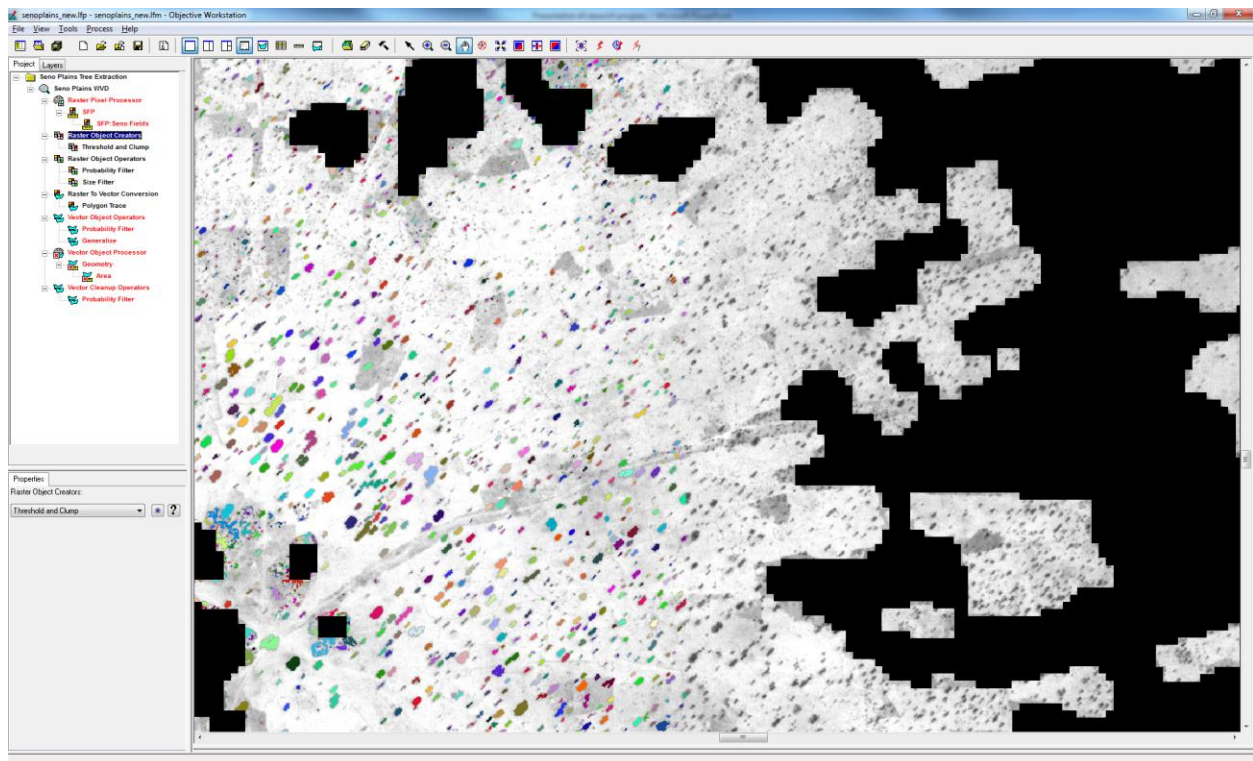


Fig. 3.12: IMAGINE Objective: Swipe showing Corona image part before (right-hand side) and result of the Raster Object Creator after (left-hand side).

3.5.1.4 Raster Object Operators (ROO)

A range of *Raster Object Operators* may be implemented here and include the *Probability* and *Size Filters*. The probability filter was at first included but following tests excluded as the

probability of the raster objects after the zonal mean calculation remains above or equal to the threshold defined in the RPP. As this threshold is mostly set rather high to begin with (in order to create as many individual objects as possible rather than large clumps), it is not deemed necessary to raise the threshold even higher. The *Size Filter* on the other hand sets a minimum and maximum size that each object may have (number of pixels). As will be seen below, in areas where the vegetation is very dense, e.g. large groups of trees in close proximity, most pixels have a high probability so that all pixels that border one another with a probability above the defined threshold are classified as a single object. The lack of contrast and resolution are primarily responsible for this problem. Ideally the size filter could be used to set a maximum size of a tree to a set number of pixels. However, this would mean that all objects greater than the set maximum size would be deleted, even though these objects represent dense woody vegetation. It was therefore decided to exclude a size limit and use the information provided by this relatively small number of large objects (i.e. objects greater in size than an individual tree) to model the approximate tree number (see chapter 3.5.4), let alone retain the information on vegetation cover. Furthermore, the size of the objects may be analysed at a later stage following the vector conversion if necessary.

3.5.1.5 Raster to Vector Conversion (RVC)

This fifth operation performs a polygon trace on the raster objects, thus converting them to vector objects. The output is a shapefile including an attribute table containing the unique ID as well as the probability of each feature. This shapefile also forms the basis of all further object operations. Fig. 3.13 again shows a swipe of a section of the Corona image where a village can be seen with the surrounding sparsely vegetated fields. The results of the RVC are displayed here only for the image part “Sparsely Vegetated”. This image also exemplifies that the grey-scales of the background pixels in the “Densely Vegetated” bush fallow areas are much darker than the background pixels of the “Sparsely Vegetated” cropland areas. After clipping the densely vegetated areas out, the contrast increases greatly so that the feature extraction in these areas is much easier.

3.5.1.6 Vector Object Operators (VOO)

Although multiple VOO are available, only the *Smooth* function is included in this process node. The aim here is to smooth the edges of the features so that they take on a more circular form rather than remaining too squared. The final results of the feature extraction are illustrated in Fig. 3.14 for a section of a sparsely vegetated Corona image part.

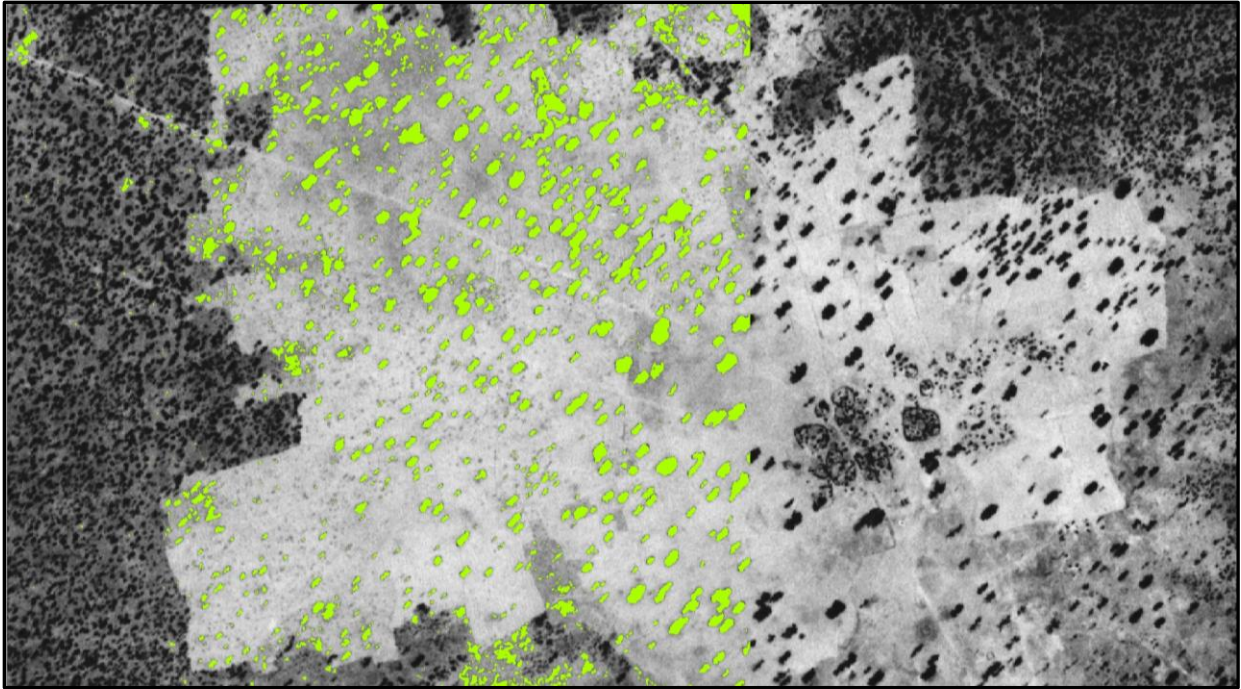


Fig. 3.13: IMAGINE Objective: Example of RVC results in a sparsely vegetated area.

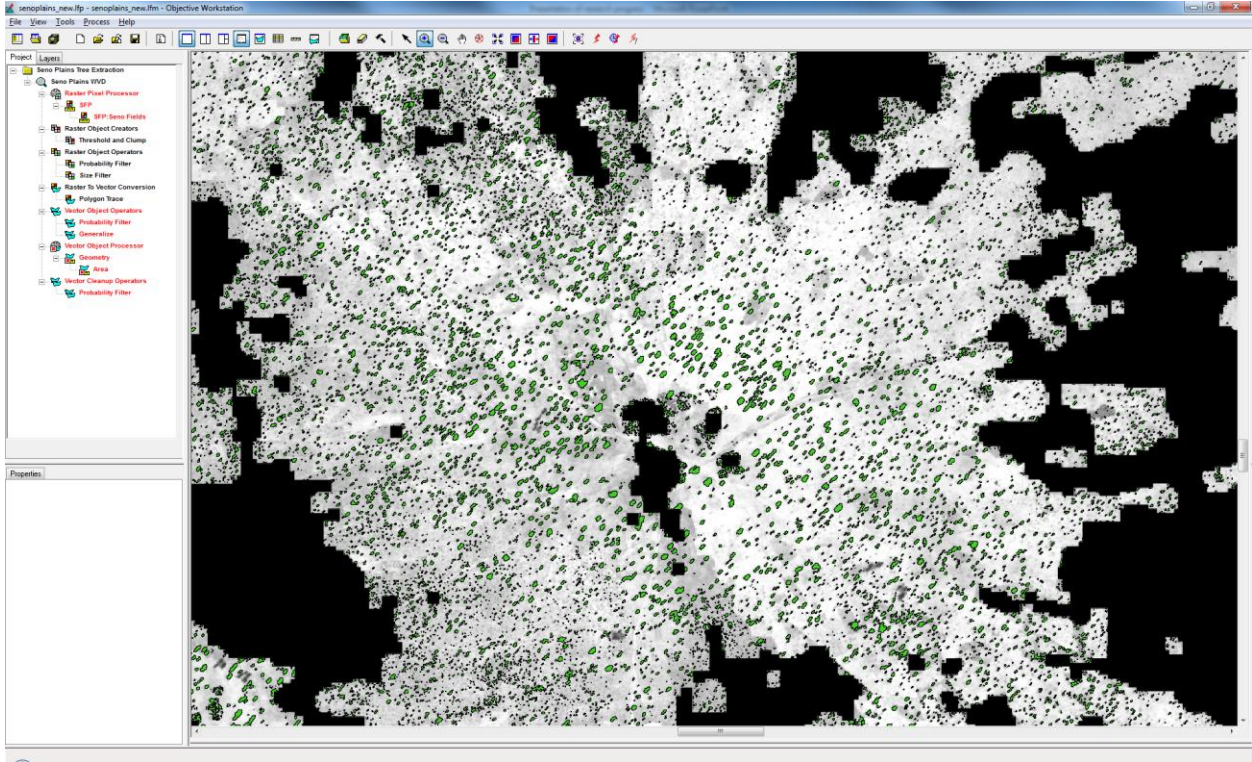


Fig. 3.14: IMAGINE Objective: Example of the final results of the woody vegetation feature extraction for a section of the sparsely vegetated Corona image part.

3.5.1.7 Vector Object Processor (VOP)

The VOP uses an object classifier to calculate the probability of each vector object, again based on training samples. In contrast to the pixel level cues, the object level cues calculate the probability of each vector object based on spatial characteristics such as area and circularity (Chepkochei 2011). This seventh and last possible process node is not used for the woody vegetation assessment, simply because it would exclude too many features based on geometric characteristics of the vector objects. It is important to bear in mind here that the aim is not to have the maximum number of perfectly shaped and sized trees but to include all woody vegetation within the parameters set above, regardless of size and shape. The primary goal is to maximize the count of individual trees and shrubs that may be mapped and, where this is not possible (e.g. in areas of dense vegetation), to retain information on vegetation coverage. With a resolution of 5 m, a tree in RapidEye may often be represented by five or six pixels. This same tree in a World View-2 image would in contrast be represented by several dozen pixels, making it possible to work with geometric characteristics. Although 5 m is a very high resolution for multispectral images, it also has its limits and these are important to acknowledge. Unfortunately RapidEye does not have a panchromatic band at a higher resolution.

3.5.2 Corona 1967

As can be seen in Table 3.11, the major difference between the feature models is the probability threshold set in the *Raster Object Creator*, i.e. for the *Threshold and Clump* operator. The quality of the results of the woody vegetation feature extraction depends almost entirely on the value set by the probability threshold, which again depends on the quality of the *Single Feature Probability*. For this reason, each feature model needs to be run several times until the desired results are obtained. This also means editing the training samples by adding, deleting, correcting existing polygons, etc., as the statistics of the training samples are decisive for the pixel classifier. The major challenge for the Corona images is the single band of greyscales. The contrast of the images differs greatly from one area of the image to another and because each input (see Table 3.10) is a part of a mosaic of many images, the differences of contrast increase even more.

Table 3.11: Feature model process nodes of Corona image parts.

CODE	RPP	ROC	ROO	RVC	VOO
CSPSV	SFP	TC: Prob. 0.100	Size Min. 2	Polygon Trace	Smooth 0.20
CSPDV	SFP	TC: Prob. 0.900	Size Min. 2	Polygon Trace	Smooth 0.20
CDPSV	SFP	TC: Prob. 0.600	Size Min. 2	Polygon Trace	Smooth 0.20
CDPDV	SFP	TC: Prob. 0.800	Size Min. 2	Polygon Trace	Smooth 0.20

As an example, trees in one area may be entirely black, in another area trees may be a medium shade of grey, simply because of the quality of the scanned images. An attempt was made to process the images using various filters and enhancement techniques, but it was decided that this decreased or distorted the original information and often also changed the reality of the situation (size and extent) of the trees and shrubs on the ground.

Because contrast represents such an important factor in the panchromatic images, the land cover plays a major role in increasing contrast. Fig. 3.15 shows the difference of contrast in an area of dense vegetation before and after clipping out the densely vegetated areas from the Corona mosaic in the Seno Plains. Prior to the clipping, it was impossible to extract woody vegetation features from these areas of dense natural vegetation because the contrast was not sufficient. By separating these areas, i.e. sparsely vegetated areas from densely vegetated areas using the land cover maps, woody vegetation also in these areas could be assessed. In this way the land cover classifications proved to be invaluable for work in IMAGINE Objective.

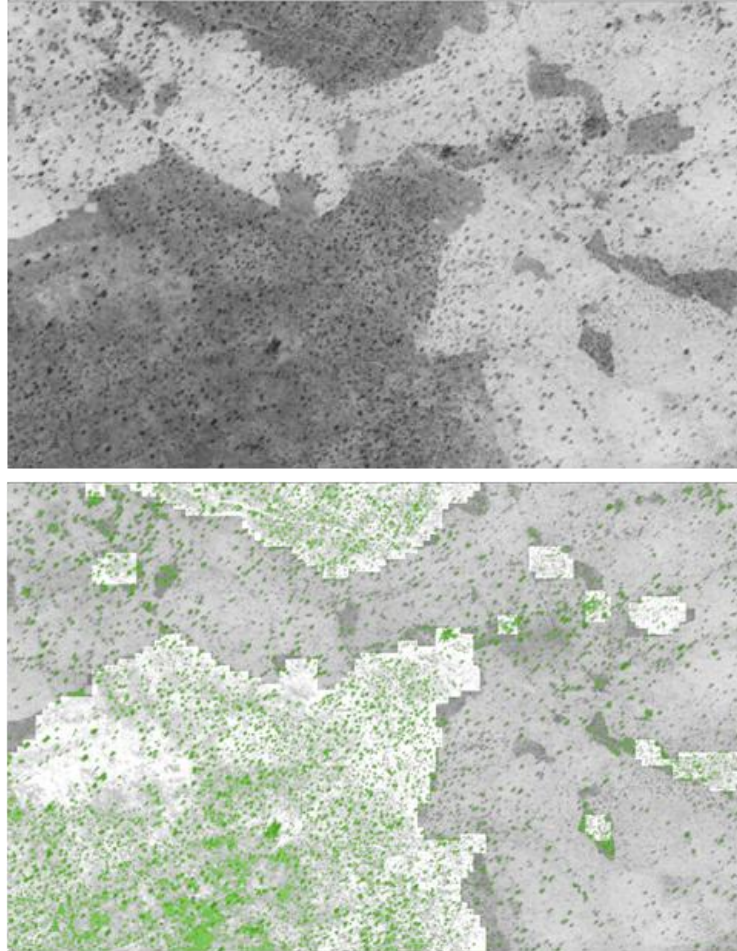


Fig.3.15: Example of contrast in Corona image before and after clipping of bush fallow areas enabling improved detection of woody vegetation.

3.5.3 RapidEye 2011

The advantage of the RapidEye images is obviously the 5 bands (6 when including the NDVI band in each image) that offer greater statistical depth for the pixel classifier. To increase the contrast within the RapidEye images, the land cover maps are used here to assess the woody vegetation within the sparsely and densely vegetated areas only. This means the RapidEye images are clipped accordingly. This is achieved by resampling the land cover maps from a 20 m resolution to a 100 m resolution using a cubic convolution filter in ERDAS Imagine, and converting the rasters to polygons. These shapefiles are then used to clip the RapidEye imagery with the Subset and Chip tool, for the sparsely vegetated and densely vegetated areas separately (apart from the image code REDP07 – see Table 3.10). The tree assessment for the remaining land cover classes is not of relevance, as the woody vegetation cover in these areas

is negligible (degraded area, riverbed, rock, infrastructure, water). The main research aim is however to map woody vegetation within the areas of natural vegetation and in agriculturally used areas, so as to analyse the change of woody vegetation within the land cover classes between 1967 and 2011. Table 3.12 offers an overview of the process nodes of each feature model. In a similar way to the Corona images, the feature models need to be adjusted so as to optimize results. Again the time consuming process of adjusting training samples and the probability threshold is necessary. No minimum size is set on the ROO as a single 5 m pixel may represent a single tree or woody shrub and the size limit of each polygon may also be adjusted if necessary in any GIS. The *Smooth* tool is also reduced to 0.10 on the vector objects.

Table 3.12: Feature model process nodes of RapidEye image parts.

Image Code	RPP	ROC	ROO	RVC	VOO
RESPSV	SFP	TC: Prob. 0.900	-	Polygon Trace	Smooth 0.10
RESPDV	SFP	TC: Prob. 0.800	-	Polygon Trace	Smooth 0.10
REDPSV	SFP	TC: Prob. 0.900	-	Polygon Trace	Smooth 0.10
REDPDV	SFP	TC: Prob. 0.800	-	Polygon Trace	Smooth 0.10
REDP07	SFP	TC: Prob. 0.995	-	Polygon Trace	Smooth 0.10

3.5.4 Woody Vegetation Density and Cover

An algorithm is developed to calculate woody vegetation as follows:

- 1) Woody vegetation density: Count of woody vegetation objects per hectare (100 x 100 m pixels)
- 2) Woody vegetation cover: Area of woody vegetation objects per 250 m x 250 m pixels

The outputs of the woody vegetation analysis are shapefiles. Because shapefiles have limitations regarding size, i.e. both the *.shp* and *.dbf* components may not exceed 2 GB, the shapefiles are converted to feature classes within a Personal Geodatabase. The features listed in Table 3.13 on the plateau and plains are merged for the woody vegetation density calculations that follow. The feature classes have the advantage of not having the limitations of shapefiles and are capable of processing the millions of features stored within them.

Table 3.13: Results (number of features per image part) of woody vegetation assessment.

Results of Woody Vegetation Assessment	No. Features	Merged for Density Assessment	No. Features
CSPSV	492,590	Corona Seno Plains	1,119,205
CSPDV	626,615		
CDPSV	2,180,747	Corona Dogon Plateau	3,467,988
CDPDV	1,287,241		
RESPSV	363,421	RapidEye Seno Plains	422,822
RESPDV	59,401		
REDPSV	378,895	RapidEye Dogon Plateau	735,690
REDPDV	270,178		
REDP07	86,617		

The model in Fig. 3.16 offers an overview of the process of converting the tree objects to density and coverage maps. In general, the features are converted to points and the points are counted for every 100 x 100 m pixel/hectare. Slight alterations are necessary as often groups of trees are mapped as a single feature, thus a single point would often represent much more than a single tree. Therefore the area of the features is calculated prior to converting them to points. The attribute "Area" of each feature is available for a more accurate calculation of woody vegetation density per hectare. A threshold for a single tree is set at 225 m² as it is hypothesized as well as compared to field data, that an average tree is represented by 3x3 5 m pixels within a RapidEye image due to the spectral adjacency effect. A tree crown with a diameter of 10 m on the ground is not necessarily represented by the corresponding spectral characteristics of the tree in just four pixels. Rather the neighbouring pixels are also affected by the scattering reflection of the tree crown. This is also shown to be true after verifying this theory using geo-tagged photography of trees, measured during the field trip. Single trees are found to have a high NDVI value in the eight neighbouring pixels, although this obviously depends on the size of the trees. This also represents a source of error, as the exact size and shape of the tree crowns cannot be perfectly mapped at a resampled geometric resolution of 5 m (originally 6.5 m). A different source of error is found with the Corona images. The shadows of trees and shrubs increase the size of the mapped objects by up to a third of the real size. For this reason and for the sake of finding a common denominator, all (groups of) trees and shrubs mapped with an area larger than 225 m² are divided by this figure to approximate the actual number of trees and shrubs represented by the single feature. The output of the calculation is set as an integer, thus rounded to the nearest number of trees (e.g. a feature with an area of 764 m² is concluded to represent a group of three trees).

Furthermore, all features larger than a hectare are selected and calculated as a separate feature class, in order to display these on the maps in a different manner and because the actual number of trees and woody shrubs is a very rough estimate. These features represent areas of very dense vegetation, which is why the individual trees and shrubs could not be detected as such in Imagine Objective. Such features are also not contained within a single 100 x 100 m pixel so that they are not converted to points in the first place. Rather, the approximate tree density is modelled by dividing the area by 225 m² followed by converting the polygon to a raster to thus represent the total area occupied by the large polygon.

In a similar way, each polygon smaller than 10,000 m² is only represented by a single point even though the polygon may extend beyond the bounds of a single 100 m pixel. This may lead to one pixel having a high density, the neighbouring having a low density, simply because the point is located at the centre of the former polygon and attributed to a single pixel. It is important to bear this in mind when studying the density maps as it represents another minor source of error.

A similar operation is used for the woody vegetation cover maps. The raster resolution is adjusted to 250 m for this purpose so that the regional scaled maps are given an overall smoother appearance. Again the attribute "Area" of the point feature class is used to calculate the cover. Polygons larger than 62,500 m² are converted to raster with the value "99", meaning areas with very high cover percentages, assumed to be at least 40% because of the absence of background pixels in these areas so that individual trees could not be extracted.

The results of both the woody vegetation density and cover mapping are displayed in chapter 4.

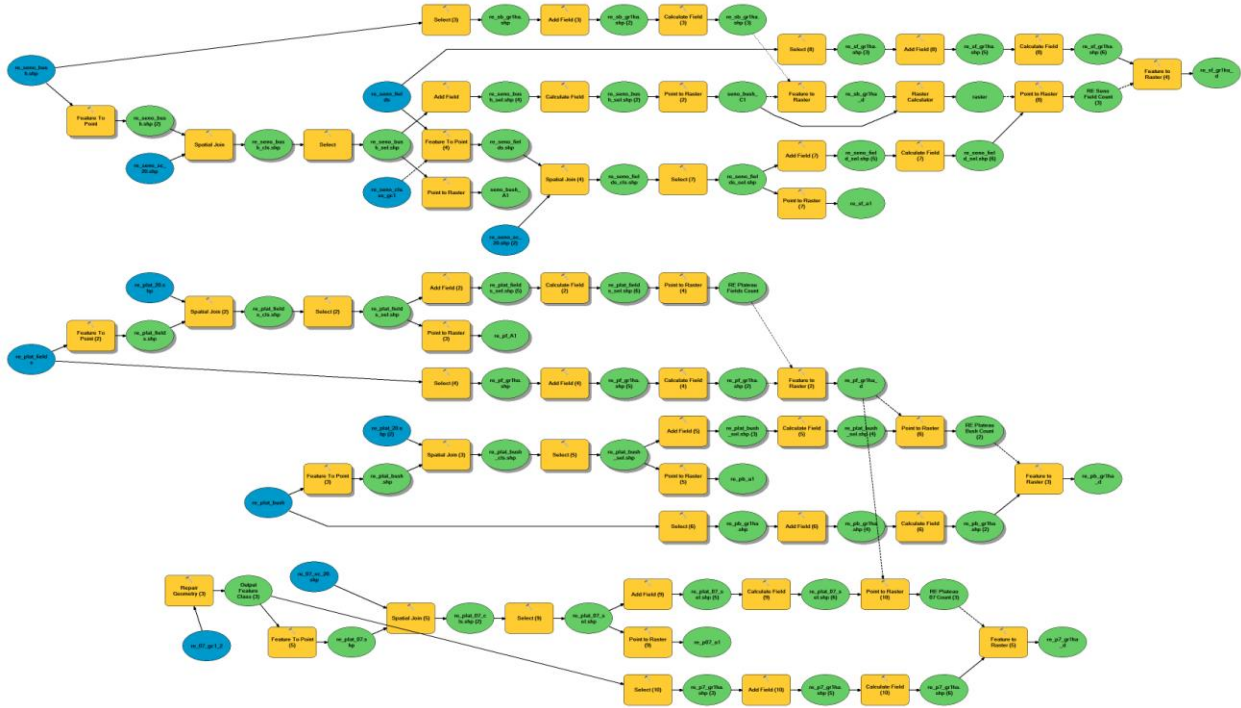


Fig.3.16: Model in ArcGIS 10 used to calculate woody vegetation density and cover maps.

3.5.5 Woody Vegetation Density and Cover Change

In order to assess the woody vegetation density and cover change, the density and cover maps of 1967 and 2011 are processed in ArcGIS using the Raster Calculator. In a first step the *Null Values* are converted to 0 to allow the subtraction of the two raster files. This is achieved with the conditional function *Con* in combination with the *IsNull* function within the Raster Calculator. Furthermore the extent of the raster that covers the smallest area is set for the subtraction with the use of a mask to ensure that the extent is equal (RapidEye on the Plateau, Corona on the Plain (due to the gaps)). The tool *Extract by mask* may then be used to calculate statistics for the various land cover classes. Only the classes “Sparsely Vegetated” and “Densely Vegetated” are of particular interest here.

4. Results

4.1 Land Cover

4.1.1 Land Cover 1967

The results of the classification for 1967 are displayed in Fig. 4.1 and in Table 4.1. Table 4.1 shows that the class “Sparsely Vegetated” dominates in both the Seno Plains and the Dogon Plateau. 59.8% (representing more than 55,000 ha) of the Seno Plains is covered by sparsely vegetated areas, compared to the 52.7% (an area totalling 142,000 ha) on the Dogon Plateau. However, the remaining 40.2% of the Seno Plains remain “Densely vegetated”. Similarly, 37.1% of the Plateau is covered by dense vegetation, i.e. areas of dense natural vegetation, in 1967. This considerable proportion of the Seno Plains had largely not been cleared for cultivation purposes in 1967 as determined by the limited demand for cropland areas due to a relatively low population density. The location of villages and towns can be identified by the degree to which the fields had been cleared for cultivation. The areas surrounding all major towns, e.g. Bankass and Bandiagara, are to a large extent free of dense vegetation, reflecting the extensive use of land there. As mentioned above, the “Rock” class is the same as that of 2011. The plateau-plains border may be identified by the rocky area in the east of the map, which represents the steep Bandiagara escarpment. The densely vegetated areas are also determined by the morphology, with large areas of dense vegetation found in the comparatively moist river valleys. In 1967 extensive areas of tiger bush (banded vegetation stripes) can still be identified on parts of the plateau, as will be shown in the case study of Diamnati in chapter 4.14.

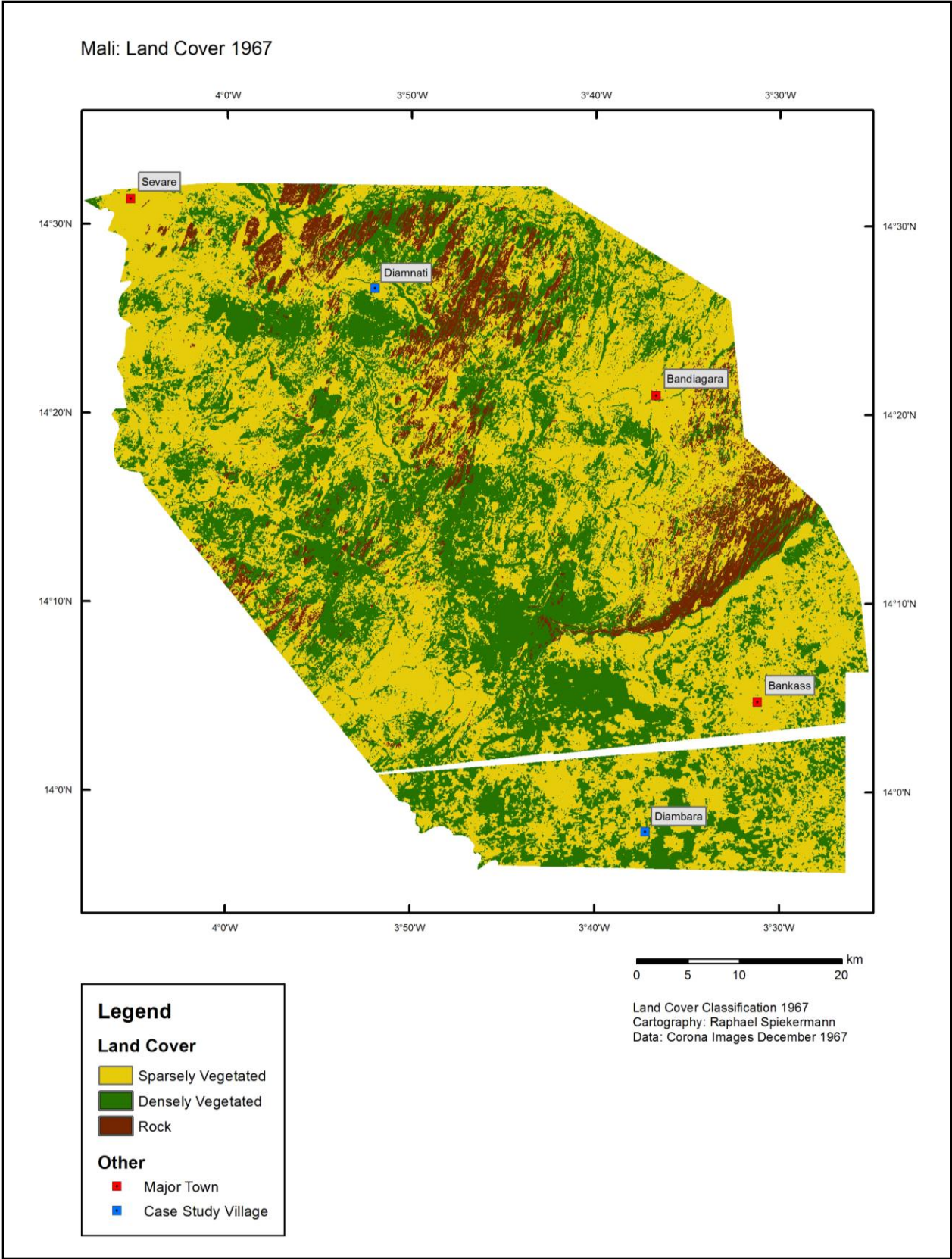


Fig.4.1: Land cover classification 1967.

Table 4.1: Land cover classification 1967 results (total area (ha) and percent).

<i>Class</i>	<i>Corona SP (ha)</i>	<i>Corona DP (ha)</i>	<i>Corona SP %</i>	<i>Corona DP %</i>
Sparsely Vegetated	55056.5	142083.0	59.8	52.7
Densely Vegetated	36971.9	100096.8	40.2	37.1
Rock	NA	27675.2	NA	10.3
Total Area	92028.4	269855.0	100.0	100.0

4.1.2 Land Cover 2011

The results of the RapidEye 2011 land cover classification are shown in Fig 4.2 and Table 4.2. As the classification method is very different to that of the Corona images, the results are more detailed considering the number of classes used. Regardless of the additional classes, compared to the Corona land cover classification, the class “Sparsely vegetated” now represents 73.2% (69943.6 ha) of the Seno Plains and only 25.8% (24629.0 ha) remain as “Densely Vegetated”. 0.9% is classified as bare rock, and the 160 hectares of infrastructure may be attributed to the main road and town of Bankass. The land cover of the Dogon Plateau in 2011 is somewhat surprising as the sparsely vegetated areas now only cover an area of 44.3% compared to the 52.7% in 1967. The degraded areas in 2011 encompass an area totalling more than 25,000 ha and represent almost 10% of the total area on the Dogon Plateau. The land cover 2011 map shows quite a complex pattern of land cover types in comparison with the relatively simple land cover pattern of the Seno Plains. Large areas of the plateau are now degraded and the interplay of sparsely and densely vegetated areas is to a large extent determined by the rough morphology of the plateau. The rocky outcrops are often outlined by dense vegetation, mostly bush, as these areas are commonly more difficult to reach and thus remain largely undisturbed. In the northwest, the classification of the RapidEye image dated 07.12.2011 shows mainly sparsely vegetated areas. The lack of the class “Rock” in this area of the plateau indicates that the morphology here is more even due to the proximity of the Niger Delta. The land cover of the Seno Plains may also reflect certain morphological features, such as the river northwest of Bankass, flowing off the Bandiagara escarpment at various locations and providing the water requirements for dense tree growth. The area with very dense natural vegetation in the west of the Seno Plains is a large rock island that extends roughly 100 m above the surrounding plain and is covered by woody natural vegetation.

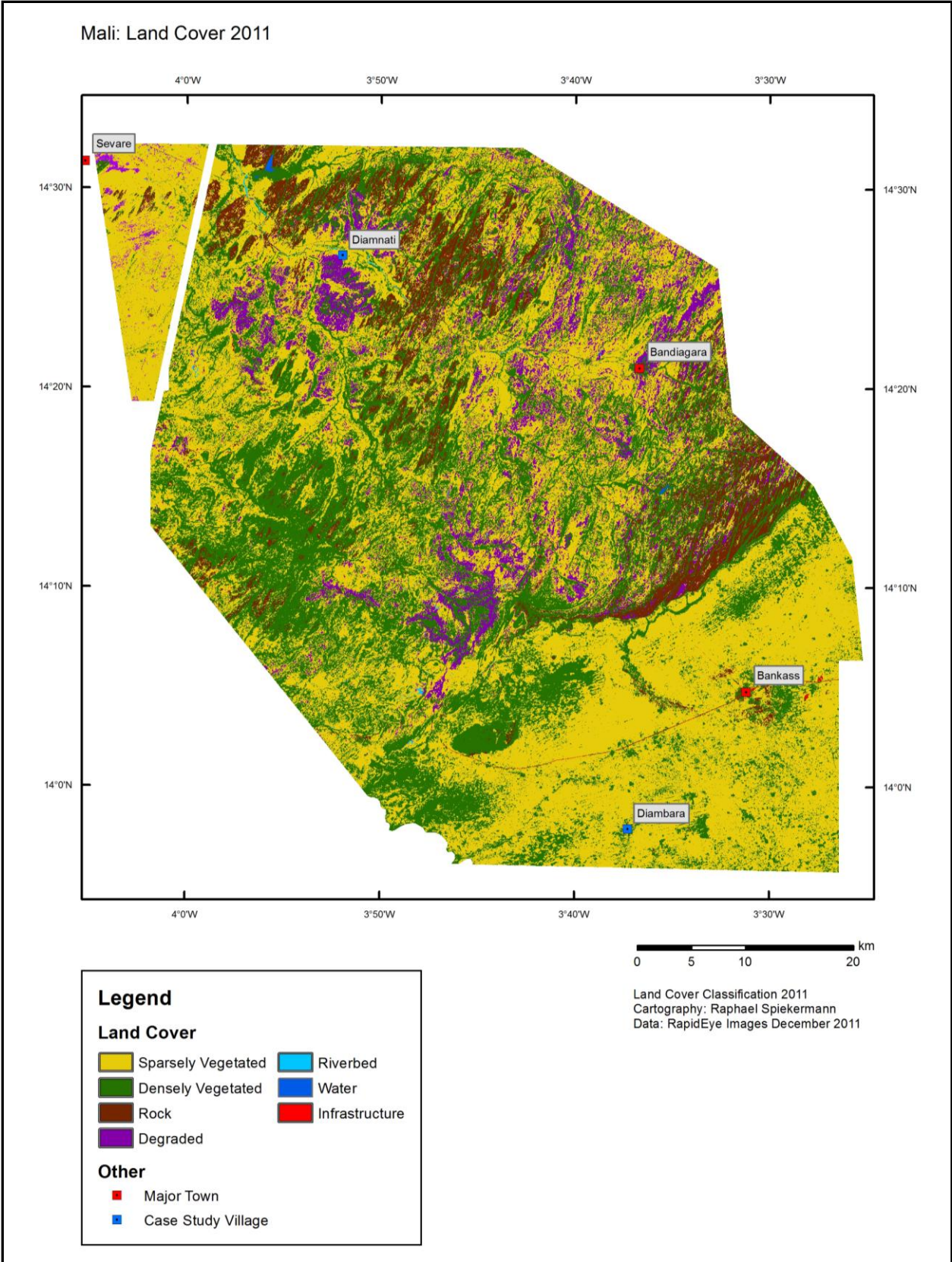


Fig.4.2: Land cover classification 2011.

Table 4.2: Land cover classification 2011 results (total area (ha) and percent).

<i>Class</i>	RE SP (ha)	RE DP (ha)	RE SP %	RE DP %
Sparsely Vegetated	69943.6	112819.2	73.2	44.3
Densely Vegetated	24629.0	93547.4	25.8	36.8
Rock	876.0	22494.9	0.9	8.8
Water	1.0	141.2	0.0	0.1
Riverbed	NA	338.4	NA	0.1
Degraded	NA	25155.4	NA	9.9
Infrastructure	159.8	NA	0.2	NA
Total Area	95609.5	254496.4	100.0	100.0

4.1.3 Land Cover Change 1967 - 2011

The land cover change map is displayed in Fig. 4.3 and shows the changes that occurred between 1967 and 2011 for all overlapping areas of the two datasets. Bearing in mind that the land cover classifications use two different methods and datasets and the land cover map from 1967, as displayed in Fig. 4.1, only contains three classes compared to the seven of 2011, the change of land cover in regard to the two main classes –“Sparsely Vegetated” and –“Densely Vegetated” are of particular interest. As can be seen, large areas of the Seno Plains have been converted from densely vegetated to sparsely vegetated areas. This reflects major land use change in the Seno Plains during the last fifty years, most likely due to wide-spread population increase. During this time the land required for cropping purposes increased so that large areas of natural bush were cleared and prepared for cultivation. Exceptions do exist however where the reverse is shown to be true. An example is the area surrounding Bankass, which shows an increase of densely vegetated areas.

The changes on the plateau are far more diverse. Large, often clustered, degraded areas are visible, particularly in the northwest and south of the plateau. Interestingly enough, large areas to the southwest of the plateau, which in 1967 were sparsely vegetated, are now densely vegetated. The area in the northwest mainly experienced change to sparsely vegetated areas, with one of the exceptions the north-eastern tip of the airport just outside of Sevaré.

The land cover change between 1967 and 2011 is further summarized in Table 4.3 and shows the various changes that occurred during these 44 years. On the Dogon Plateau, 13% of the total area changed from densely vegetated to sparsely vegetated areas. However 14.1%, i.e.

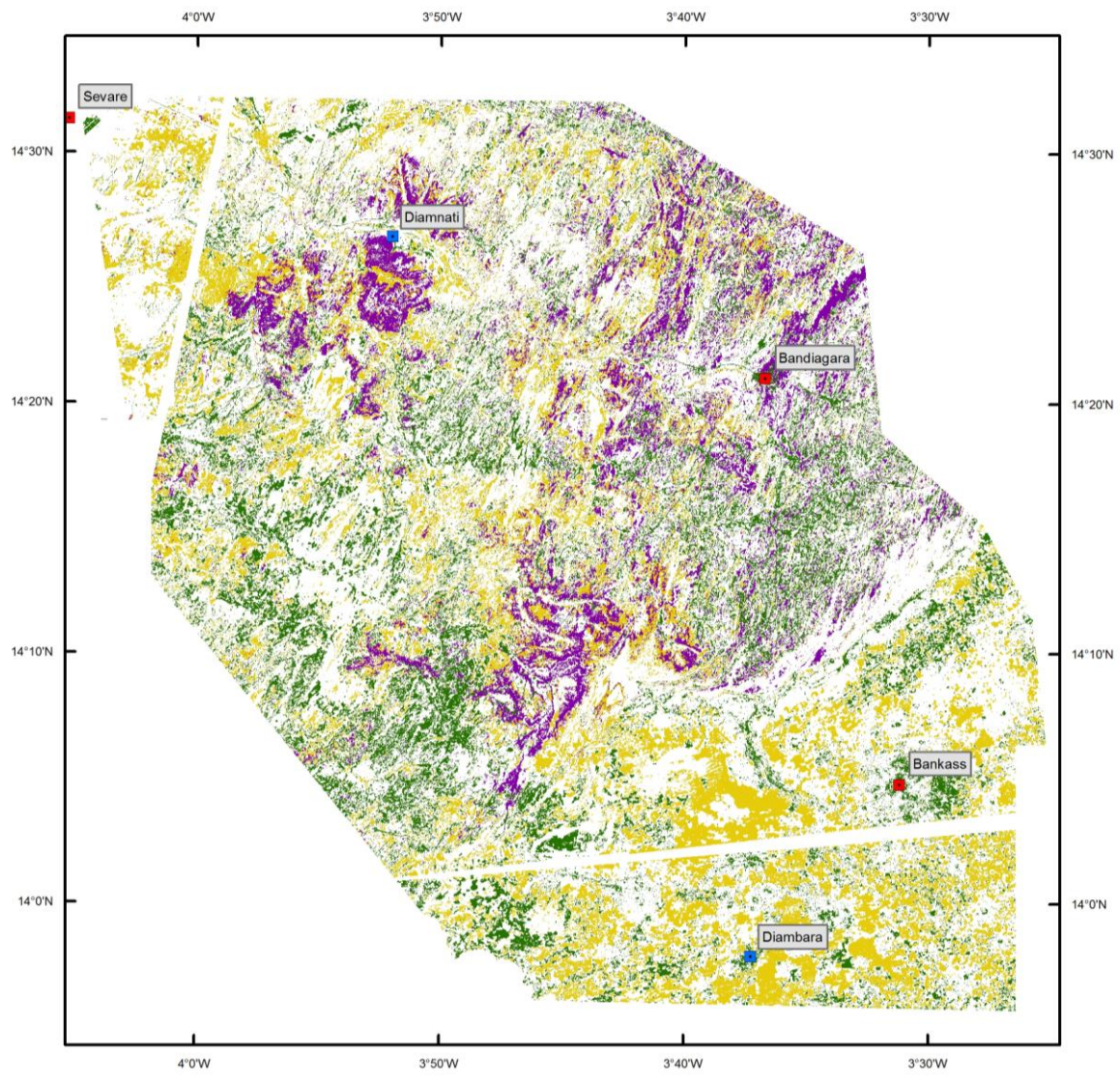
879,000 ha, changed from densely vegetated to sparsely vegetated land cover. The 25,000 ha of degraded areas classified originate from densely and sparsely vegetated areas alike, with 3.5% of the total area changing from densely vegetated to degraded land and 6.2% of all areas changing from sparsely vegetated to degraded land.

Table 4.3: Land cover change 1967 – 2011 in hectare and percent. DV: Densely vegetated; SV: Sparsely vegetated; R: Rock; W: Water; RB: Riverbed; I: Infrastructure.

Change Code	DP Change (ha)	DP Change (%)	SP Change (ha)	SP Change (%)
DV-SV	32362.1	13	24487.3	26.6
DV-DV	53367.7	21.4	12242.1	13.3
DV-R	902.3	0.4	198.5	0.2
DV-W	36.4	0	0.2	0
DV-RB	144.8	0.1	0	NA
DV-D	8764.7	3.5	0	NA
SV-SV	78270	31.4	42661.8	46.4
SV-DV	35157.5	14.1	11623.3	12.6
SV-R	1584.8	0.6	630.2	0.7
SV-W	95.7	0	0.8	0
SV-RB	193	0.1	0	NA
SV-D	15495.5	6.2	0	NA
R-SV	1905	0.8	0	NA
R-DV	0	0	0	NA
R-R	19998.7	8	0	NA
R-W	0	0	0	NA
R-RB	0.2	0	0	NA
R-D	862.6	0.3	0	NA
DV-I	0	NA	20.7	0
SV-I	0	NA	127	0.1
Total	249140.9	100	91991.8	100

To show the extent of land cover changes at a large scale, two case study sites – one on the plateau and one on the plains – will be presented in the following two chapters. This will also assist in understanding of the methods explained above and show the spatial differences at village level.

Mali: Land Cover Change 1967 - 2011



Legend

Land Cover Change

- Densely Vegetated to Sparsely Vegetated Areas
- Sparsely Vegetated to Densely Vegetated Areas
- Change to Degraded Areas

Other

- Major Town
- Case Study Village



Land Cover Change 1967 - 2011
Cartography: Raphael Spiekermann
Data: Corona Images December 1967,
RapidEye Images December 2011

Fig.4.3: Land cover change 1967-2011.

4.1.4 Case Study: Diamnati

To exemplify the land cover (changes) at a large scale on the Dogon Plateau, the area surrounding the village of Diamnati (the exact location can be seen in Fig. 4.1 and Fig. 4.2) is presented. The two images used as the data base are shown in Fig. 4.4. Already here the land cover can be identified to a certain extent. The Corona image of 1967 shows Diamnati village (the huts are shown in the window) with the Yamé River to the north and the cleared fields surrounding the village. Diamnati was founded in 1954 in agreement with the nearby town of Fiko (which until today has rights to the land) by families emigrating from the Seno Plains. Within thirteen years since the first families arrived, fairly large areas have already been cleared for cultivation. To the south typical formations of tiger bush can be identified. This area must have been very dense bush, which was used primarily for gathering wood. At that time, according to information provided by the village chief, lions could still be found roaming through these untouched areas.

In 2011, the RapidEye image shows the same fields to the east of Diamnati village with many large trees covering and surrounding the fields. Within the village itself, large fully grown trees offer relief from the sun. To the southwest of Diamnati, what was once tiger bush is now to a large extent free of vegetation and represents a typical form of degraded land. Only remnants of the tiger bush remain, seen here as a skeleton-like pattern. Even in the 1980s, the vegetation here was much denser than today (see Brandt *et al.*, in review) and the degradation continues.

Fig. 4.5 shows the results of the classifications for the years 1967 and 2011 for the same case study area of Diamnati. As can be seen, the detail in 1967 is not as great as in 2011 with the Yamé River mostly classified as densely vegetated, due to the trees surrounding the river, but in general the classification is reasonably good when compared to the data base in Fig. 4.4 and the photographic evidence in Fig. 4.6. Due to the additional land cover classes for 2011, the detail of the land cover map is much better and also more accurate. Groups of trees on the fields and even within the village are correctly classified as densely vegetated areas. The sparsely vegetated cropland areas are also classified correctly and the magnitude of degraded land may at first seem exaggerated but truly represents an accurate account of the reality on the ground, as shown by the photos in Fig. 4.6. Furthermore, the class "Riverbed" accurately shows the location of the then dry Yamé riverbed, however also depicts an area obviously "falsely" classified to the west of Diamnati village. At closer inspection, this area is formed by the accumulation of fluvial deposits originating from the gentle slopes to the southwest and is thus similar in nature to a riverbed, i.e. composed of very fine-grained material, as seen in Fig. 4.6-D2.

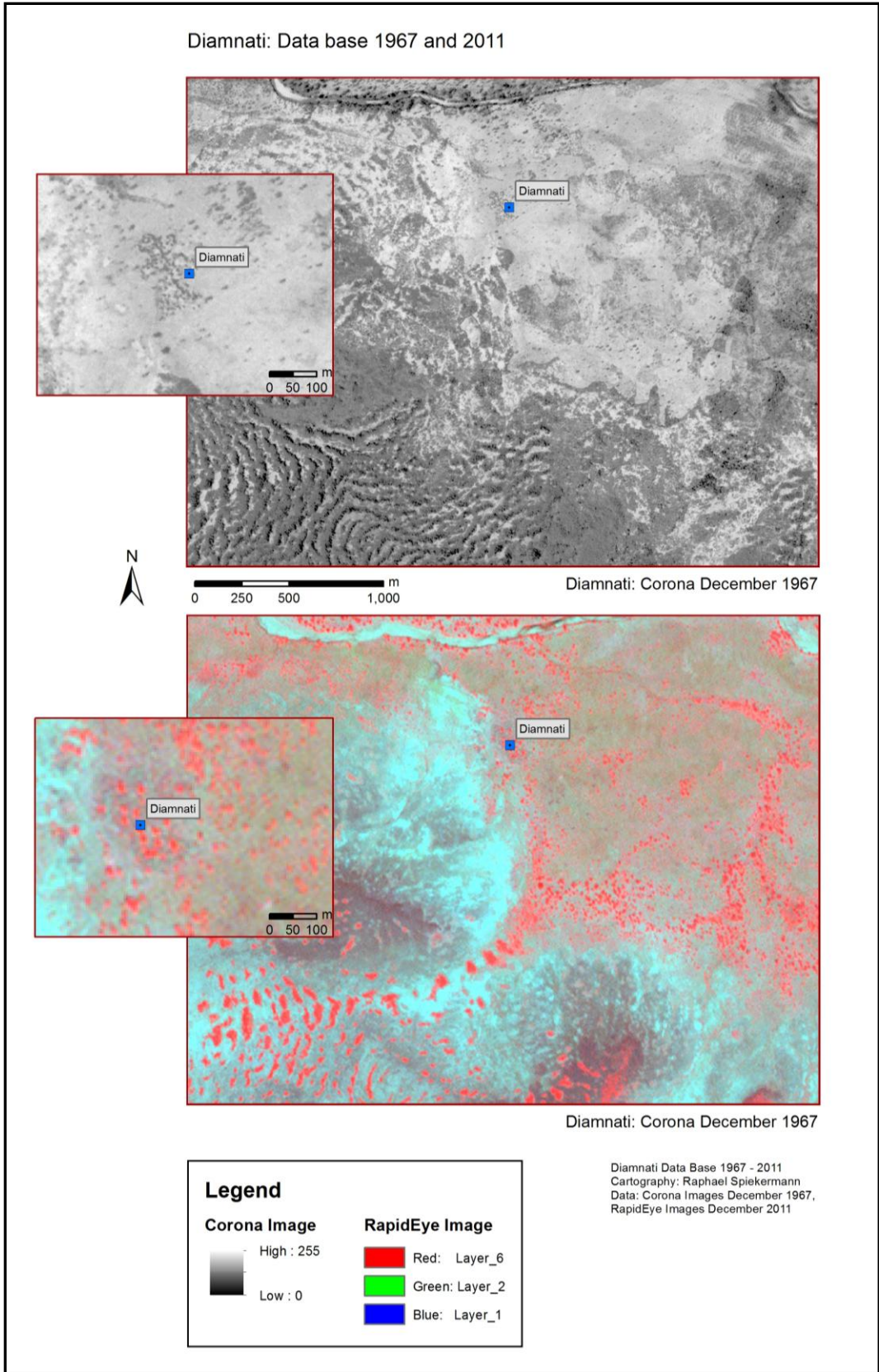
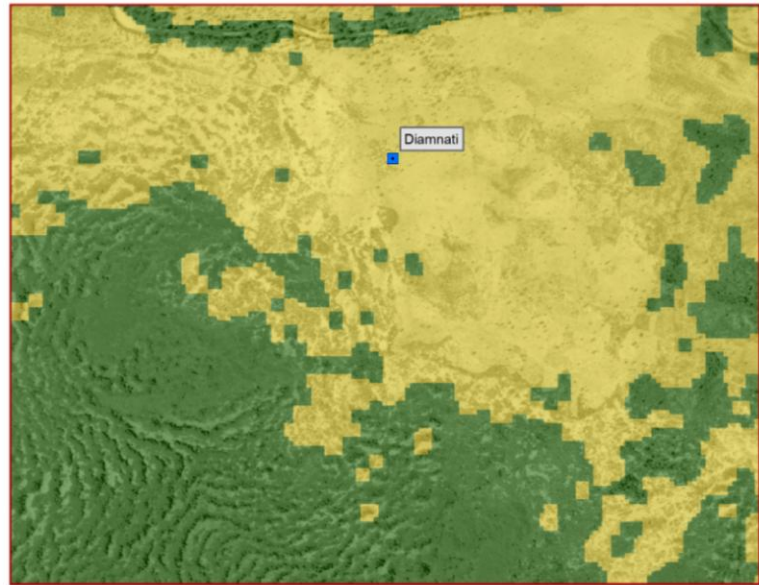
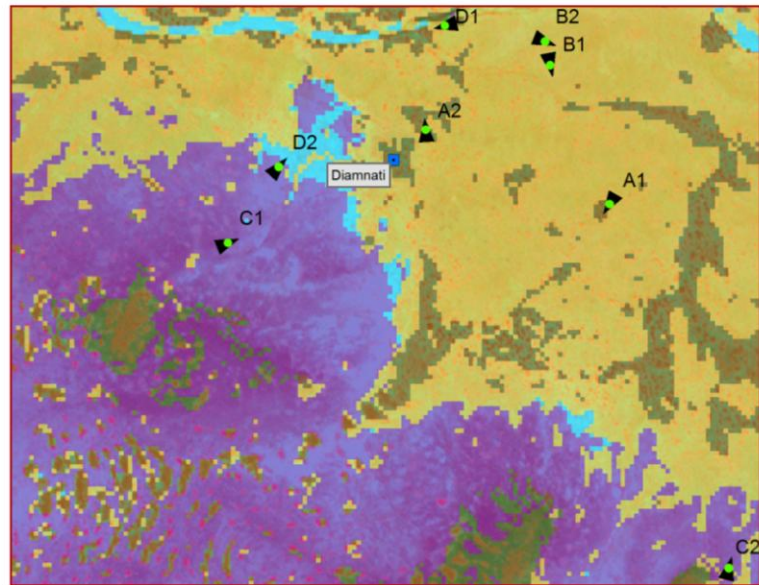


Fig. 4.4: Diamnati, Dogon Plateau: Data base 1967 and 2011.

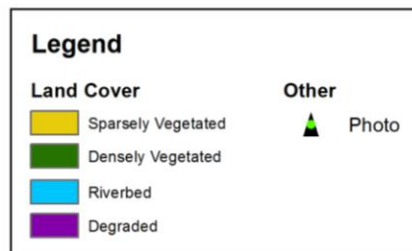
Diamnati: Land Cover 1967 and 2011



Diamnati: Corona December 1967



Diamnati: RapidEye December 2011



Diamnati Land Cover 1967 and 2011
 Cartography: Raphael Spiekermann
 Data: Corona Images December 1967,
 RapidEye Images December 2011

Fig. 4.5: Diamnati, Dogon Plateau: Land cover classification 1967 and 2011.



Fig. 4.6: Photographs of land cover types in the Diamnati case study area: A1, A2: Densely vegetated cropland; B1, B2: Sparsely vegetated cropland and fallow; C1, C2: Degraded land; D1, D2: Examples of the "Rierbed" class.

Fig. 4.7 is a map showing the changes to the land cover for the Diamnati area between 1967 and 2011. On the one hand, tree growth on fields has led to an increase of densely vegetated areas, and presents a typical form of agroforestry. Additional clearing of former bush fallow areas, particularly in the southeast has increased the sparsely vegetated areas. The most astonishing change that occurred is the extent to which the densely vegetated tiger bush in the southwest has become degraded land. Almost half of the case study area is now degraded and cannot be used for agricultural purposes apart from grazing during the wet season where patches with a thin layer of soil enable grass to grow.

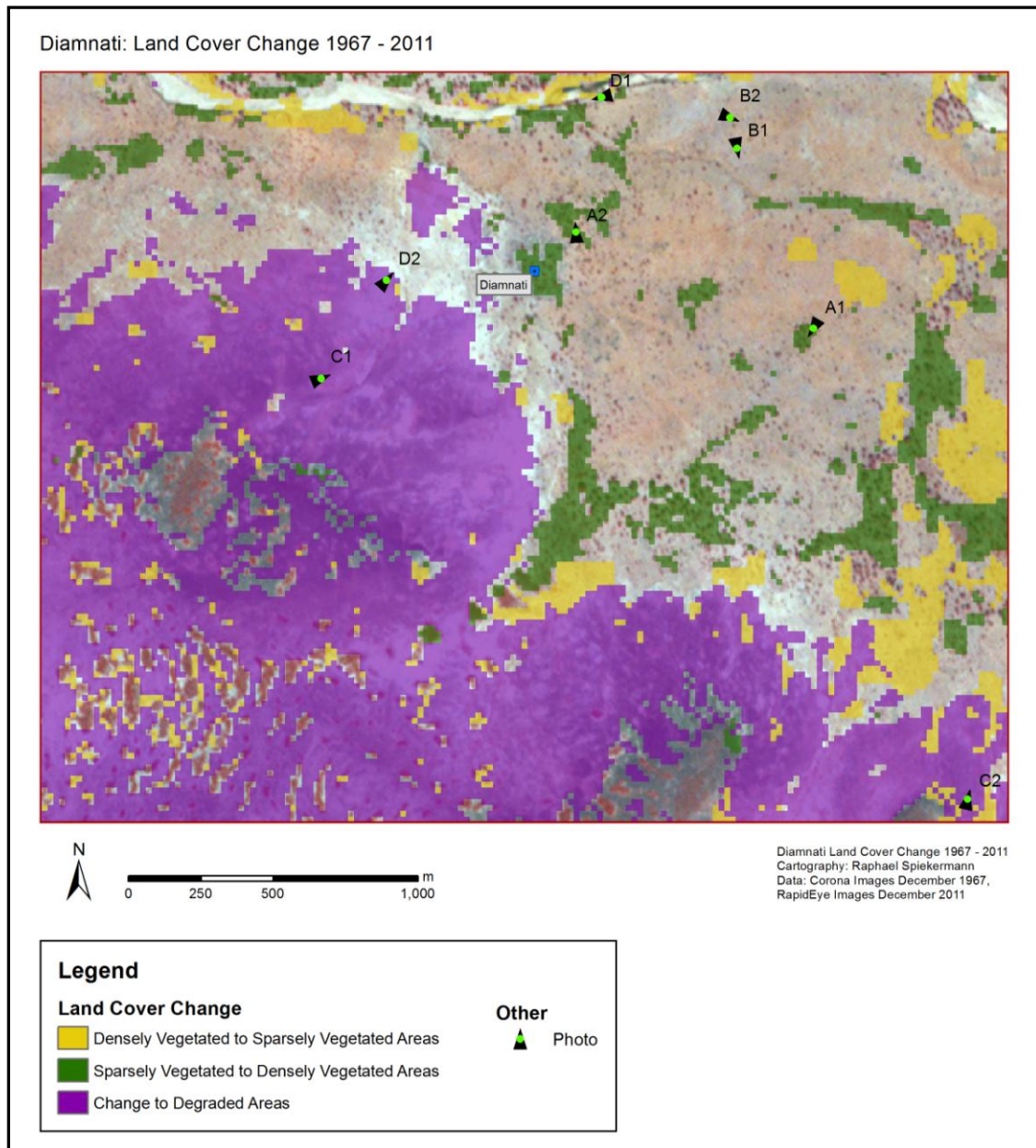


Fig. 4.7: Diamnati, Dogon Plateau: Land cover change 1967-2011.

4.1.5 Case Study: Diambara

Diambara is a typical village on the Seno Plains and is located in the far south of the study area (see Fig. 4.1 and Fig. 4.2). Diambara has had no outside influence by external projects such as the area around Bankass. Therefore the assumption is made that the development of the Diambara area has progressed “naturally”, i.e. with limited external disturbances. This case study intends to show the changes to the land cover that has occurred for a number of reasons and typifies the overall change on the Seno Plain. Fig. 4.8 shows the data base images used for the assessment. In the Corona image, the location of Diambara is given and the large-scaled window enables the exact location of the groups of buildings to be identified. The RapidEye image (at the same scale) shows the same extent of the Seno Plains around Diambara in 2011. The window shows that the village has grown in the last fifty years, particularly the group of buildings in the southwest of the large-scaled window. The NDVI band (red layer) shows that a large number of trees are located within the village itself, and particularly in the immediate surroundings of the village. The darker shades of grey on the Corona image to the east and south of Diambara represent typical bush fallow areas, which have been classified as “Densely Vegetated” (see Fig. 4.9). These areas no longer exist as such in 2011. However, due to an increase of woody vegetation on the sparsely vegetated fields surrounding Diambara, many of the cultivated areas are classified as “Densely Vegetated” areas. Almost a total reverse of land cover has thus occurred in the space of half a century (see the land cover change map in Fig. 4.10). Tree growth has obviously been encouraged by farmers on the older fields that are used for cropping. A more detailed look at tree density and cover will be given in the following chapter and the land cover changes are discussed in chapter 5.

Diambara: Data base 1967 and 2011

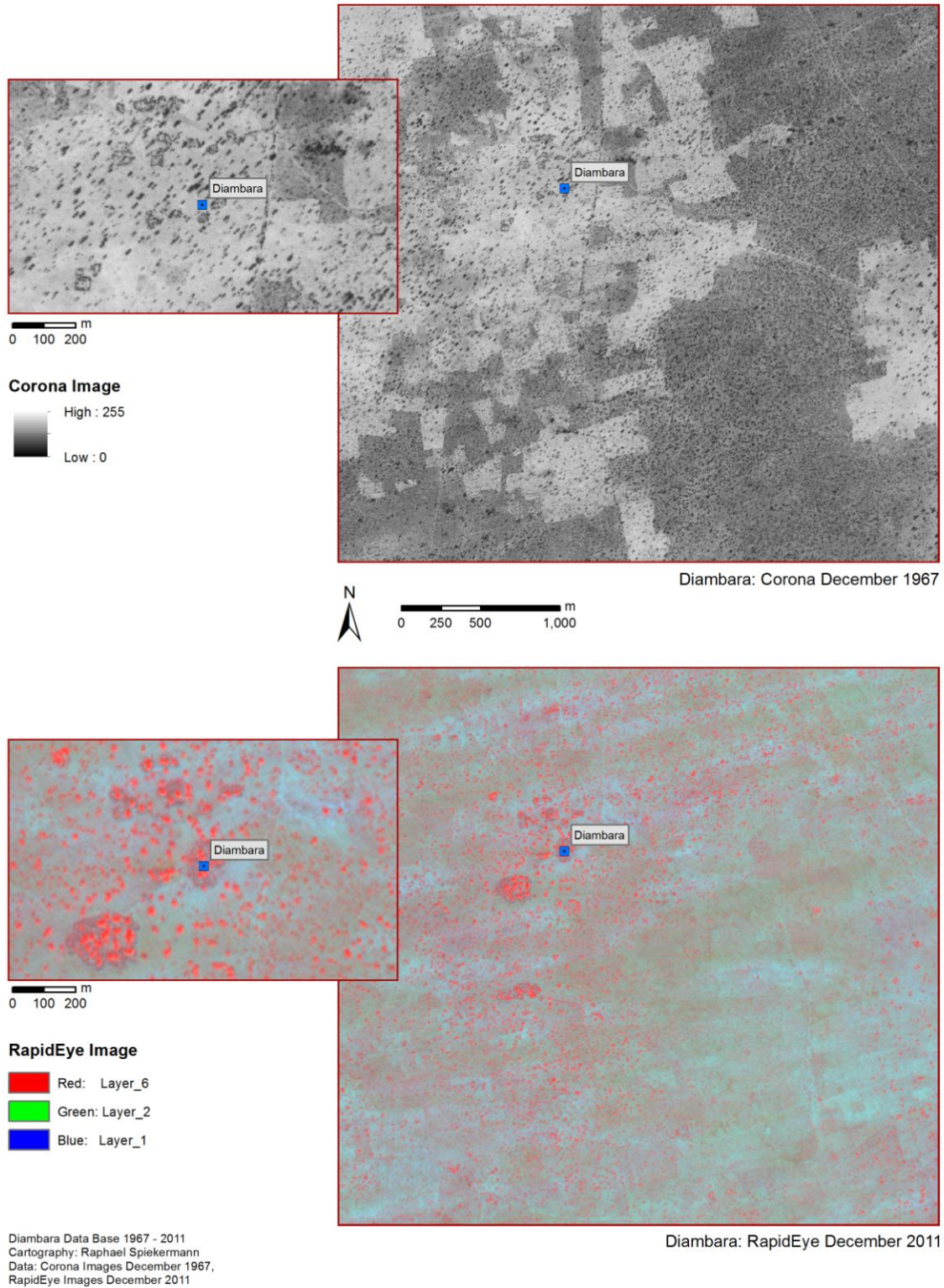


Fig. 4.8: Diambara, Seno Plains: Data base 1967 and 2011.

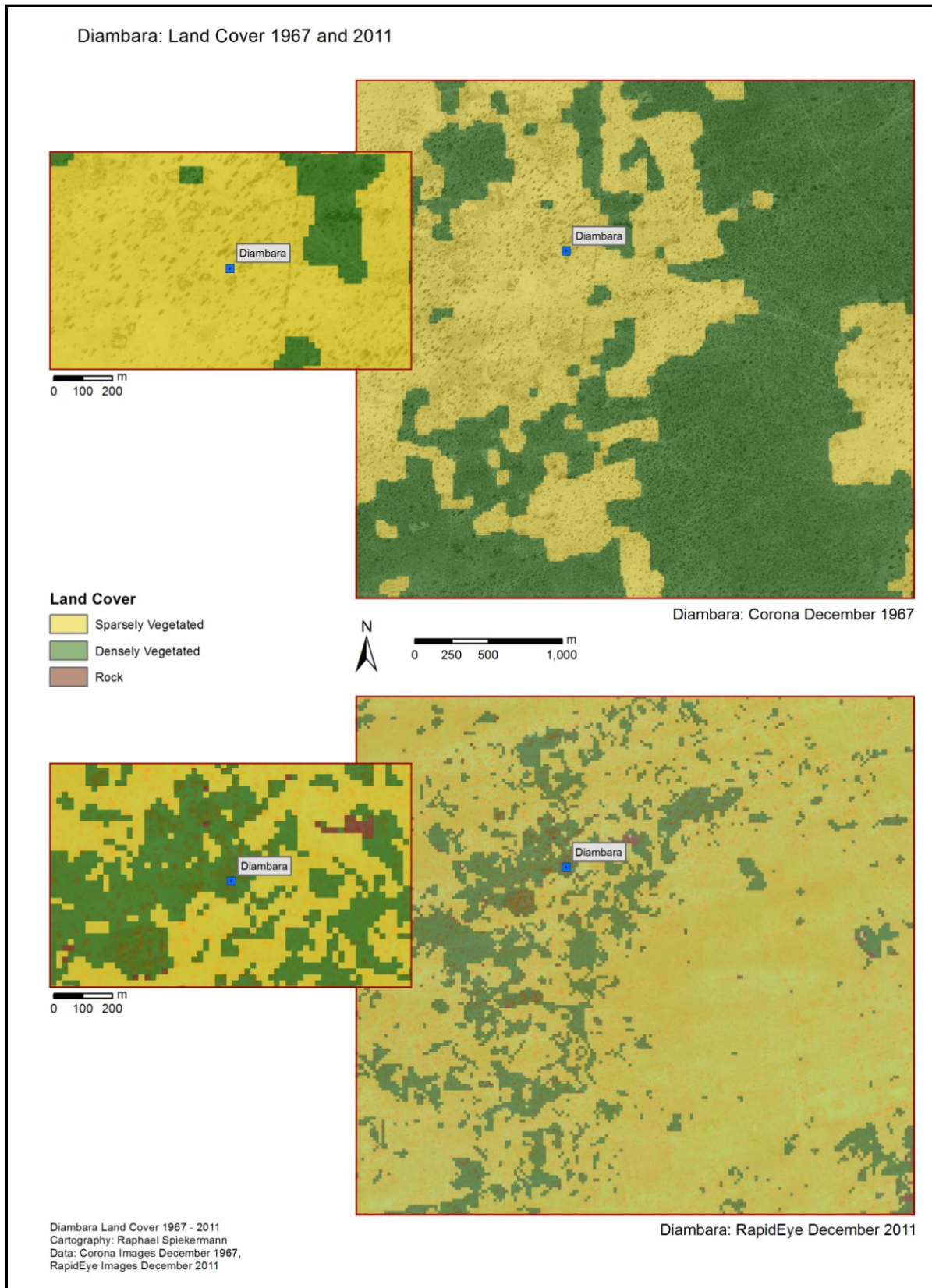
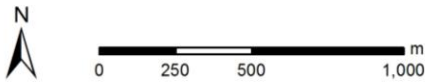
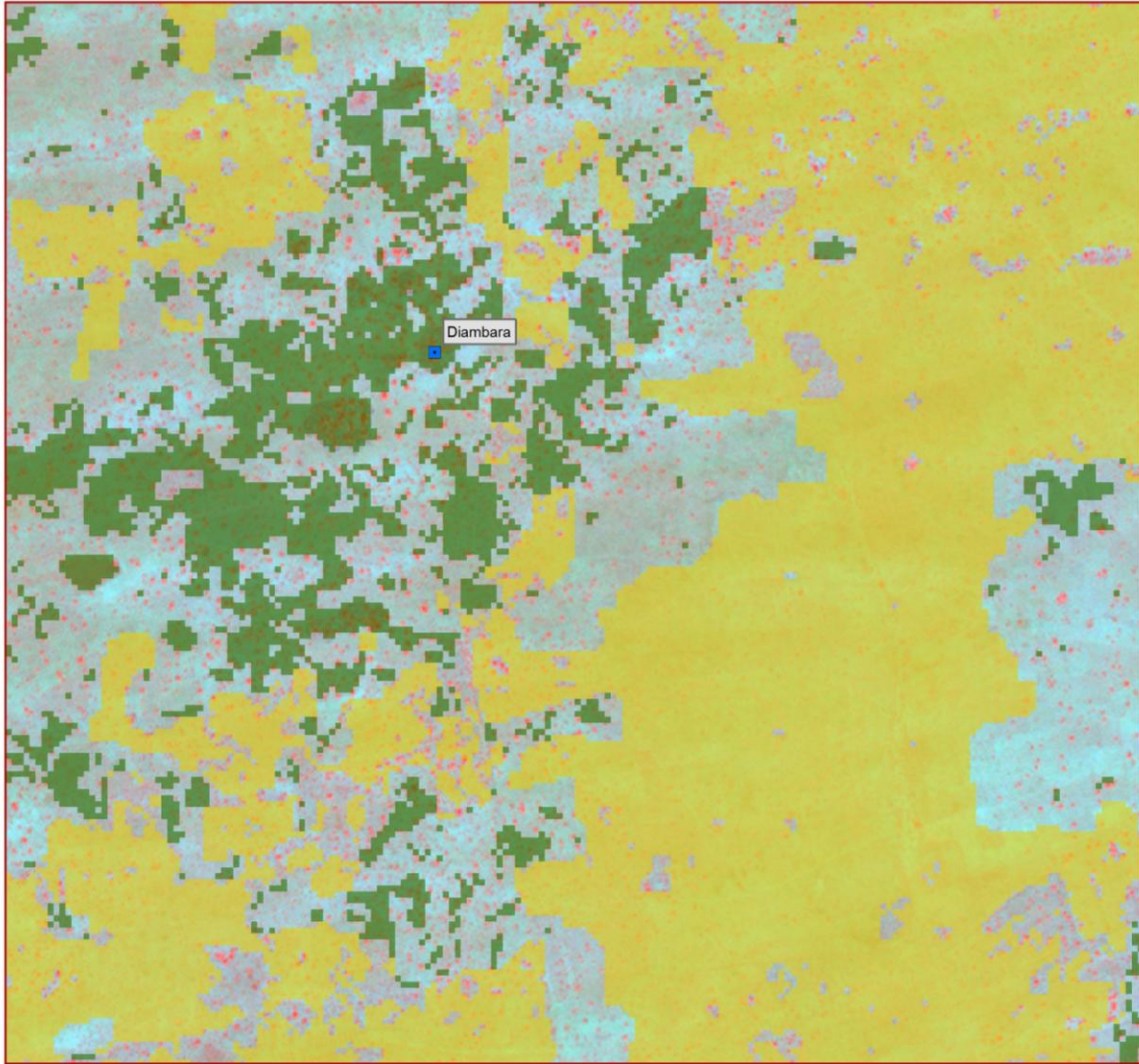


Fig. 4.9: Diambara, Seno Plains: Land cover classification 1967 and 2011.

Diambara: Land Cover Change 1967 - 2011



Diambara Land Cover Change 1967 - 2011
Cartography: Raphael Spiekermann
Data: Corona Images December 1967,
RapidEye Images December 2011

Legend

Land Cover Change

-  Densely Vegetated to Sparsely Vegetated Areas
-  Sparsely Vegetated to Densely Vegetated Areas

Fig. 4.10: Diambara, Seno Plains: Land cover change 1967-2011.

4.2 Woody Vegetation Density and Cover

4.2.1 Woody Vegetation Density and Cover 1967 and 2011

The results of the woody vegetation feature extraction for 1967 and 2011 are displayed in Fig. 4.11 and Fig. 4.12 respectively. These maps show the woody vegetation density in number of features per hectare as each pixel is 100 x 100 m large. When comparing the woody vegetation density map of 1967 with the land cover map of 1967 in Fig. 4.1, certain correlations are visually identifiable. The areas of dense vegetation, i.e. the bush fallow, clearly exhibit a higher density than the cropland areas with sparse vegetation. The pattern in the Seno Plains is particularly clear. The missing information (white signature) on the plateau is mainly due to the fact that the woody vegetation feature extraction was not carried out for areas classified as "Rock". The areas coloured brown represent areas where the features were larger than one hectare so that the number of trees could only be approximated, as described above. These features represent areas with very dense vegetation so that the individual trees cannot be singularly extracted due to the lacking contrast. These relatively small amounts of pixels are displayed in brown in order to distinguish between the two different models used.

The same woody vegetation density classes are used for 2011 and thus summarize the results of the feature extraction at the same scale of 100 x 100 m in Fig. 4.12. The map at first sight looks much "emptier" or lighter, i.e. most pixels are represented by the classes "4-5" or "5-10" features per hectare. Again various linear features are identifiable and show the location of river valleys and gorges with greater woody vegetation density. Regions with higher vegetation density may be identified, especially in the northwest of the plateau and the area surrounding Bankass. A "hot spot" of low density is located ten to fifteen kilometres west of Bankass on the fossil sand dunes west of a large river valley coming from the Bandiagara escarpment. The woody vegetation density in this particular area north of Dimal on the Seno Plains (see Fig. 3.4 for location) has obviously seen a stark decrease in past decades, similar to other areas where changes to land use have caused the same effect.

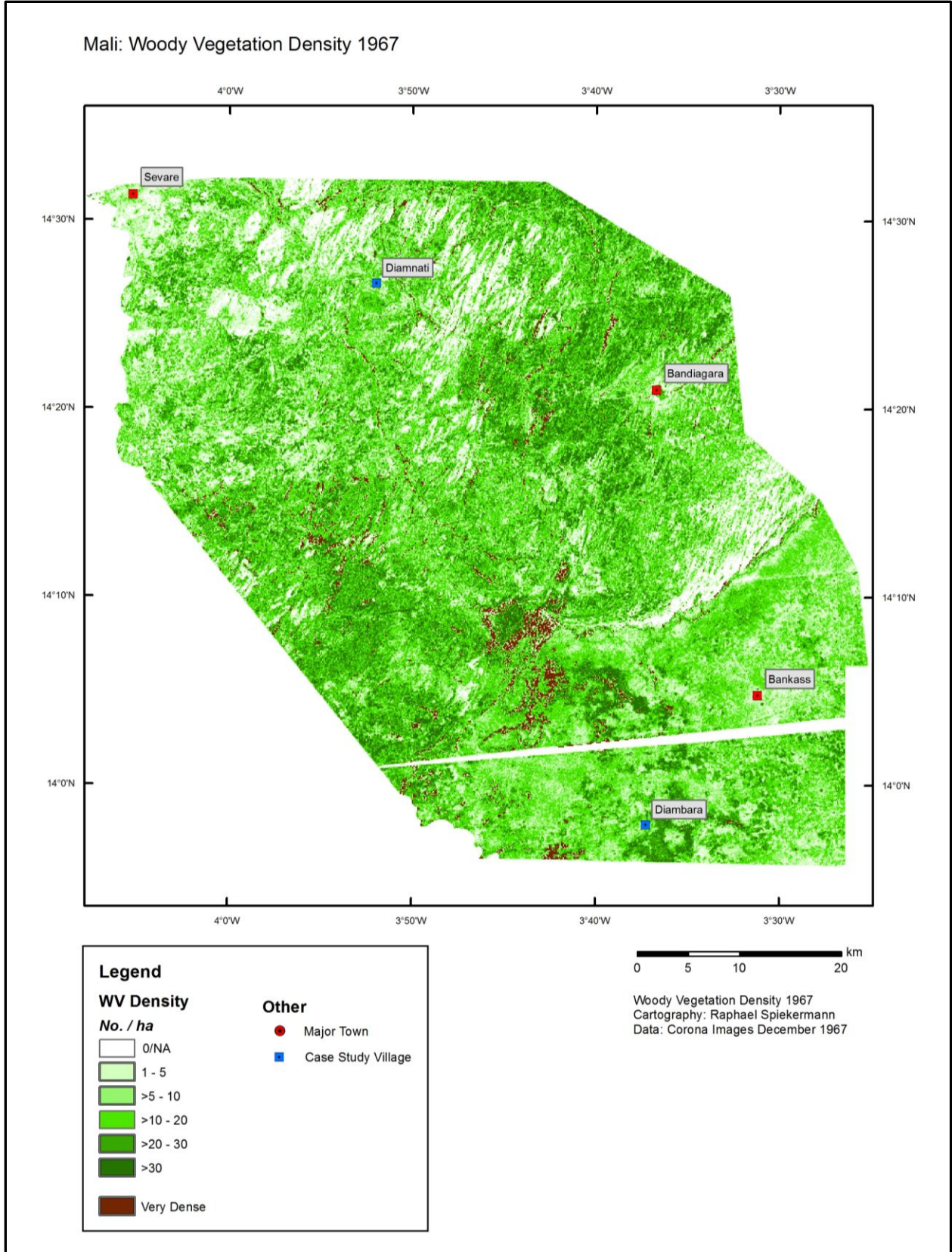


Fig. 4.11: Woody vegetation density map of study area 1967.

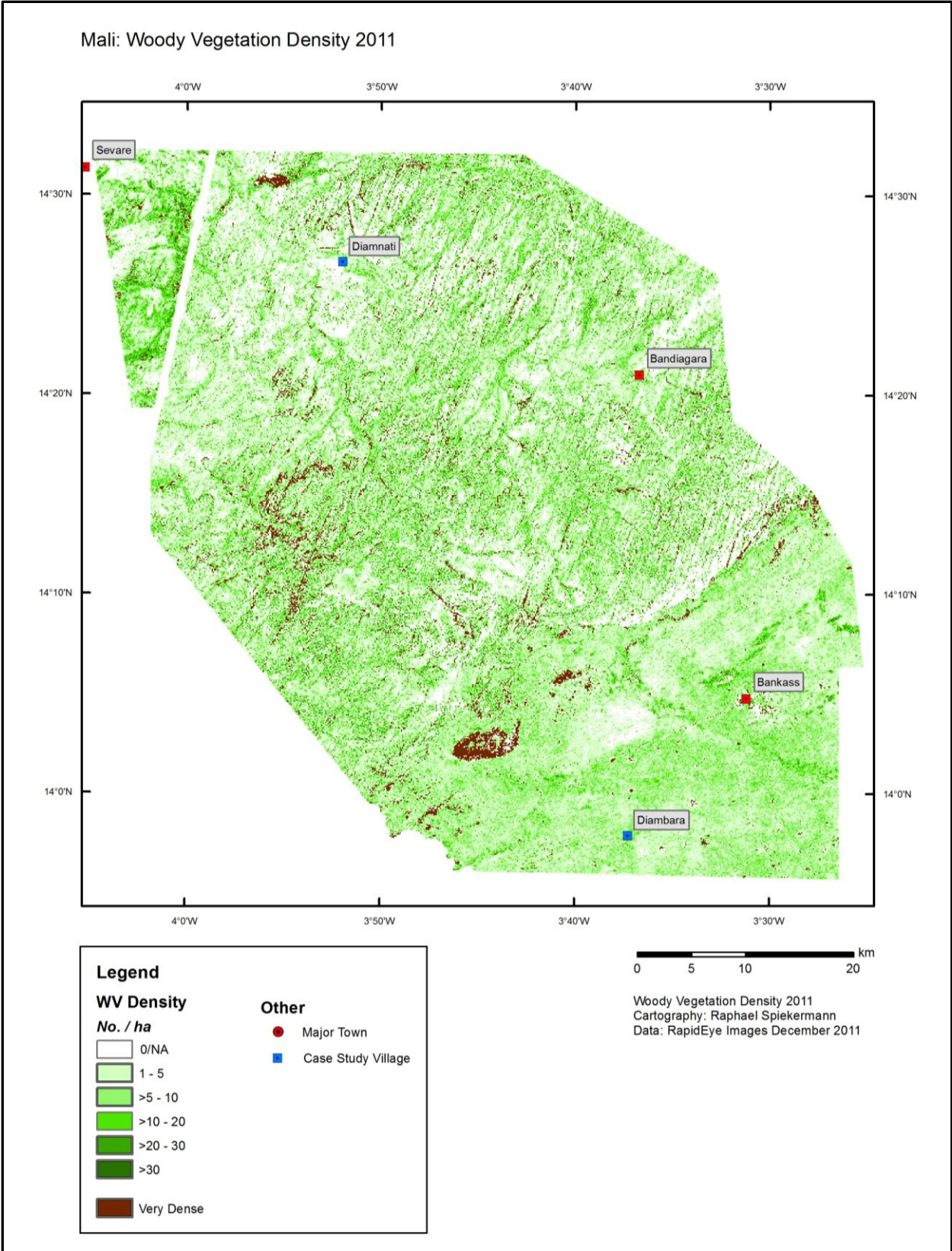


Fig. 4.12: Woody vegetation density map of study area 2011.

The statistics of the 5.75 million polygons representing large shrubs, trees and groups of trees are presented in Table 4.4. 4,587,193 polygons were mapped in the Corona dataset with a total area of 43,899.8 ha. In comparison only a quarter as many, i.e. 1,158,512 features are extracted in the RapidEye images; however with a similar total area of 41,662.5 ha. The individual features are thus on average four times the size of the features extracted with the Corona images. The mean area of a polygon for Corona is 105 m² compared to 389 m² of RapidEye.

Table 4.4: Summary of feature extraction results for each Corona and RapidEye image part.

Dataset	No. Polygons	Total Area (m ²)	Mean Area (m ²)	Min. Area (m ²)	Max. Area (m ²)	StD Area (m ²)
CSPSV	492590	52826597.7	107.24253	4.5	9700.387682	166.1191
CSPDV	626615	73800541.5	117.776	5.2	3103167.2	5321.76
CDPSV	2180747	151360118.4	69.4	6.0	4100.1	171.9
CDPDV	1287241	161010495.4	125.1	6.0	4612726.3	5581.9
RESPSV	363421	56289684.8	154.9	4.8	779792.2	1621.6
RESPDV	59401	37938154.2	638.7	40.3	9372150.3	39256.2
REDPSV	378895	160756881.1	424.3	15.5	40190.8	1142.9
REDPDV	270178	145381916.5	538.1	12.4	2093653.4	7666.0
REDP07	86617	16257981.6	187.7	12.4	301120.2	1733.1

Table 4.5 offers more detail of the feature extraction results. As is described in the Methods chapter above, the results are classified according to size to produce the density and vegetation cover maps. Once again, it can be seen that the size of the features mapped is considerably different with only 5.6% and 8.9% of the features on the plateau (1967) and on the plains (1967) being larger than 225 m² respectively. In comparison, 26.2% of all features extracted from the RapidEye image on the plateau are larger than 225 m², which corresponds to the size of nine 5 meter pixels of the RapidEye image, and means that this significant proportion of all features represents groups of woody vegetation.

The first subset of Table 4.5 displays the results of the woody vegetation density assessment for all features smaller than one hectare (D1). The mean density is higher on the Dogon Plateau compared to the Seno Plains both in 1967 and 2011. In 1967 the mean density on the Dogon Plateau was 15.1 trees per hectare (trees here includes all types of woody vegetation) compared to the 13.4 trees per hectare on the Seno Plains. In 2011 the mean density on the Dogon Plateau, again for all features smaller than 1 hectare, was 7.1 trees per hectare on the plateau and 5.9 trees per hectare on the plains.

As for the features greater than one hectare (D2), the woody vegetation density is entirely modelled, thus the results listed are most likely very inaccurate. In general, these polygons represent areas with a high woody vegetation density, which is why the pixels in the Corona images and RapidEye images are grouped into single polygons. However polygons with an area greater than one hectare are limited in number when compared to the number of those smaller than one hectare. Because of the difficulty to assess the true number of trees represented by these areas, the density maps display these areas as areas with very dense woody vegetation coverage (brown symbology of maps in figures 4.11 and 4.22).

In a similar manner to the density maps, the woody vegetation cover maps for both 1967 and 2011 are displayed in Fig. 4.13 and 4.14 respectively. The pixel size now is 250 m and the cover is determined by the total area of all features within a 250 m pixel given in percent of the total possible area, i.e. 250 m x 250 m. Features larger than one of these pixels, i.e. larger than 62,500 m² are displayed qualitatively in blue as very high coverage. The cover map of 1967 naturally has a similar trend to the woody vegetation density map in Fig. 4.11. Particularly on the Seno Plains, the patterns similar to that of the land cover maps are visible. It may be assumed that areas with a cover of greater than 20% represent areas of dense natural vegetation and areas with coverage below 20% most likely signify cropland.

In comparison with the woody vegetation density maps, the two cover maps are surprisingly similar. In 2011 the general coverage ranges between 10% and 30%, similar to that of 1967. Again the Bankass region stands out as an area of high coverage on the Seno Plains and the same gap north of Dimal is again present here. The coverage on the plateau is in general higher than on the Seno Plains with many more pixels attributed values greater than 30% cover.

The statistics in the lower half of Table 4.5 offer further detailed information regarding the coverage. The coverage of woody vegetation in 1967 and 2011 is in contrast to woody vegetation density fairly similar, as can be seen by the number of 250 m by 250 m pixels of coverage smaller than 62,500 m² in Table 4.5 (C1). The mean coverage in percent of each pixel is greater in 2011 on the plateau than in 1967 (11.8% to 10.1% respectively). On the other hand, the plains in 2011 have a much lower mean coverage in 2011 with 7.8% than in 1967 with 11.2%. The number of polygons with very high coverage (C2), i.e. polygons with an area that exceeds the pixel area, is limited in number for both years.

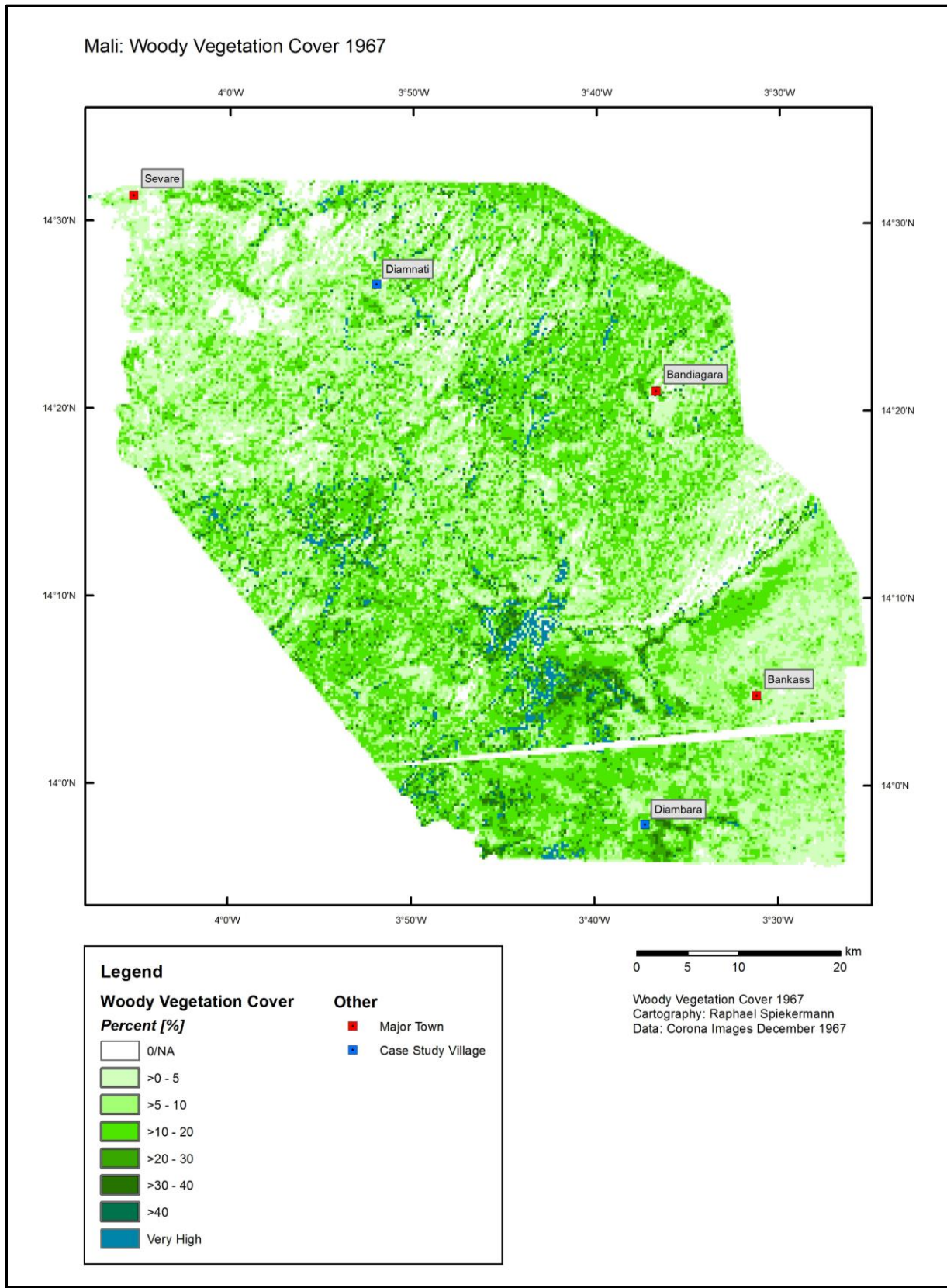


Fig. 4.13: Woody vegetation cover map of study area 1967.

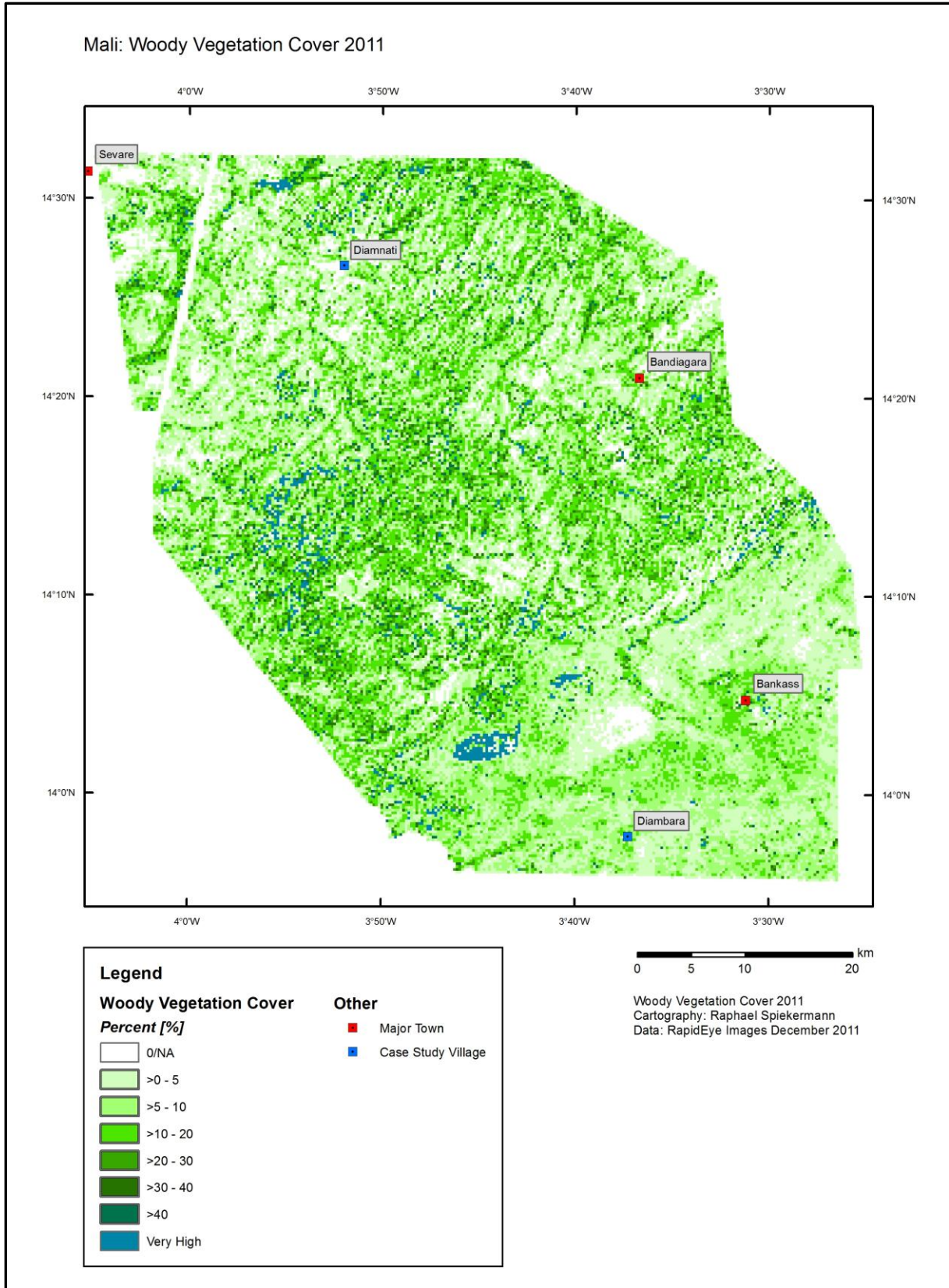


Fig. 4.14: Woody vegetation cover map of study area 2011.

Table 4.5: Detailed statistics of woody vegetation feature extraction results, classified acc. year and plateau/plain.

Subset	Item	Corona Plateau	Corona Plains	RapidEye Plateau	RapidEye Plains
D1: WV smaller than 1 ha area (excl. 0 in statistics)	No. Polygons > 225m ² (%)	5.6	8.9	26.2	19.8
	No. Polygons (<10,000m ²)	3466687	1118870	732966	422448
	No. Pixels (100 x 100 m)	252492	91954	200277	87962
	Mean Density (trees/ha)	15.1	13.4	7.1	5.9
	Min. Density (trees/ha)	1.0	1.0	1.0	1.0
	Max. Density (trees/ha)	89.0	92.0	80.0	58.0
	StD. Density (trees/ha)	9.7	8.4	7.4	4.2
D2: WV greater than 1 ha area (excl. 0 in statistics)	No. Polygons (>10,000m ²)	1301	335	2724	374
	No. Pixels (100 x 100 m)	6531	2191	8035	2480
	Mean Density (trees/ha)	565.4	4078.8	882.0	16316.6
	Min. Density (trees/ha)	44.0	45.0	44.0	45.0
	Max. Density (trees/ha)	20501.0	14796.0	9305.0	41654.0
	StD. Density (trees/ha)	1337.0	5438.6	1175.3	19590.5
C1: Coverage of WV smaller than 62500 m ² (excl. 0 in statistics)	No. Polygons (<62,500 m ²)	3467794	1119145	735484	422779
	No. Pixels (250 x 250 m)	40556	14942	37301	14713
	Mean Coverage (% of 250m)	10.1	11.2	11.8	7.8
	Min. Coverage (% of 250m)	1.0	1.0	1.0	1.0
	Max. Coverage (% of 250m)	151.0	126.0	157.0	130.0
	StD. Coverage (% of 250m)	8.8	9.1	11.4	7.5
C2: No. Pixels with 100% Coverage	No. Polygons (>62,500 m ²)	194	60	206	43
	No. Pixels (250 x 250 m)	702	269	580	273

4.2.2 Woody Vegetation Density and Cover Change

4.2.2.1 Woody Vegetation Change

In order to compare the two density maps in a reasonable way, the change map in Fig. 4.15 may be viewed in combination with statistics listed in Table 4.6.

The change map shows a strong decrease overall, indicated by the orange and red tinge. Most of the yellow areas on the plateau, signifying no change, occupy the areas marked by the bare rock, for which the feature extraction was not carried out. Only minimal green positive areas may be identified. These are located in the Bankass region, along the Bandiagara escarpment

to the north of Bankass and in particular in the northwest of the plateau. However the majority of the study area is marked by a decrease of at least -5 trees/shrubs per hectare.

Table 4.6 offers more detail. Of the 254,489 ha that changed on the plateau during the given time period, only 18% saw an increase of woody vegetation compared to 76% with a decrease. Similarly, 16% of the 93,381 ha on the Seno Plains increased in woody vegetation, with 80% showing negative change. The mean change on the plateau is – 8.7 trees per hectare and -8.2 on the plains. The direction of change of the pixels representing the features greater than one hectare is relatively even for both the plateau and plain (–change to very dense areas”). Possible reasons for this negative change obviously have to do with the number and average size of the extracted individual polygons. This will be discussed in more detail below in chapter 5.

Table 4.6: Summary of woody vegetation density change 1967 – 2011.

Woody Vegetation Density Change 1967 - 2011	Statistics	Plateau	Plains
WV smaller than 1 ha area (D1)	No. Pixels Total (100 x 100 m)	254489	93381
	Positive Change (%)	17.9	15.9
	Negative Change (%)	76.0	79.6
	No Change (100 x 100 m)	6.0	4.5
	Mean Density Change (trees/ha)	-8.7	-8.2
	Min. Density Change (trees/ha)	-89.0	-88
	Max. Density Change (trees/ha)	69.0	57
WV greater than 1 ha area (excl. 0 in statistics) (D2)	StD. Density Change (trees/ha)	12.01	34.2
	No. Pixels Total (100 x 100 m)	13089	4036
	Positive Change (%)	55.6	47.4
	Negative Change (%)	44.4	52.6
	Mean Density Change (trees/ha)	-366.0	1906.9
	Min. Density Change (trees/ha)	-20501.0	-14796.0
	Max. Density Change (trees/ha)	9305.0	41654.0
	StD. Density Change (trees/ha)	3016.6	9476.3

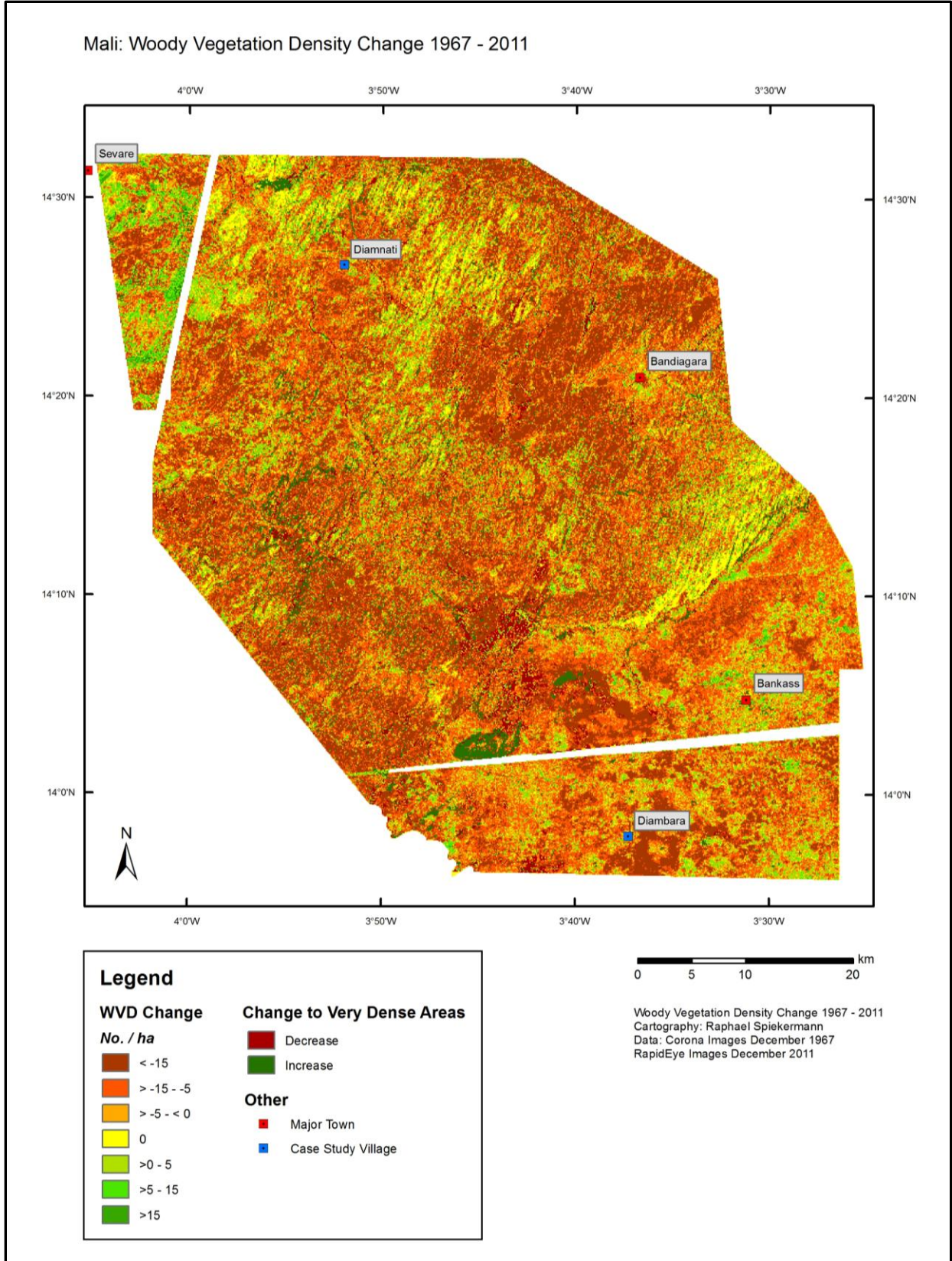


Fig. 4.15: Woody vegetation density change 1967 – 2011.

4.2.2.2 Woody vegetation cover change

In regard to the change to cover, the overall impression offered by the change map in Fig. 4.16 is rather positive, supported by the statistics in Table 4.7. 45% of the change on the plateau is positive, which is comparatively high given the change of the woody vegetation density, which is shown to be overall negative. 43.7% of pixels on the plateau saw a decrease of coverage, which is low compared to the 61.6% of pixels that decreased in woody vegetation coverage on the plains. Again the area surrounding Bankass is a hotspot for positive change and the fossil dunes generally show a decrease (including the area around Gama, as described in the introduction above) as well as areas which have been cleared for cropping during the past fifty years. Coverage has largely decreased in areas that are classified as “Degraded” in the land cover classification of 2011 on the plateau (compare with Fig. 4.2).

Possible reasons for the major differences between the woody vegetation density and cover maps will be discussed in the following chapter. First though, the results of the density and cover classifications are analyzed according to land cover class.

Table 4.7: Summary of woody vegetation cover change 1967 – 2011.

Woody Vegetation Cover Change 1967 - 2011		Plateau	Plains
Cover of WV smaller than 62500 m ² (C1)	No. Pixels (250 x 250 m)	40885	14957
	Positive Change (%)	44.9	25.4
	Negative Change (%)	43.7	61.6
	No Change (%)	11.4	13.0
	Mean Cover Change (%)	0.6	-4.3
Cover of WV greater than 62500 m ² (C2)	StD. Density Change (trees/ha)	13.2	11.0
	No. Pixels (250 x 250 m)	1148	472
	Positive Change (%)	49.9	48.9
	Negative Change (%)	39.5	43.0
	No Change (%)	10.6	8.1

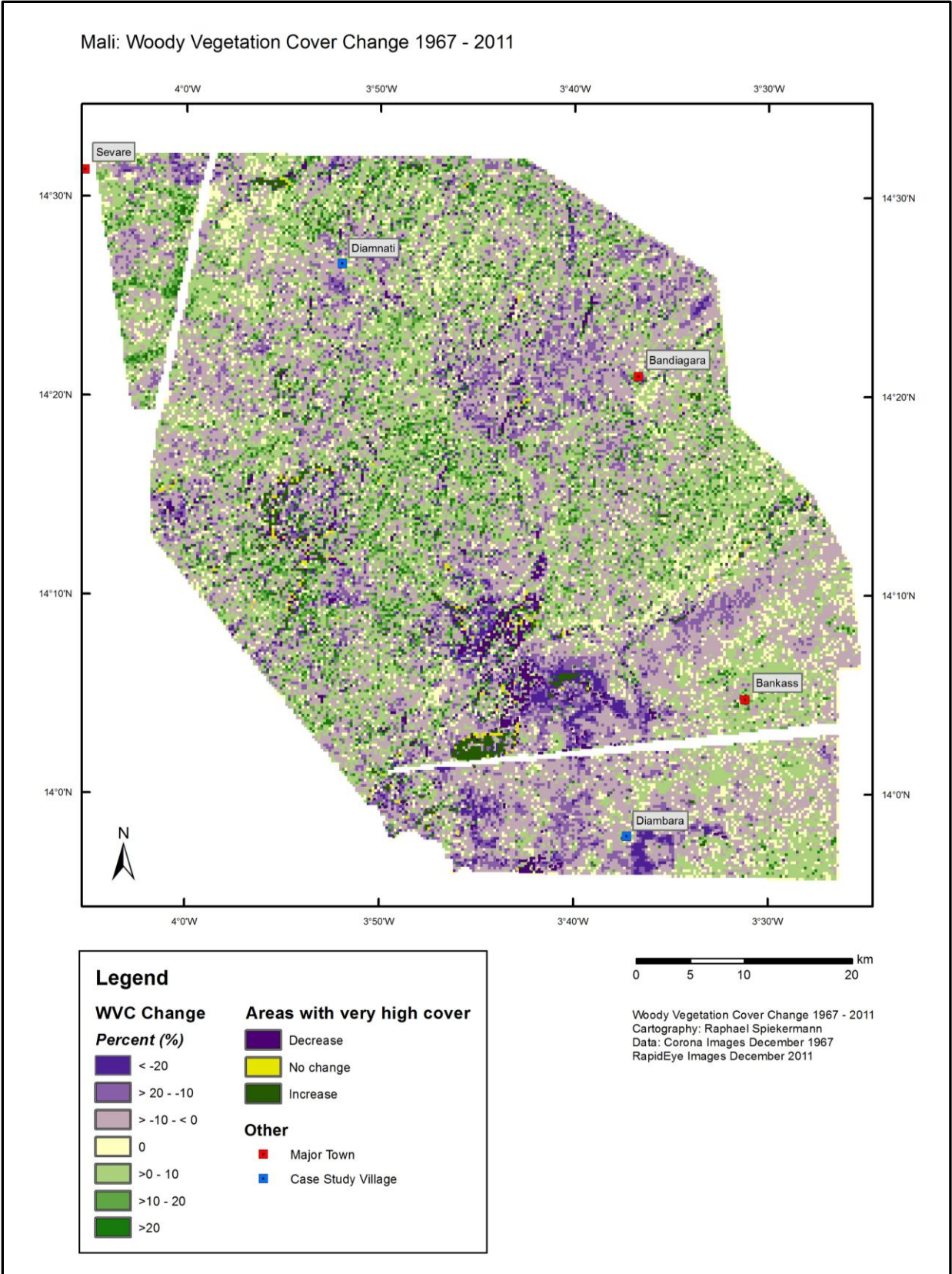


Fig. 4.16: Woody vegetation cover change 1967 – 2011.

4.2.2.3 Woody vegetation density and cover change acc. to land cover

Table 4.7 lists the statistics for the woody vegetation density and coverage results for the plateau and plain specifically for the two land cover classes –“Sparsely Vegetated” and –“Densely Vegetated” separately, in order to compare tree density and cover in cultivated areas and in bush fallow areas. The first row indicates the total area (ha) of each class of the woody vegetation density (D1). For the year 2011 on the plateau, an average of 5.6 trees/ha are found on the sparsely vegetated areas compared to 8.8 in densely vegetated areas, which mostly consist of naturally vegetated bush fallow but may also represent densely vegetated cropland areas. Because these areas are often fallow or untouched, many bushes and shrubs growing here, depending on the size, are not mapped and counted within this category. On the plains, the average density of woody vegetation for the same year 2011 is practically the same on sparsely vegetated as on densely vegetated land. For one, the sparsely vegetated areas dominate on the plains (65,000 ha compared to 21,000 ha of densely vegetated areas), and the densely vegetated areas often consist of fallow land with dense shrubbery, which may often be too small to be identified in the feature extraction. The number of trees in sparsely vegetated areas and in densely vegetated areas is comparably similar with only the number of shrubs being decisively different. The figures listed thus suggest that the shrubs cannot be detected at a resolution of 5 meters.

The plateau in 1967 appears to host a similar number of trees on both sparsely vegetated and densely vegetated areas, with even more features extracted within sparsely vegetated areas than in densely vegetated areas (16.2 and 15.1 respectively). This ironic fact may be explained by viewing the feature extraction in Diamnati (see Fig. 4.18). Because the land cover class –“densely vegetated areas” is used to assess the woody vegetation density separately from the –“sparsely vegetated areas” in order to increase contrast, only actual trees and large woody shrubs are extracted and thus exclude smaller low-lying shrubs, unless the shrubs are of such a size identifiable by the feature extraction tool.

The situation on the plains is however quite different in 1967. Here the mean woody vegetation density is 10.4 in sparsely vegetated areas compared to 18.3 in densely vegetated areas. An explanation for this is perhaps the better quality of the land cover map on the plains for 1967 compared to that of the plateau. Due to the more complex nature of the plateau and the limited information provided by the panchromatic images, the land cover classification may not have distinguished satisfactorily between the two classes so that grasslands or areas of dense shrubbery with darker grey values than cropland areas may well have been classified as –“densely vegetated”. The feature extraction may then not have been capable of identifying the relatively small shrubs in these areas, especially after the contrast adjustments created by

masking out all sparsely vegetated areas, so that only trees within the densely vegetated areas are mapped.

Table 4.8: Woody vegetation density and cover on sparsely vegetated (SV) and densely vegetated (DV) areas on the Seno Plains and Dogon Plateau 1967 and 2011.

	Plateau 2011 SV	Plateau 2011 DV	Plains 2011 SV	Plains 2011 DV	Plateau 1967 SV	Plateau 1967 DV	Plains 1967 SV	Plains 1967 DV
D1:No. Pixels (100 x 100 m)	92573	82268	65373	21238	138955.0	96436	56437	38804
Mean Density (trees/ha)	5.6	8.8	5.8	5.9	16.2	15.1	10.4	18.3
Min. Density (trees/ha)	1.0	1.0	1.0	1	1.0	1.0	1.0	1.0
Max. Density (trees/ha)	71.0	80.0	54.0	55	65.0	89.0	64.0	92.0
StD. Density (trees/ha)	5.4	8.7	3.8	5.1	9.4	9.7	5.9	9.2
D2:No. Pixels(100 x 100 m)	NA	7644.0	174.0	2258.0	NA	8.0	NA	2166.0
Mean Density (trees/ha)	NA	616.6	1961.4	17371.3	NA	3663.6	NA	4100.4
Min. Density (trees/ha)	NA	44.0	41.0	45.0	NA	413.0	NA	45.0
Max. Density (trees/ha)	NA	9305.0	41654.0	41654.0	NA	20501.0	NA	14796.0
StD. Density (trees/ha)	NA	1812.0	5453.3	19853.0	NA	6854.8	NA	5451.6
C1:No. Pixels (250 x 250 m)	19650.0	16235.0	11182.0	3961.0	22758.0	16012.0	8827.0	5805
Mean Coverage (% of 250m pixel)	9.0	15.4	6.7	9.5	9.6	10.8	9.2	14.8
Min. Coverage (% of 250m pixel)	0.0	0.0	0.0	0.0	0.0	0.0	0.0	0
Max. Coverage (% of 250m pixel)	115.0	157.0	104.0	130.0	139.0	151.0	122.0	126
StD. Coverage (% of 250m pixel)	9.2	13.5	5.5	11.1	6.7	11.5	6.7	11.5
C2:No. Pixels (250 x 250 m)	10.0	568.0	16.0	248.0	26.0	699.0	14.0	269

The mean coverage of the same classes for 1967 and 2011 has the same trends as the density maps. A mean coverage of 9.0% on sparsely vegetated areas compared to 15.4% within densely vegetated areas on the plateau highlights the differences between these two land cover types in 2011. The differences of the mean coverage on the plateau in 1967 are – similar to the density - not great with a mean coverage of 9.6% for sparsely vegetated areas and 10.8% for densely vegetated areas recorded. The plains show stronger differences in 1967, with an average of 9.2% within sparsely vegetated areas and 14.8% in densely vegetated areas. The average coverage appears to be lower on the plains in 2011, with an average of 6.7% in sparsely vegetated areas and 9.5% in densely vegetated areas. The standard deviation within the densely vegetated class is always greater as is the maximum coverage, which for both extends beyond 100%, as a handful of pixels include the area of a number of features which

extend beyond the borders of the pixel, the centre of these features however happen to be within the same pixel so that the total area is greater than 10,000 m².

Table 4.9 offers further detailed information in regard to the change of woody vegetation density and coverage between 1967 and 2011. The change refers to the classes –Sparsely vegetated” and –densely Vegetated” of the year 2011. The mean change of woody vegetation density is in all cases negative, the minimum mean density change being -7.2 trees per hectare for the sparsely vegetated areas on the Seno Plains. The high standard deviation of 12.66 shows that large variations exist. The change of cover is however not as great, with a positive average change of 3.9% recorded for the densely vegetated areas on the Dogon Plateau.

Table 4.9: Woody vegetation and cover change 1967 – 2011 for the sparsely vegetated (SV) and densely vegetated (DV) areas of 2011.

	Plateau Change SV (2011)	Plateau Change DV (2011)	Plains Change SV (2011)	Plains Change DV (2011)
D1 No. Pixels (100 x 100 m)	112492	92648	67389	24011
Mean Density (trees/ha)	-10.3	-7.2	-7.5	-9.3
Min. Density (trees/ha)	-75.0	-89.0	-68.0	-88.0
Max. Density (trees/ha)	57.0	68.0	45.0	50.0
StD. Density (trees/ha)	11.0	12.66	9.4	10.2
D2 No. Pixels (100 x 100 m)	419.0	1048.0	150.0	369.0
Mean Density (trees/ha)	-35.8	-346.6	36.2	2157.8
Min. Density (trees/ha)	-20501.0	-20501	-14796	-14796
Max. Density (trees/ha)	6040.0	9305	41654	41654
StD. Density (trees/ha)	740.3	2985.49	5062.643	9768.7
C1 No. Pixels (250 x 250 m)	15893.0	14903.0	10791.0	3843.0
Mean Coverage (% of 250m pixel)	-1.1	3.9	-3.3	-4.8
Min. Coverage (% of 250m pixel)	-90.0	-121.0	-114.0	-121.0
Max. Coverage (% of 250m pixel)	100.0	137.0	116.0	89.0
StD. Coverage (% of 250m pixel)	9.8	16.1	8.9	14.8
C2 No. Pixels Increase (250 x 250 m)	0.0	437.0	16.0	192.0
C2 No. Pixels Decrease (250 x 250 m)	102.0	426.0	0.0	130.0

4.2.3 Case Study: Diamnati

The Diamnati area illustrates in more detail the results of the woody vegetation assessment for an area on the plateau. It has already been shown that the land cover here has changed significantly during the period from 1967 to 2011. The results of the feature extraction in IMAGINE Objective are shown in Fig. 4.18. A large number of features have been identified, primarily within the bush fallow areas and the trees and shrubs forming the tiger bush in the south west are also extracted. The dark shaded spaces in between the tiger bush islands are most likely dense grasses and low-lying shrubs. At closer inspection, the shrubs within the sparsely vegetated areas (see the land cover map in Fig. 4.5 above) are also detected and mapped.

The feature extraction results for the RapidEye image for the same area around Diamnati is displayed in the lower half of Fig 4.18. The number of individuals extracted is not nearly as many as that of 1967, although the features are on average larger. A large proportion of the trees have been identified within the areas used for cultivation but many of the remnants of the tiger bush in the south west are excluded. The windows at a larger scale of 1:10,000 show that the number trees within the immediate surroundings of Diamnati village have increased. The limitations of the feature extraction method are also clearly visible. The buildings in Diamnati cannot be distinguished from trees as the contrast of grey-scales of the buildings with the background pixels is similar to that of woody vegetation. Thus the buildings are falsely classified here as trees. In comparison, the near infrared band of the RapidEye image enables vegetation to be identified and mapped more easily. Woody vegetation can be distinguished from background pixels far more accurately than is possible when working with panchromatic imagery. Because of the fine line between woody and non-woody vegetation, and because a threshold is set to distinguish between these, not all of the woody vegetation has been extracted. A visual estimation may conclude that some 20% to 30% of the woody vegetation has been excluded in this particular part of the map. The results in other areas of the study area are perhaps more successful, as will be shown in the discussion below. Fig. 4.19 displays the tree density map for the Diamnati territory. Each pixel is one hectare large and provides information on the number of features per hectare. The individual features are shown in red so that the actual number and coverage of these can be compared to the density. As mentioned above, the village area has seen an increase of tree density since 1967. The three pixels directly around Diamnati showing 10-20 features per hectare in 1967 actually refers mainly to the number of buildings in the village. This again demonstrates the same source of error as discussed above. Because the average size of the features on the Corona image (see Table 4.4) is much smaller than that of RapidEye, the density is greater. However, an attempt is made to model the true number of trees and shrubs in the RapidEye image by dividing the area of each feature by 225

m², as is explained in the methods chapter. One of the pixels in the 2011 woody vegetation density map is marked brown. This pixel is covered by a feature, whose area is larger than the size of the pixel, i.e. greater than 10,000 m² (D2). Because this feature is associated with only one pixel, only one pixel is marked brown in order to express that this area has a particularly high woody vegetation density. This qualitative value is attributed to only a relatively small number of similar cases in the study area and intends to replicate the real situation on the ground without distorting or exaggerating the true woody vegetation density. Some of the tiger bush remnants were not mapped as woody vegetation, an example of incomprehensive feature extraction. The change to woody vegetation is given in Fig 4.20. The woody vegetation density in the degraded area (see Fig. 4.5) to the southwest of Diamnati has drastically decreased, whereas an increase of up to 5-15 features per hectare is seen on most cultivated areas to the northeast and southeast of Diamnati village. Many of the areas to the east of Diamnati with a decrease of woody vegetation density represent areas that were once bush fallow (compare with the land cover map in Fig. 4.5). So even though the feature extraction within the RapidEye image is not entirely capable of including all of the trees within the feature extraction, an increase on the fields is nevertheless the result of the change calculation. This result can be seen as a positive result, and the photos A1 and A2 in Fig 4.6. witness to the healthy environment of the cultivated fields east and south-east of the village. The degraded area to the southwest of Diamnati stands in stark contrast to the rest of the area. The sharp border between healthy and degraded land is a stunning phenomenon. Farmers are doing what they can to prevent further advances of the degraded area west of Diamnati by construction of small retaining walls as shown in Fig. 4.17.



Fig.4.17: Retaining walls designed to capture soil and hinder progression of degraded areas west of Diamnati, Dogon Plateau.

Diamnati: Woody Vegetation 1967 and 2011

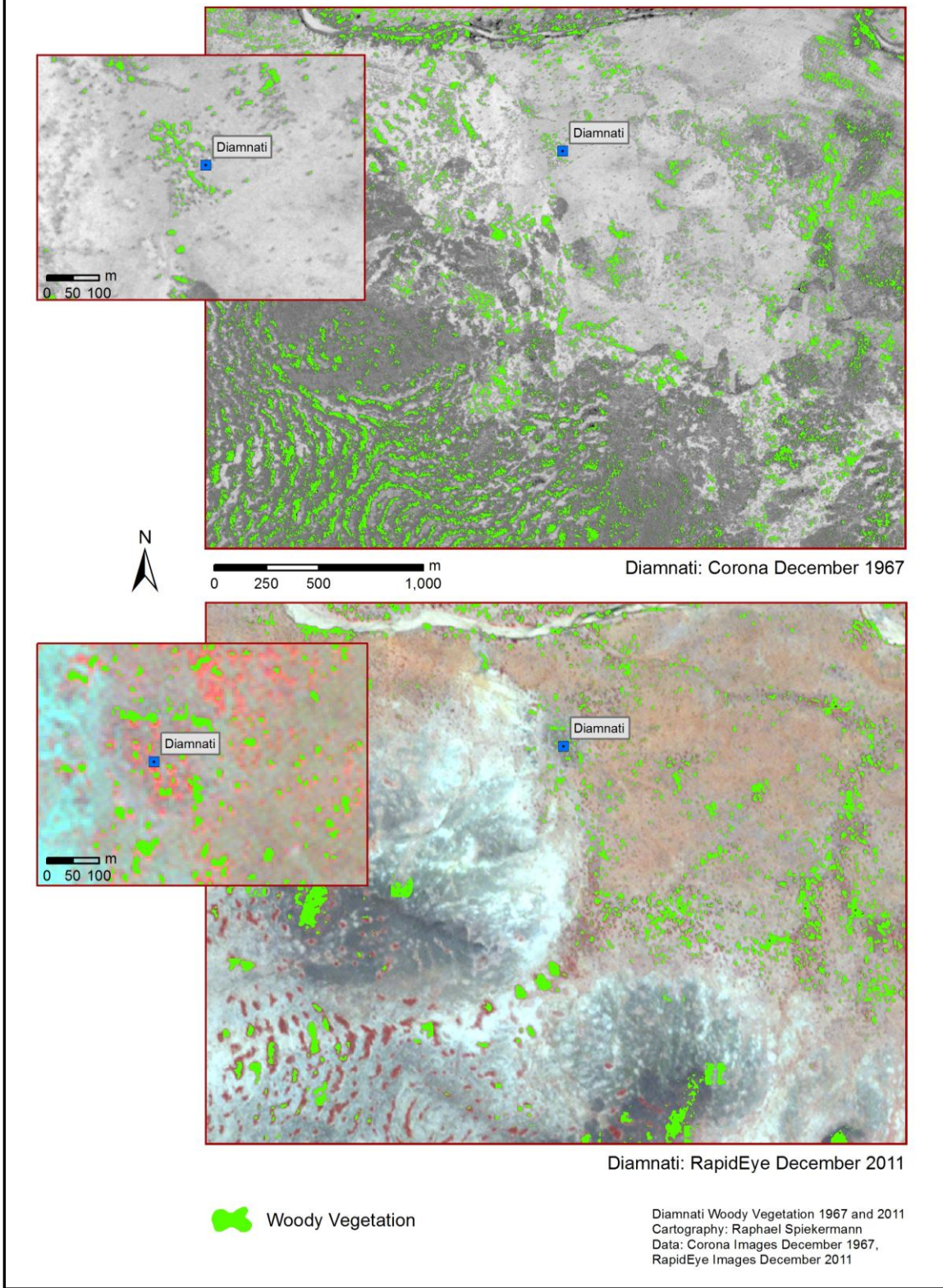


Fig.4.18: Woody vegetation feature extraction results in Diamnati 1967 and 2011.

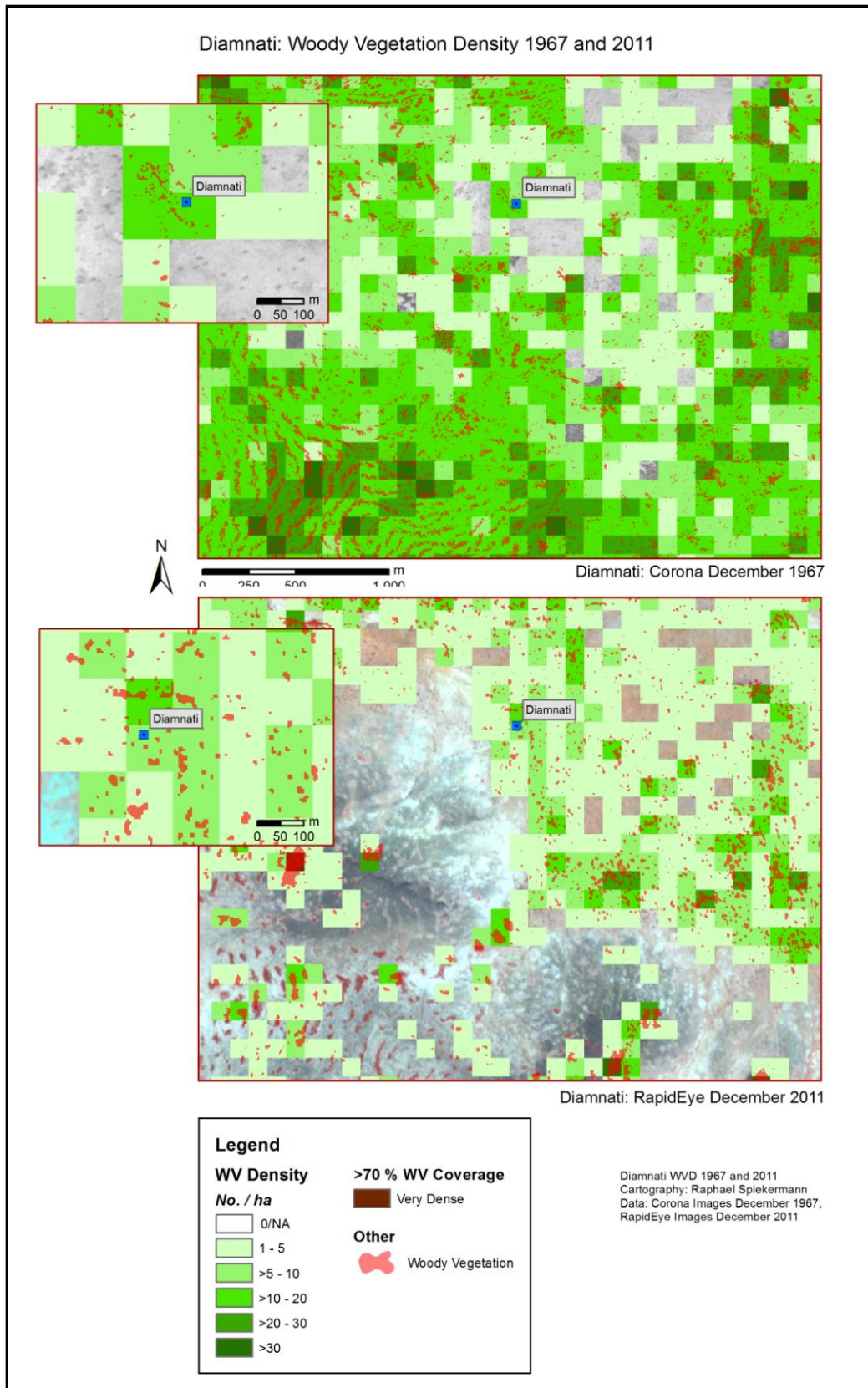


Fig. 4.19: Tree density in Diamnati 1967 and 2011.

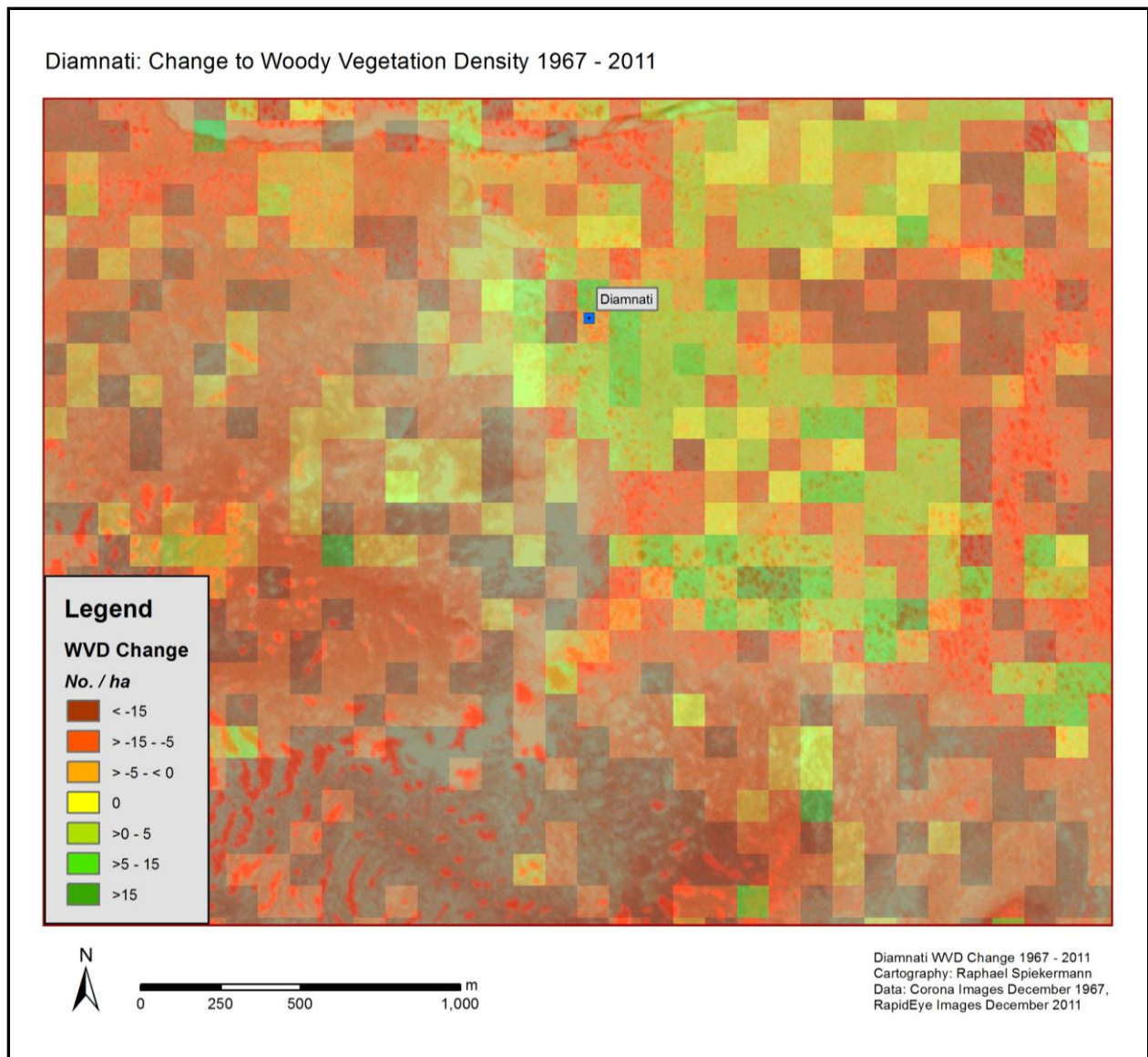


Fig. 4.20: Change to woody vegetation density in Diamnati 1967 – 2011.

A map of the woody vegetation cover for Diamnati in 1967 and 2011 is displayed in Fig. 4.21. The cover is similar for all areas that are not degraded. The vegetation cover ranges between 0-10% on cropland areas and 10-30% in densely vegetated bush fallow areas in 1967 (compare with the land cover map in Fig. 4.4). As was shown, the degraded areas host very little woody vegetation, but the cover in cropland areas has increased to between 5 and 20%. The tree cover change map in Fig. 4.22 shows the areas of change. The fields directly surrounding Diamnati village have a greater tree cover than in 1967, an increase of up to 10%. More cropland areas in the southeast have also seen a strong increase of cover. The purple shades again show the vast areas of degraded land to the southwest of Diamnati.

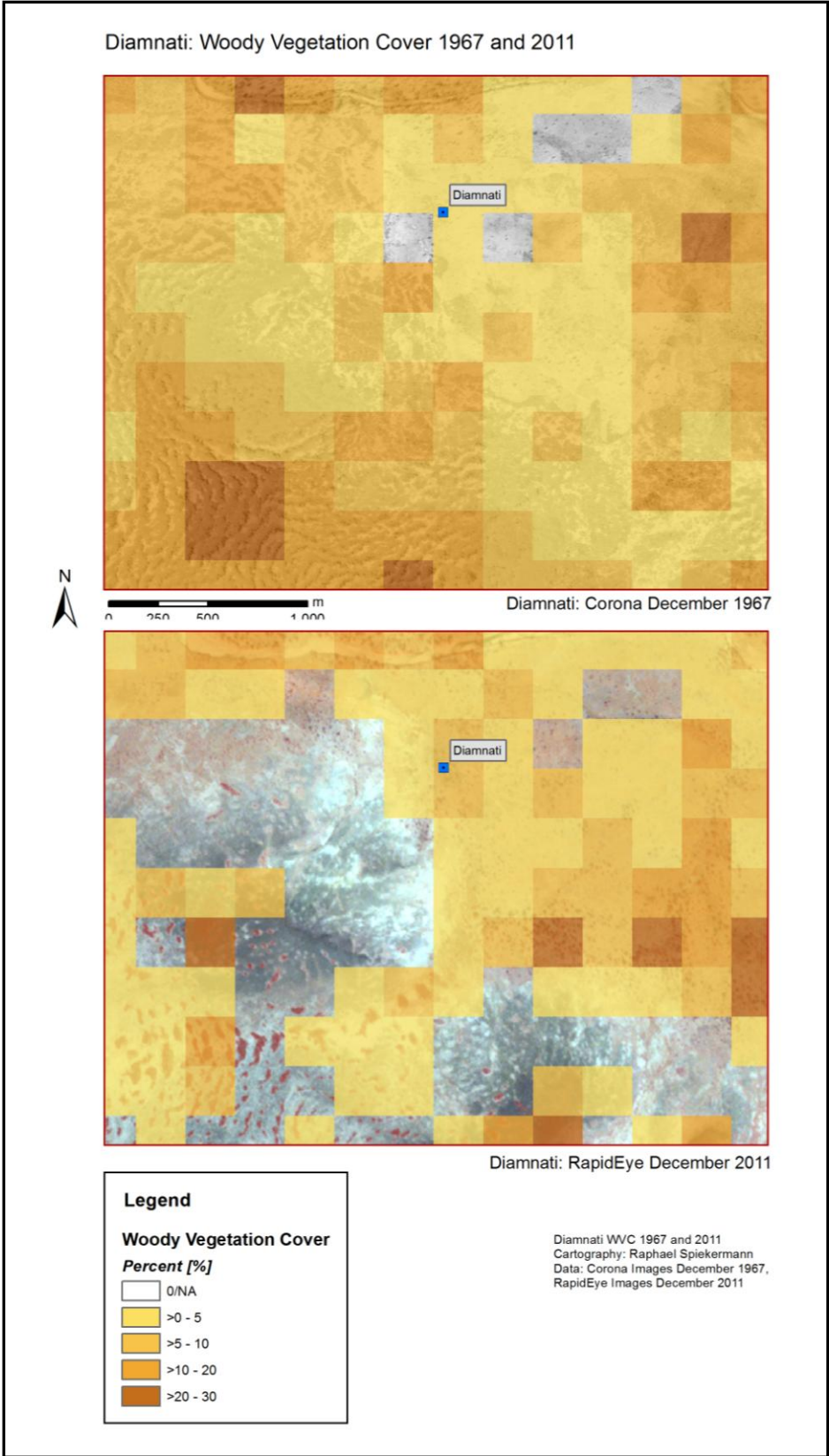


Fig. 4.21: Woody vegetation cover in Diamnati 1967 and 2011.

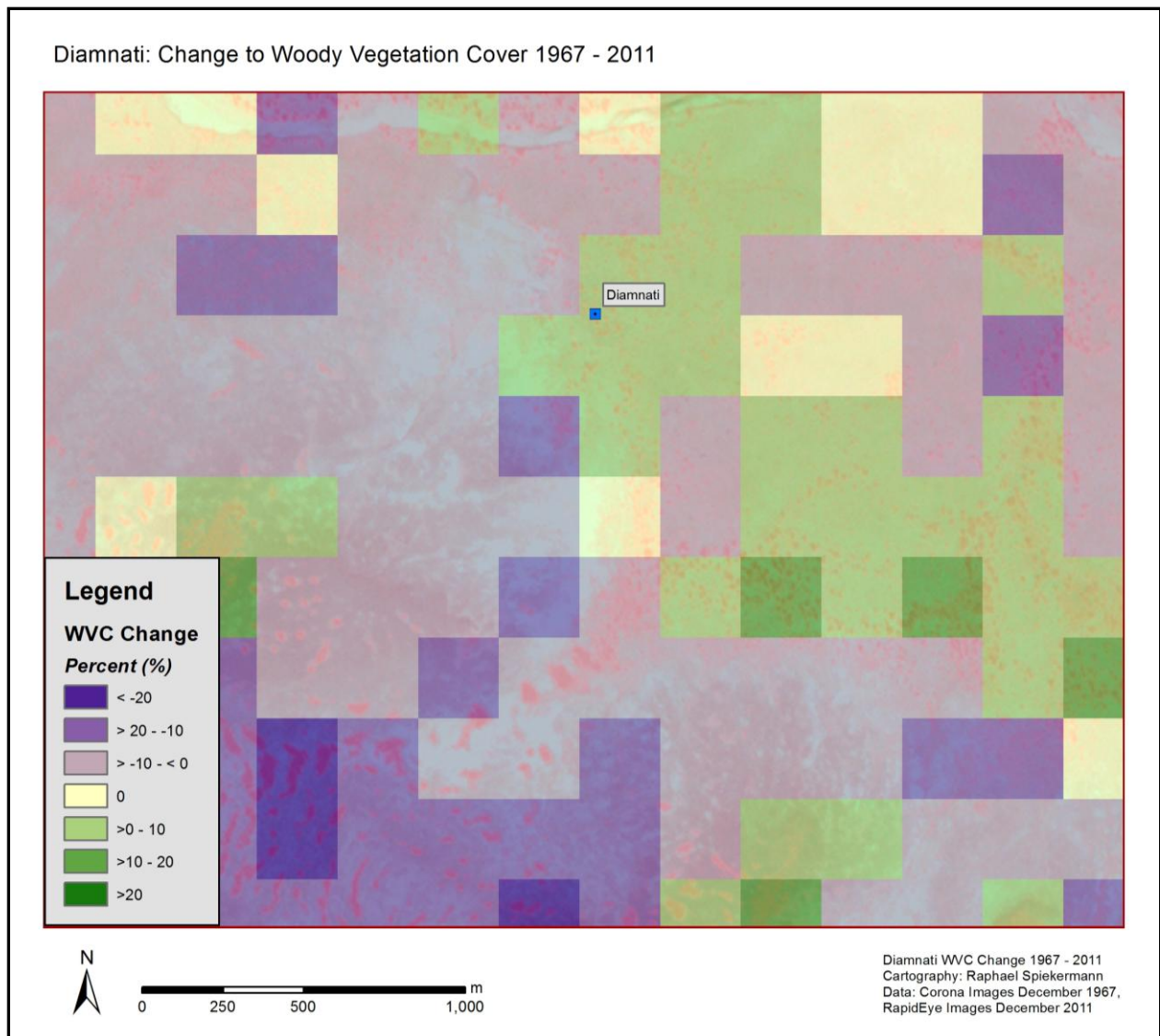


Fig. 4.22: Woody vegetation cover change in Diamnati 1967 – 2011.

4.2.4 Case Study: Diambara

In similar fashion to the land cover case study above, Diambara will showcase the tree density and cover of 1967 and 2011 and its change, as a representative for the Seno Plains. The map in Fig. 4.23 depicts the results of the woody vegetation feature extraction for the years 1967 and 2011. It was shown by the land cover classification that only certain areas around the village were needed for cropping, so that many areas remained as bush fallow with dense natural vegetation. The results show that these areas in particular were densely covered with woody shrubs and trees in 1967. Until 2011, the former densely vegetated areas had been cleared in order to cultivate these areas. These areas were cleared in such a manner that little remains of the woody vegetation. What was once a densely vegetated area is now only extremely sparsely

populated by trees. The tree density maps for 1967 and 2011 are to be viewed in Fig. 4.24 and show the stark spatial differences for the Diambara territory. This phenomenon is best seen in the density change map of Fig. 4.25, which shows the major differences of woody vegetation density between 1967 and 2011, particularly to the northeast and southeast of Diambara. In 1967 many areas of the bush fallow contained over 30 trees or large shrubs per hectare. On the cropping and grazing fields, the number generally ranged between 1 and 20 trees per hectare. In 2011, these same fields that existed in 1967 had a similar number of trees growing on them as in 1967. Only a small number of trees are growing on the former bush fallow areas today.

The woody vegetation cover map in Fig. 4.26 tells the same story as the density map. In 1967 the woody vegetation cover in the densely vegetated areas ranged between 20% and over 40%. Grasses and low-lying shrubs will have grown in between the woody vegetation, which is the reason for the dark shades in the Corona image in this area. The sparsely vegetated areas, i.e. the cropping areas, have a woody vegetation cover up to 20% both in 1967 and 2011. As one can see, the land use is not just the decisive factor for woody vegetation cover, but particularly the subjective value given to the cropland by farmers. The older fields boast a large number of trees, the newer fields are only thinly populated. These former bush areas were found to be fallow in 2011 and are only used when needed by farmers or in a cropping cycle of three to four years.

A similar phenomenon as in Diamnati can be found in Diambara as well. On viewing the change maps in Fig. 4.9 and 4.10 the only increase of woody vegetation is found on the fields surrounding the village. This again shows a higher value attributed to these fields than cropland on the outskirts of Diambara's territory. This appears to be the case when viewing the vegetation cover change map in Fig. 4.27. Farmers provide particular care and protection for the trees growing in close proximity to the village, which is why the tree cover here has increased by 10-20%. However, as will be discussed below, comparing the two images quantitatively has its difficulties, mainly because of the different spatial and spectral resolutions of the data base imagery. The margin of error is such that a decrease of up to -5 trees/ha or -10% coverage does not necessarily mean that a decrease has occurred in reality. Anything beyond that however is certain to accurately depict the direction of change.

Whether or not the values of woody vegetation density and coverage are comparable for the years 1967 and 2011, given the different data bases and also the slightly dissimilar methods applied, is a legitimate question and shall be discussed below. Before we do so, we turn our attention to the vegetation composition, as an interesting point is how the vegetation differs between the two major land use classes, i.e. the impact of land use on the vegetation composition.

Diambara: Woody Vegetation 1967 and 2011

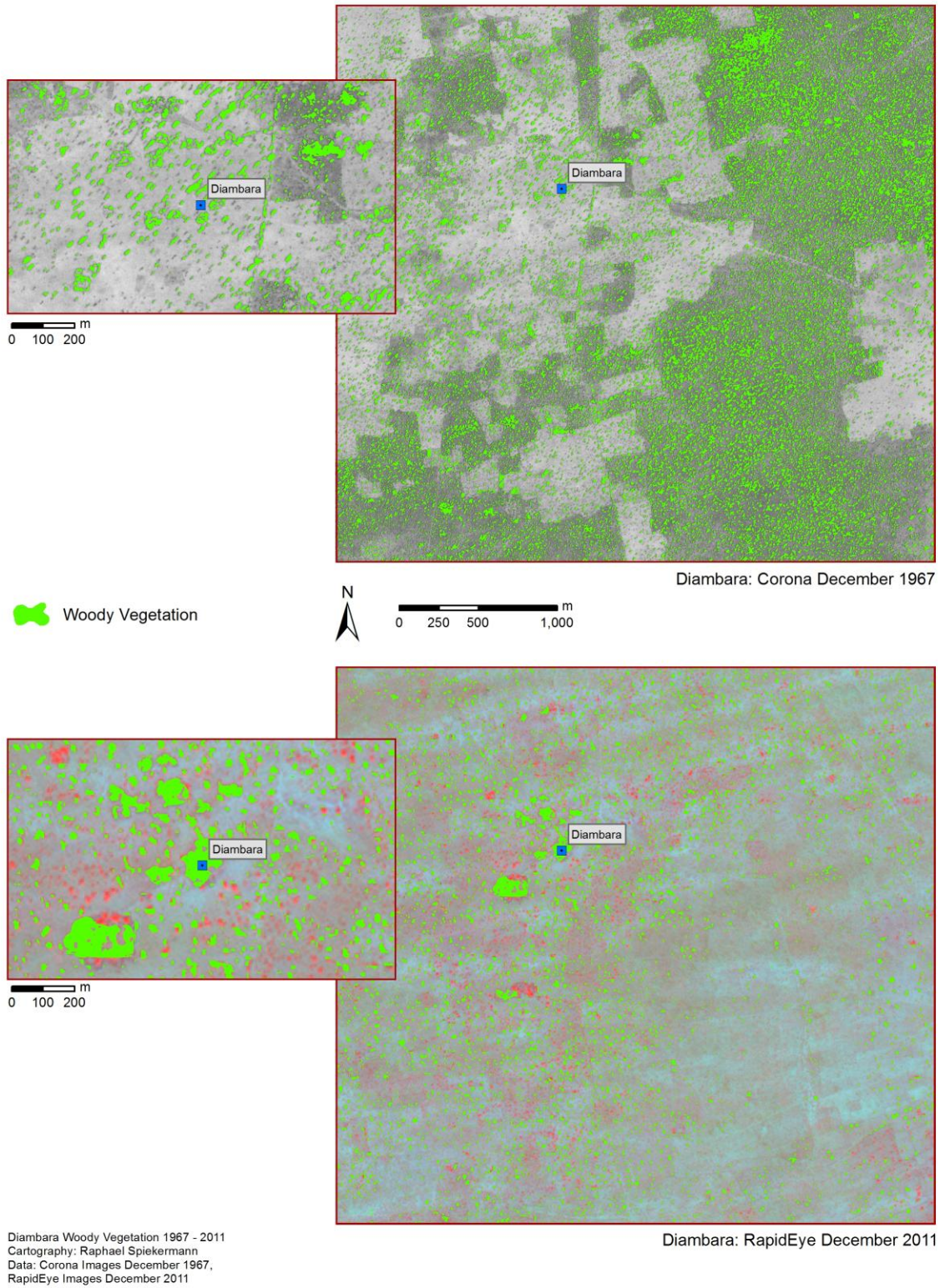


Fig. 4.23: Woody vegetation feature extraction results in Diambara 1967 and 2011.

Diambara: Woody Vegetation Density 1967 and 2011

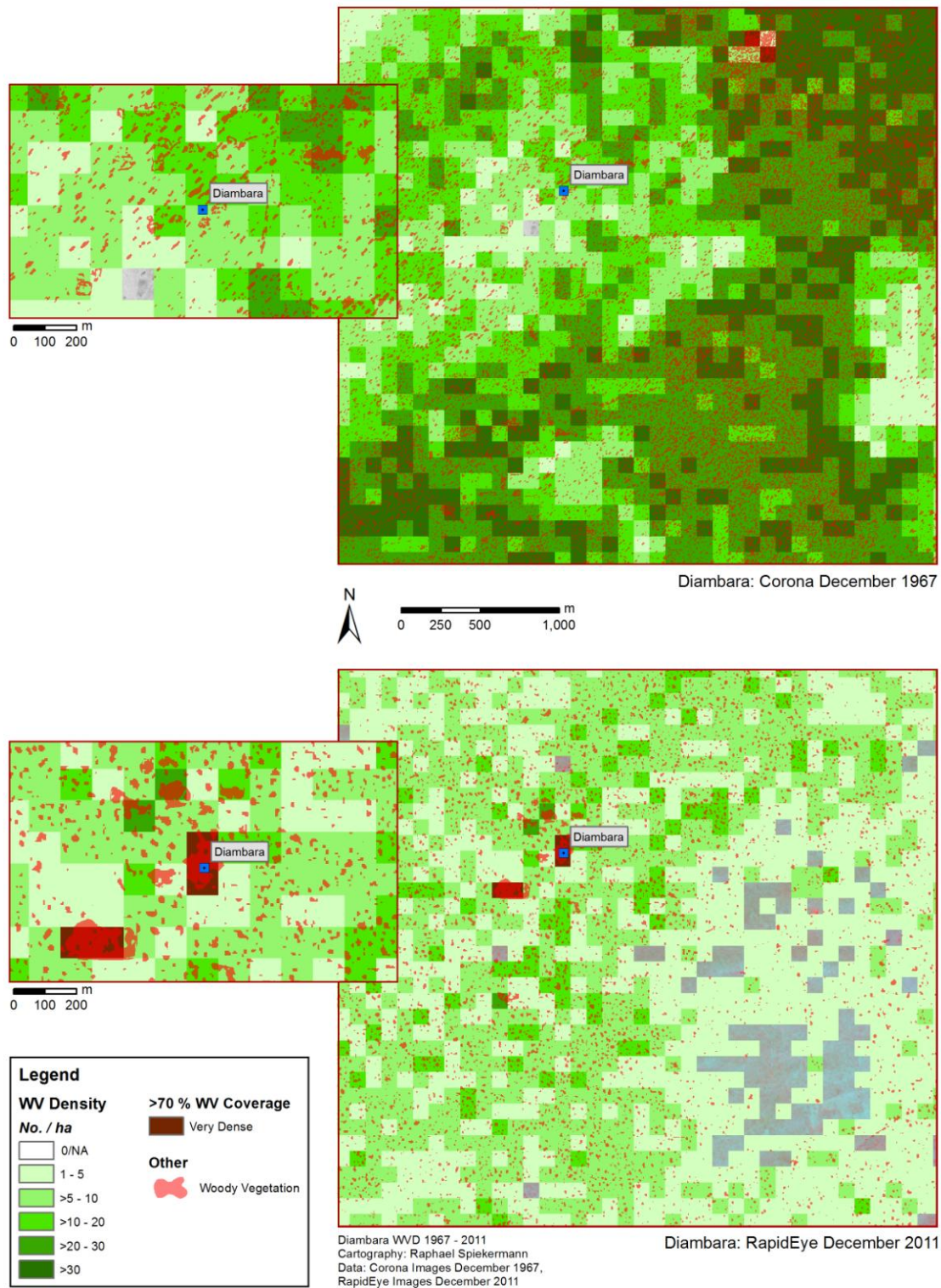


Fig. 4.24: Tree density in Diambara 1967 and 2011.

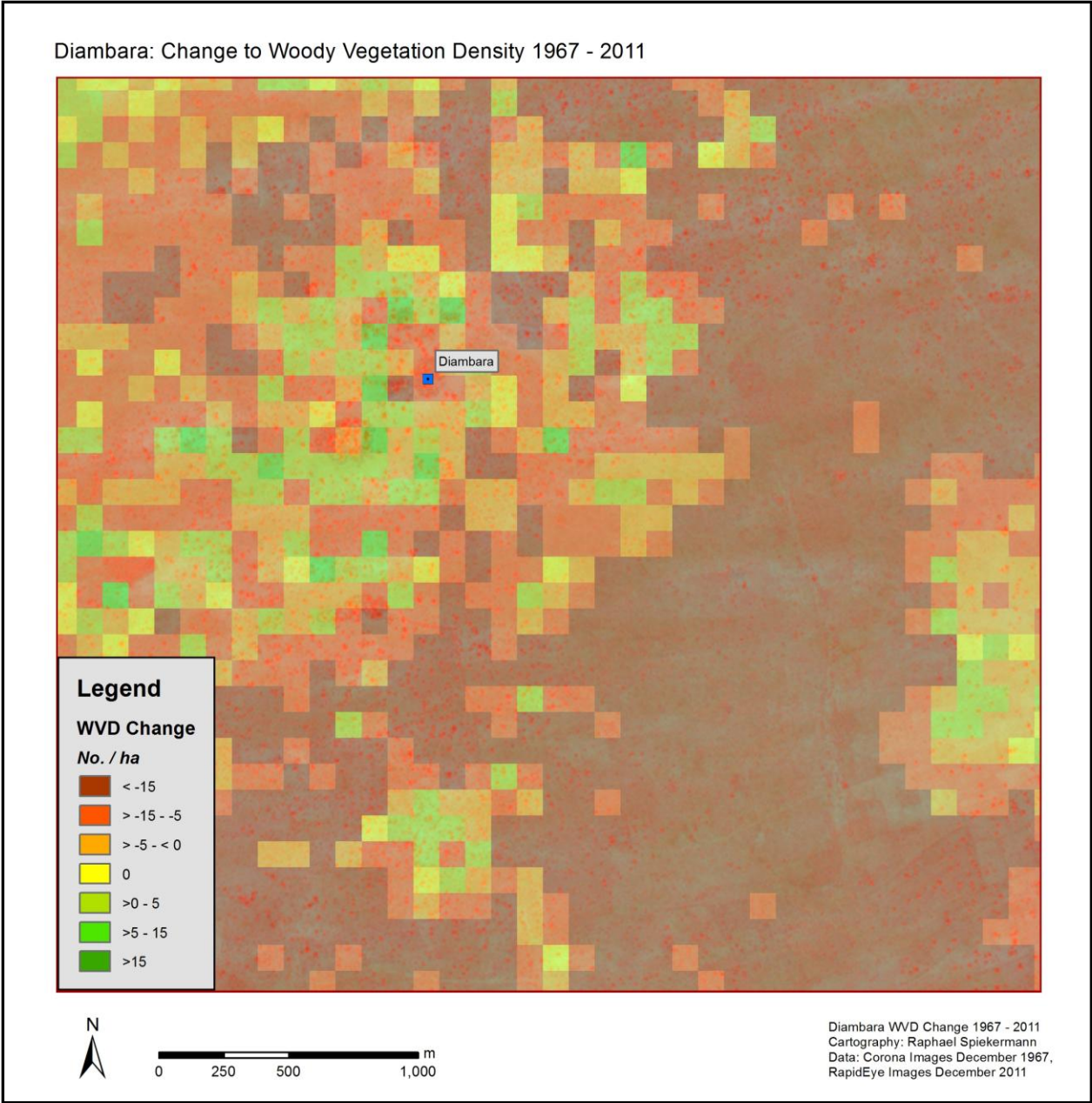
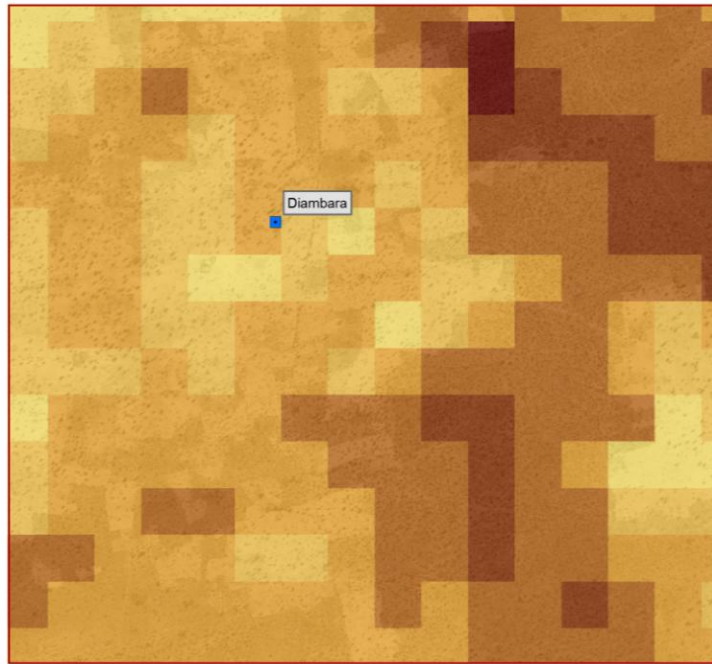
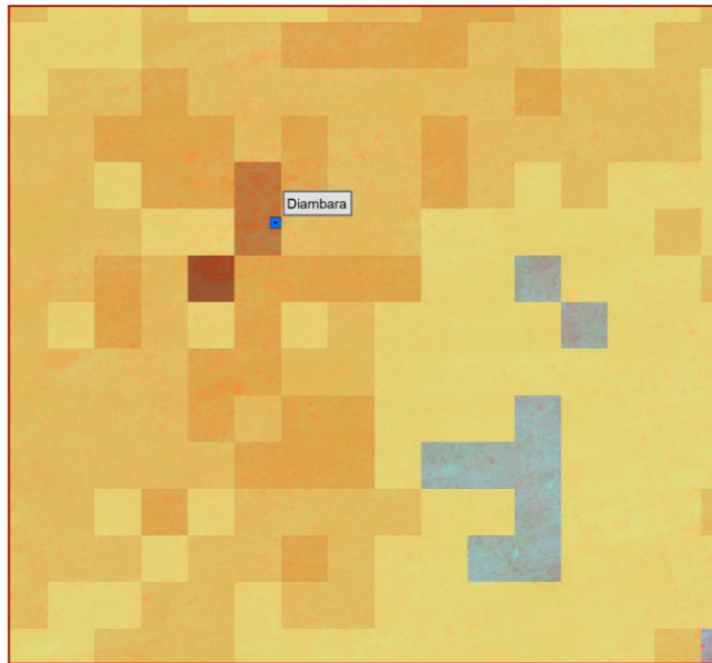
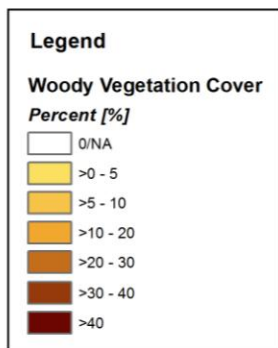
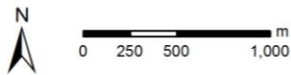


Fig. 4.25: Change to woody vegetation density in Diambaara 1967 – 2011.

Diambara: Woody Vegetation Cover 1967 and 2011



Diambara: Corona December 1967



Diambara: RapidEye December 2011

Diambara WVC 1967 - 2011
Cartography: Raphael Spiekermann
Data: Corona Images December 1967,
RapidEye Images December 2011

Fig. 4.26: Woody vegetation cover in Diambara 1967 and 2011.

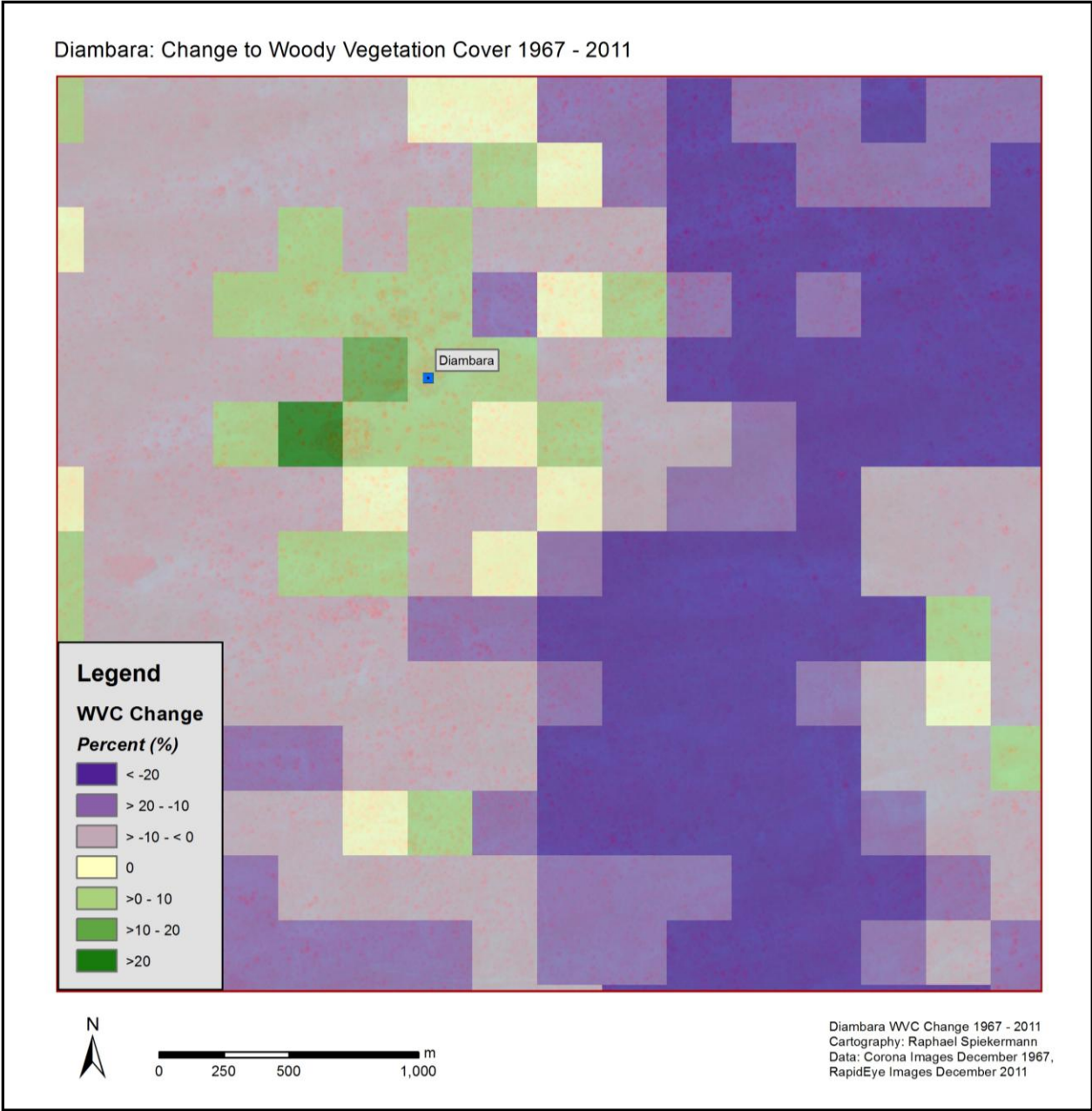


Fig. 4.27: Woody vegetation cover change in Diambara 1967 – 2011.

4.3 Vegetation Composition

One of the major open questions of Sahelian environmental science is concerned with the current and recent change to the vegetation composition. As mentioned earlier, not only the number and coverage of woody vegetation in the Sahel is of interest, but most importantly what is growing there and which species are favoured by farmers. Within the study area, 46 detailed vegetation surveys were carried out for 5,000 m² plots as described in chapter 3. Each plot is intended to represent the wider area. In this way, a good overview of the vegetation cover according to various land uses can be obtained. The land cover maps in most cases reflect the land use. More often than not, the class “Densely Vegetated” refers to bush fallow areas (particularly in 1967 where bush fallow with dense natural vegetation was more common than today) and the land cover class “Sparsely Vegetated” mostly refers to cropland areas. Care must be taken, as it was shown in the case studies that densely vegetated areas may also represent cultivated areas with a high woody vegetation cover. The results of the vegetation surveys are listed in Table 4.10 and show the land use of each plot, the number of trees and species as well as statistics related to the dominant species of each respective plot. The survey results are summarized in the graph in Fig.4.28. The dominant species on cropland are *Acacia albida*, *Balanites aegyptiaca* and *Guiera senegalensis*, which each consist of over 20% of the species found in such areas. The major difference between cropland and bush fallow land is that *Combretum glutinosum* comprises 24.7% of all species in bush fallow areas compared to just 4.8% in cropland areas. This signals that farmers are very selective in regard to which species they favour and leave to grow on cropland. *Combretum micranthum*, rarely found on agricultural land, makes up 13.1% of the species in bush fallow areas today. *Balanites aegyptiaca* is the most robust species and together with *Acacia albida* most favoured by farmers on the Seno Plains. In general, the diversity of tree species is greater on the plateau than on the plains, primarily due to the lack of unused areas on the plains.

Table 4.10: Vegetation survey results: Land use: Cropland (CL), Bush (B), Fallow (F); number of trees, vegetation species; dominant species (BAL: *Balanites aegyptiaca*, COG: *Combretum Glutinosum*, BOA: *Borassusaethiopum*, BOS: *Bosciasenegalensis*, GUI: *Guierasenegalensis*, ACA: *Acacia albida*, ACN: *Acacia nilotica*, BI: *Sclerocýaryabirrea*, COM: *Combretummicranthum*, AI: *Azadirachta indica*)

Area	Landuse	No. of Trees	No. Trees > 4m	No. Species	Dominant Species	% of Total Trees	% of Species	Species Avg. Height
1	CL	53	14	8	BAL	75.8	15.1	2.9
2	CL	52	21	6	BAL	66.7	11.5	3.8
3	CL	38	14	7	BAL	54.5	18.4	3.9
4	CL	36	11	9	COG	33.3	25.0	0.8
5	CL	36	8	12	BOA	27.3	33.3	6.0
6	CL	34	3	5	BOS	51.5	14.7	0.3
7	CL	30	5	7	GUI	54.5	23.3	0.5

8	CL	29	10	6	COG	42.4	20.7	3.6
9	CL	29	7	3	BAL	60.6	10.3	2.7
10	CL	27	3	8	GUI	30.3	29.6	2.2
11	CL	26	19	5	BAL	42.4	19.2	3.4
12	CL	26	16	3	BAL	54.5	11.5	4.9
13	CL	26	15	7	GUI	24.2	26.9	0.8
14	CL	26	8	5	GUI	36.4	19.2	0.8
15	CL	26	1	3	ACA	60.6	11.5	2.3
16	CL	23	11	3	GUI	30.3	13.0	1.3
17	CL	22	9	8	GUI	21.2	36.4	0.9
18	CL	20	8	8	ACA	12.1	40.0	5.3
19	CL	19	8	8	ACN	21.2	42.1	2.9
20	CL	16	8	7	BAL	15.2	43.8	4.0
21	CL	13	7	3	BI	21.2	23.1	6.2
22	CL	9	6	5	ACA, BOS	9.1	55.6	6.5
23	CL	9	3	1	ACA	27.3	11.1	5.0
24	CL	6	6	1	ACA	18.2	16.7	14.0
25	CL	5	4	1	ACA,	15.2	20.0	5.2
26	CL	5	0	1	BAL	15.2	20.0	
27	CL	4	4	1	ACA	12.1	25.0	10.1
28	CL	4	0	1	GUI	12.1	25.0	0.4
29	CL	1	0	1	GUI	3.0	100.0	0.6
30	BU	87	20	8	COG	136.4	9.2	3.6
31	BU	40	12	6	GUI	78.8	15.0	
32	BU	21	0	6	GUI	21.2	28.6	1.5
33	BU	14	0	9	GUI	18.2	64.3	
34	BU	10	0	2	COM	24.2	20.0	3.5
35	BU	10	0	3	COG	24.2	30.0	1.8
36	BU	8	3	5	ACA	12.1	62.5	4.3
37	BU	7	0	5	ACA; GUI	6.1	71.4	
38	BU	4	2	4	COG; COM; AI	3.0	100.0	4.0
39	FA	52	11	9	ACA	69.7	17.3	4.2
40	FA	35	11	3	BAL	81.8	8.6	1.8
41	FA	29	6	3	BAL	45.5	10.3	3.3
42	FA	28	12	7	BAL	39.4	25.0	3.3
43	FA	23	9	4	BAL	42.4	17.4	3.8
44	FA	13	6	5	COG	18.2	38.5	5.0
45	FA	3	0	3	COG; CON; GUI	3.0	100.0	1.5
46	FA	1	0	1	GUI	3.0	100.0	1.5

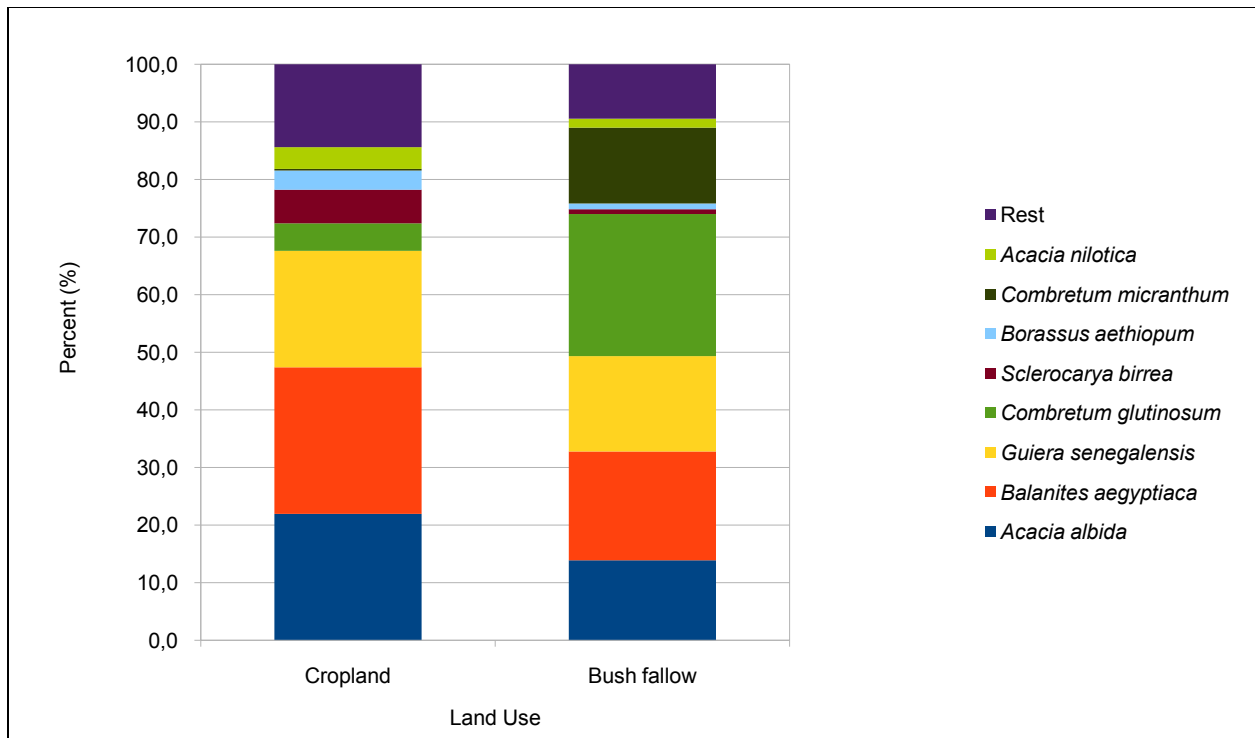


Fig. 4.28: Average proportion of vegetation species according to land use (cropland and bush fallow).

5 Discussion

The results presented in chapter 4 have shown that the change of land cover as well as tree density is spatially very diverse. The land cover on the plateau and particularly on the plains has seen significant changes during the analysed period and has had an obvious impact on environmental change in the study area. These changes range from positive to negative, although much environmental change cannot be categorised that easily.

It has been demonstrated that it is possible to map woody vegetation, i.e. individual trees and large shrubs and groups of trees in close proximity to one another. The accuracy and completeness of the feature extraction largely depends on the spatial resolution of the images used as well as the spectral resolution. On the one hand, the very high resolution (2 m) of the photographic Corona satellite imagery means that smaller features can be extracted. On the other hand a disadvantage here is that only grey-scales are available, making it difficult, if not impossible, to distinguish between objects related to vegetation and other features such as buildings in settlements or shadow. This is the clear advantage of the multi-spectral RapidEye images. The use of the near-infrared band and the NDVI makes it possible to solely map and extract features relating to vegetation. The lower geometric resolution (6.5 m / 5.0 m resample) means that shrubs are unlikely to be mapped by means of feature extraction. Groups of dense shrubs and trees however have been mapped. This is best explained by Fig. 5.1 which exemplifies the differences of the feature extraction in an area of the Dogon Plateau. Most trees and shrubs on the fields have been successfully extracted from the Corona image. It is however almost impossible to know whether the large dark shaded areas are shadows of a rocky outcrop or actually groups of trees. The near infrared band of the RapidEye image clarifies the situation, showing that the dark areas in the Corona image are indeed dense groups of trees. Fig. 5.1 also shows that due to the lack of background pixels in these densely vegetated areas, individual trees cannot be extracted but only grouped together as a large polygon.

Fig. 5.2 shows the limitations of the RapidEye images in detail. A comparison is made between *Bing Maps Aerial* imagery and the RapidEye images as well as an on-site view with the GPS photography. The arrows in 1a and 1b show the location and direction photo 1 was taken at. In this case, the trees are large and old and standing alone, so that all of the trees in this cut-out can be easily identified. Most of these trees are represented by six to twelve pixels. In photo 2, a group of young small trees are seen on the field. The very high resolution image from *Bing Maps Aerial* manages to depict the individual trees. In RapidEye, the four small trees are represented by a handful of pixels, making it impossible to extract individual trees, regardless of the software applied. The results of the feature extraction are also displayed in 2b in Fig. 5.2.

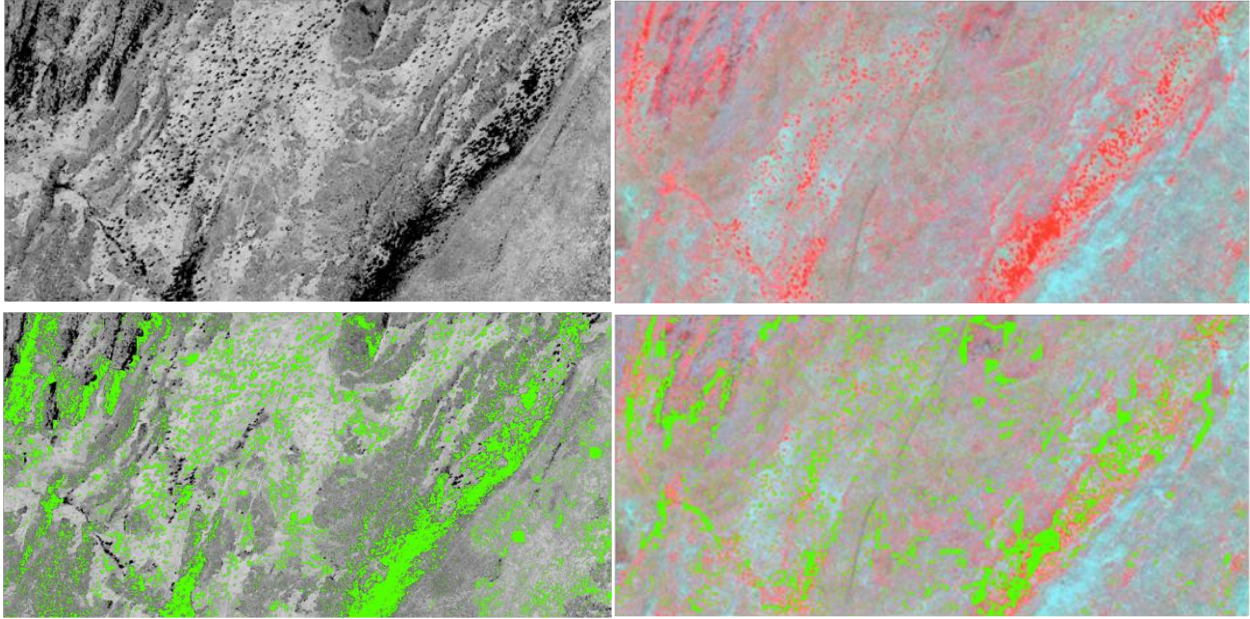


Fig. 5.1: Feature extraction results for an area on the Dogon Plateau: Advantages and disadvantages of Corona and RapidEye imagery for feature extraction.

Many of the polygons represent groups of trees, again showing the importance of dividing the total area of each polygon by 225 m² to approximate the true number of trees.

The success of the feature extraction largely depends on the size of the objects and their reflective characteristics. A 5 m tall *Acacia albida* with only a few large branches extending in various directions (often many branches are cut off for building purposes and as a source of firewood) may not be visible even with use of the NDVI, due to the small leaves and lack of greenery. An average sized *Guiera senegalensis* with numerous large green leaves is more likely to be detected. These facts are highly important to consider in light of the results presented in chapter 4. The results show stark differences of woody vegetation density in many areas between 1967 and 2011. The woody vegetation cover maps are very similar in most regions of the study area. This is simply because the number of features is no longer needed, rather the total area of the features within each pixel. The number of features extracted in the Corona images is roughly four times greater than the number extracted from the RapidEye images. The reverse is however true concerning the average area of the features, mainly due to the different pixel size of the two images. Thus the greater number of features makes up for the smaller mean area of the features in the Corona images, and the larger mean area makes up for the smaller number of features in the RapidEye images. In this way the woody vegetation cover maps of 1967 and 2011 are far more similar than the density maps for these years. There is an obvious dilemma in comparing these maps quantitatively because of the differences listed

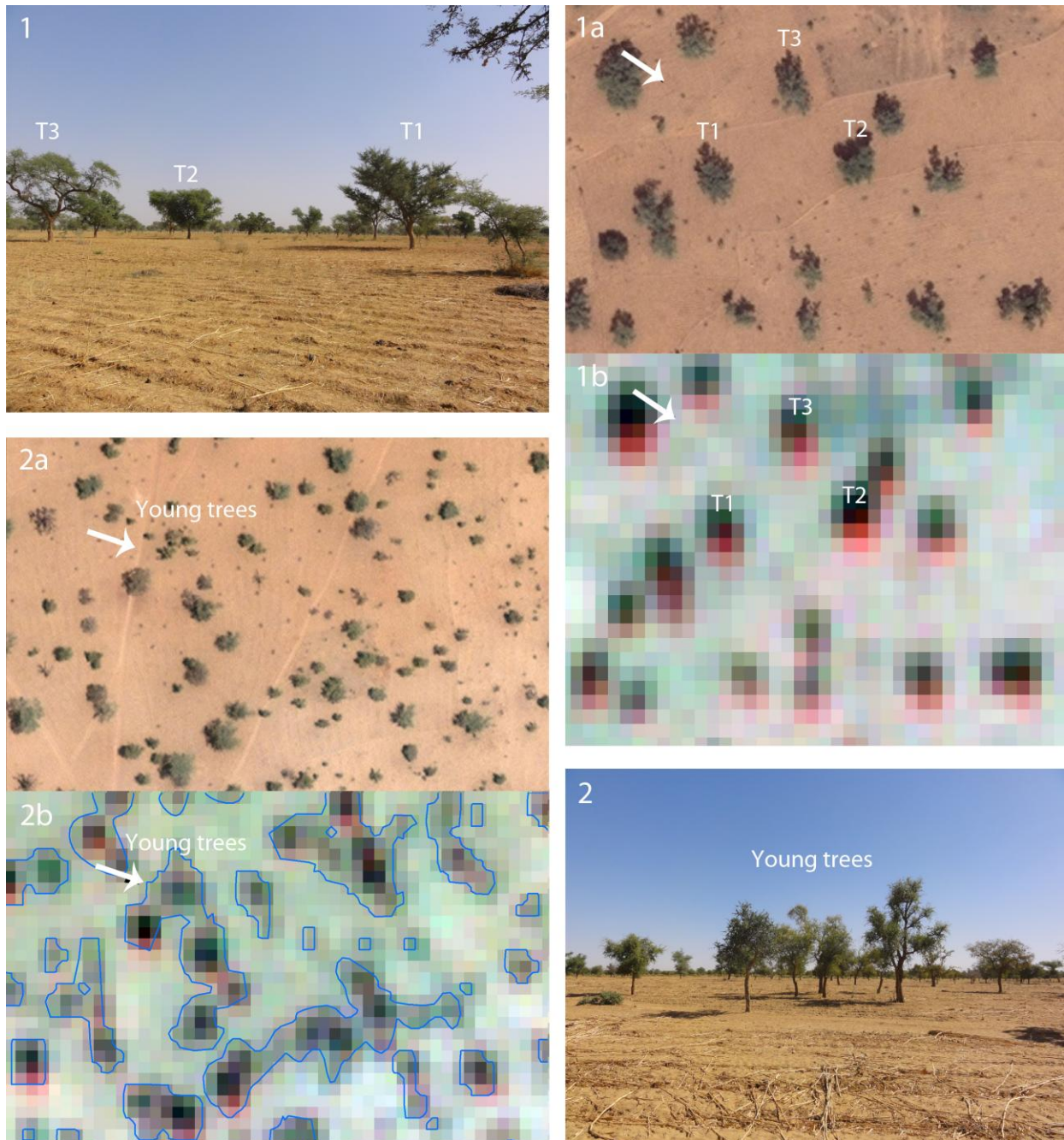


Fig. 5.2: Comparison of GPS-tagged photography (1-2) with very high resolution images (1a-2a) and RapidEye images (2a-2b). Source: Photos 1-2: R. Spiekermann; 1a-2a: © Bing maps: Microsoft Corporation and its data suppliers 2010; 1b-2b: RapidEye 2011.

above. Although the quantitative change may not be entirely correct, the trend certainly is. A slight decrease of woody vegetation density may not necessarily mean a decrease in reality. But areas with a strong decrease have certainly seen a decrease in reality. The direction of change, or better said, the tendency, is definitely correct.

Furthermore, the case studies showed that a comprehensive woody vegetation feature extraction with the RapidEye images is more difficult than with the Corona images. This has to do with the thresholds set in the feature model as well as the mapping of training areas. To be more precise, as the feature model uses the statistics of the training areas to distinguish between woody vegetation and areas not related to woody vegetation, the training areas must be selected with great care. Because the spectral characteristics of certain trees and shrubs may be quite similar to the remains of the seasonal harvest, a threshold must be set at a point where the maximum number of individual features are mapped and at the same time not including areas which are most likely not trees or woody shrubs. The lower the threshold is set, the more pixels are included, creating larger features and thus decreasing the total number of individuals. This could be improved by using a moving window, which only regards the contrast within the window rather than the contrast between desired pixels and background pixels for the entire image. The methods applied for this study make use of the capabilities within ERDAS Imagine and are subject to the limitations at the same time. A comparison of the two years must be done with regard to the limitations of the method and the information contained in each image.

For a closer discussion of the results of the feature extraction in combination with the land cover classifications, a “stroll” through the case study area of Diambara is presented. Fig. 5.3 shows the land cover change between 1967 and 2011, overlain with the woody vegetation polygons extracted from the RapidEye image for this area. The location of the photos in Fig. 5.4 and Fig. 5.5 are displayed on the map as well. The photos of areas most commonly used for cropping are marked and numbered in blue (CX) and photos of areas that are more often than not fallow in red (FX). The areas in yellow indicate areas that changed from densely vegetated to sparsely vegetated land between 1967 and 2011 and represent areas that were bush fallow in 1967, were cleared at some point and are now used for cropping. Many of these areas are considered to be second-rate fields and are often used in a three to four year rotational farming cycle. The green areas show reverse changes, i.e. from sparsely vegetated to densely vegetated areas. These densely vegetated areas are mainly primary cropping fields that are of particular value to the farmers due to their historic use and proximity to the village centre. These fields are generally used on an annual basis and fertilized regularly with both natural and artificial fertilizers. Young seedlings, depending on the species, are encouraged to grow and protected in these areas and trees are used for firewood in a sustainable manner.

Generally speaking, it can be said that photos of cropland in Fig. 5.3 are within close proximity to Diambara village and photos of fallow are more distant. Another observation is that the change to densely vegetated areas is solely around the settlement of Diambara and change to sparsely vegetated areas occurred further away from the village. This reflects the land cover

and land use in 1967. The green polygons representing woody vegetation are more numerous within a 1 kilometre radius surrounding Diambara than in areas identified as fallow by the photographs. It cannot be generalized that sparsely vegetated areas in the Diambara territory are secondary cropland areas or fallow, and densely vegetated areas primary cropland. Cropland is found in both areas. Photos C6-C9 have all been taken in sparsely vegetated cropping areas. Although quite a few trees are seen on these images, they are younger and smaller than in traditional farmland areas closer to the village. The photos C1 – C5 show larger and older trees, as these areas were already used for cropping in 1967. Photo C10 is again closer to the village centre and thus boasts large old *Acacia albida* and an *Acacia senegalesis* can also be identified. The final picture C11 also shows a well-kept cropping area after harvest with a young *Balanites aegyptiaca* in the foreground. Although this area is more distant from Diambara village and surrounded by fallow areas, many young trees are growing here and the change is from sparsely vegetated to densely vegetated. When viewing Fig. 4.8 and 4.9, one can see that this area approximately 1.5 km south of Diambara was one of the first bush fallow areas at greater distance to the village to be cleared for cropping prior to 1967. Therefore it fits the pattern that those areas already used for cropping in 1967 have a higher tree density today than areas that were deforested for cropping after 1967. In this way, the two types of cropping fields may be distinguished, depending on their historical significance and proximity to village, and can be referred to as primary and secondary fields.

The pictures in Fig. 5.5 show areas that are mostly fallow, i.e. are not used every year, rather on a rotational basis. The tree density in these areas, outside of the green belt, is relatively low and the small number remaining are in a comparatively poor state due to unsustainable use of the trees. This is another indicator of secondary fields, as the prioritisation of tree protection is much lower here and soils are less fertile due to the limited recovery time of (usually) three years, which may also lead to soil leaching. All photos of fallow land were taken at greater distances from the village centre than the cropland photos on primary fields. Picture F2 shows a field covered with *Guiera senegalensis*, which is a shrub that sprouts and grows rapidly and is used by farmers as a source of firewood. It also indicates that this particular field has not been used for cropping during the last one to two seasons as it is regarded as a weed by farmers. Similarly, photos F5 to F9 are covered with grass, another indicator of fallow land. Although pictures F10 to F12 show remnants from the harvest, the lack of woody vegetation and the distance to the village, as well as information offered by the farmers, indicate that these areas are secondary fields only used for a few years at a time and are of poorer quality than primary fields. Because these fields lie at the outskirts of the Diambara territory, they are also more difficult to access and cannot be protected from intruders looking to collect wood to sell on the market. During the field inspection in this area, this particular phenomenon was observed.

The patterns described and illustrated in this example of Diambara demonstrate that the change of land cover and woody vegetation density within a given area can be very diverse, although similar patterns are observed in many other areas, also including the other case study site of Diamnati on the Dogon Plateau. Fields that were already used for cropping in 1967 have generally seen an increase of woody vegetation and may be referred to as green belts encompassing villages. Former areas of bush fallow, which have been cleared for cropping, are today mostly sparsely populated. The extensive land use change mapped via the land cover maps (see Fig. 4.4) has of course also had an impact on vegetation diversity so that species such as *Detarium microcarpum*, *Gardenia ternifolia* and *Vitellaria paradoxa* have disappeared or become rare. Farmers know the importance of having trees on the fields and are aware of the advantages of an agroforestry system. Particularly since the droughts of the 70s and 80s, farmers have increased efforts to protect trees on cropping sites using traditional sustainable farming methods (especially *Acacia albida*, *Balanites aegyptiaca*, *Borassus aethiopum*, *Adansonia digitata*) and use the trees for various purposes efficiently and effectively without causing the trees harm. For this reason the tree density is often higher on the fields in the surroundings of settlements than in 1967 and represent an important contributing factors towards the greening of the Sahel, as this form of greening is more importantly a very useful and sustainable form of greening. On the other hand, many areas at greater distances from settlements, which at some point have been cleared from the dense natural vegetation cover of 1967, are today lacking woody vegetation and, if fallow for more than a year, are covered with shrubs such as *Guiera senegalensis*. However some indications of a positive development of these younger cropland areas were seen in many areas, where numerous young trees no older than twenty years, in particular *Balanites aegyptiaca*, *Combretum glutinosum*, and *Prosopis africana*, populated the fields. The Bankass region and the surroundings of Dimbal as well as the stretch along the Bandiagara escarpment towards Endé clearly stand out in this regard. It must be said however that vegetation diversity on the fields in the Seno Plains varies. The main species within the green belts around villages are *Acacia albida*, *Acacia nilotica*, *Acacia seyal*, *Adansonia digitata*, *Butyrospermum parkii*, *Detarium microcarpum*, *Piliostigma reticulatum*, *Prosopis africana*, and *Sclerocarya birrea*.

The degraded areas found on the plateau, and illustrated by the case study of Diamnati, exhibit an adverse effect of a complex interaction of processes involving the impact of the extreme droughts in the 1970s and 80s and the limited precipitation since the droughts (compared to pre-drought rainfall amounts). To compensate for the poor harvests during these years, local inhabitants would fell trees in the bush-covered area and sell the wood on the market or use the greenery to feed animals. Furthermore the number of livestock increased, which added to the pressure on soils and vegetation. The decreasing vegetation cover only accelerated the erosion

processes due to the increased susceptibility to soil erosion. Interviews with locals led to the conclusion that many useful vegetation species on the plateau are rare or no longer exist (e.g. *Detarium microcarpum*, *Gardenia ternifolia* and *Vitellaria paradoxa*).

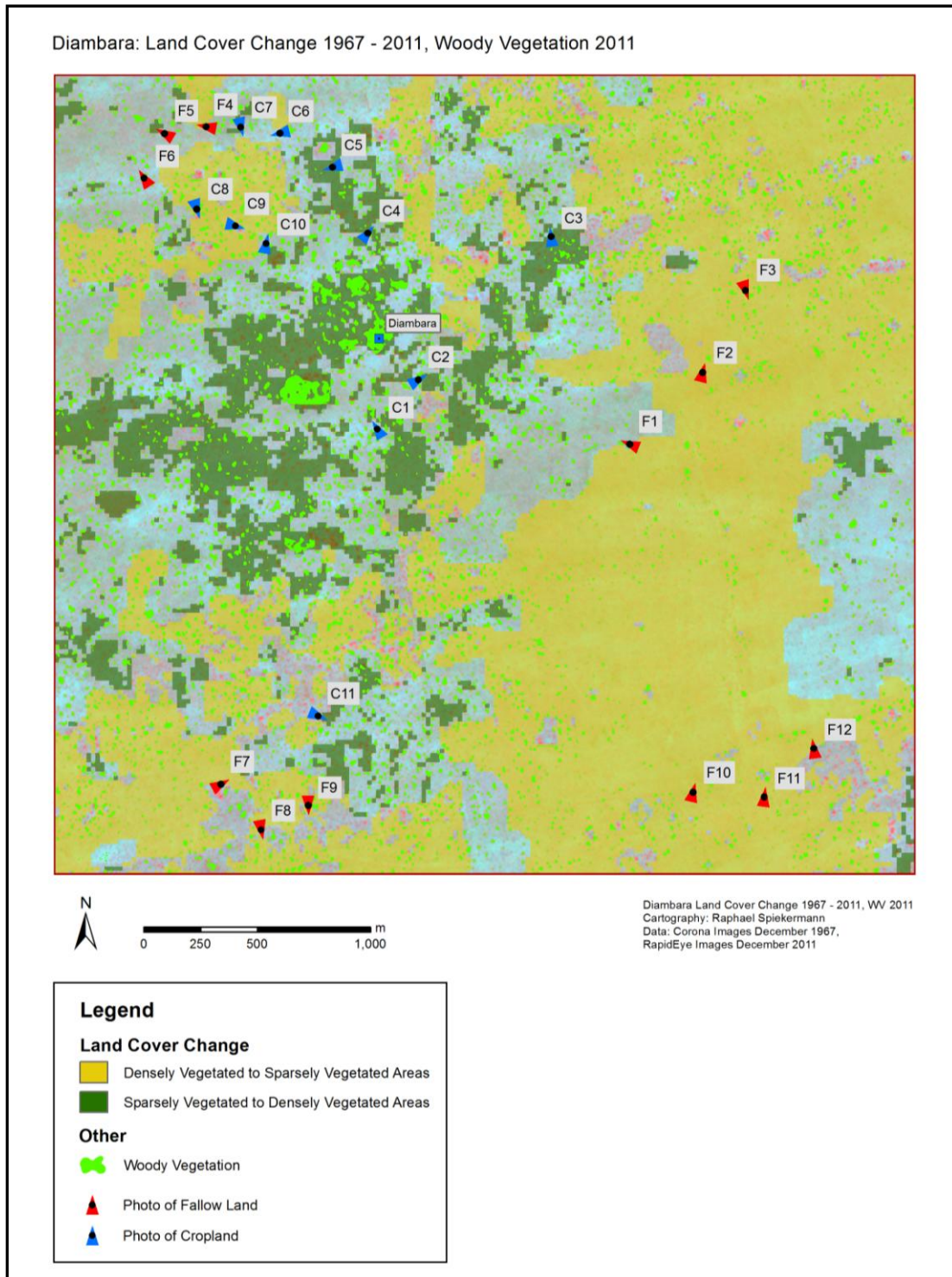


Fig. 5.3: Diambara: Land cover change 1967-2011 and woody vegetation 2011 with photo locations.

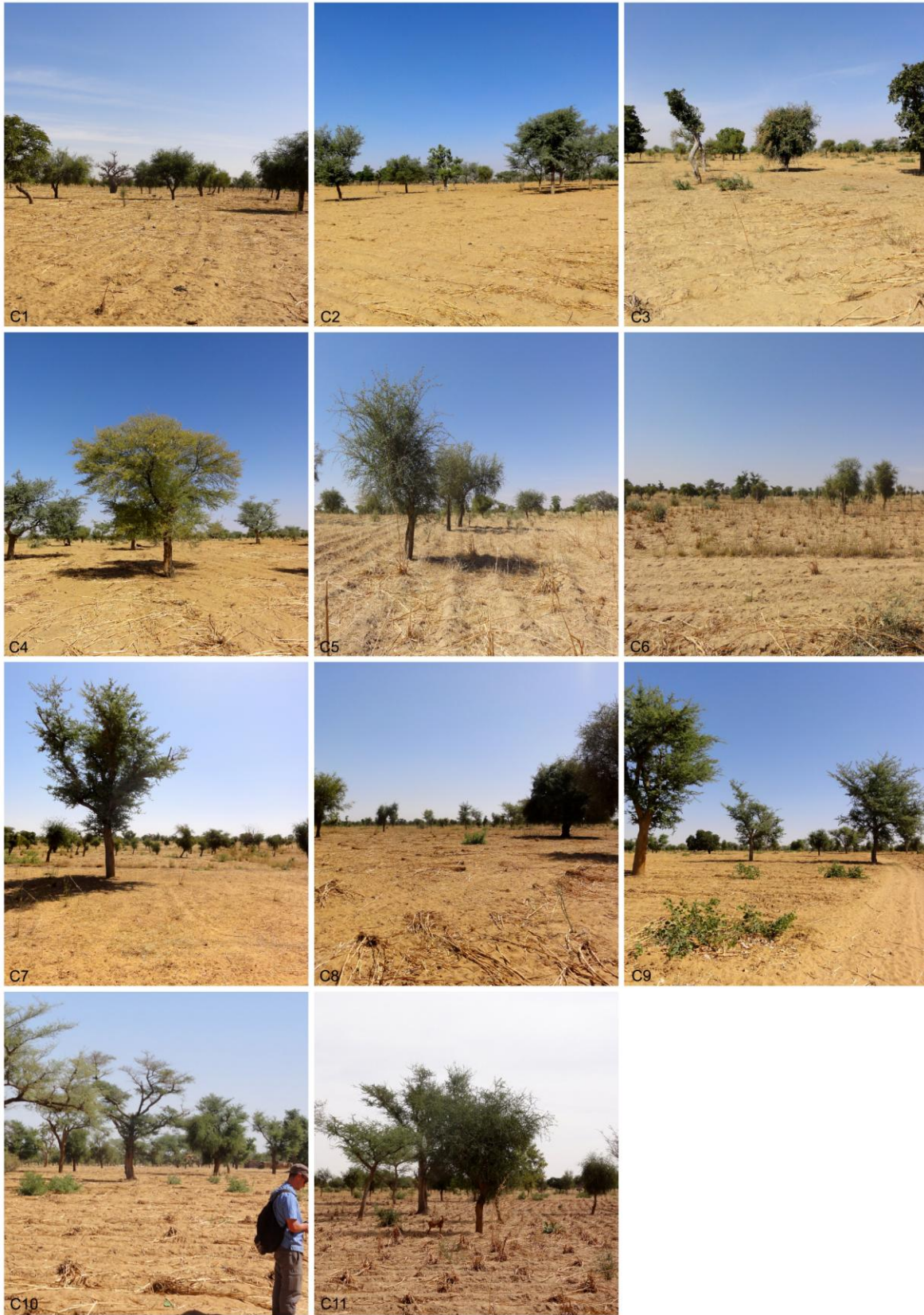


Fig. 5.4: Photos of cropland (C1 – C11 in map of Fig. 5.3).



Fig. 5.5: Photos of fallow land (F1 – F12 in map of Fig. 5.3).

6 Conclusion

The research presented in this thesis offers detailed insight on the state of the environmental change in the West African Sahel at a regional/local scale. Quantitative information on the woody vegetation cover is provided. Remote sensing, making use of high resolution images of the years 1967 and 2011, in combination with field work is shown to be a very useful tool for quantifying and comparing the woody vegetation cover over the past fifty years at tree level. This study goes further than previous works dealing with environmental change in the Sahel, which mostly remain qualitative or descriptive, or else provide small scaled studies with lack of detail. By means of an object-oriented approach, individual and groups of woody vegetation features could be extracted and displayed as woody vegetation density and cover maps. A total of 5,745,705 polygons representing single, as well as groups of trees and shrubs are extracted for the years 1967 (Corona images) and 2011 (RapidEye images) in an area totalling 3660 km² on the Dogon Plateau and Seno Plains of Mali. The same imagery is used to produce land cover maps at a resolution of 20 m, which offer detailed information regarding changes to land cover and the linkage to land use is explored. Two case study sites, Diamnati on the Dogon Plateau, and Diambara on the Seno Plains, demonstrate the evolution of the environment at a large scale as well as displaying the limitations of the methods. Geo-tagged photos, vegetation surveys and interviews with locals enable an in-depth interpretation of results and show that remote sensing alone does not permit a sufficient clarification of processes at a local level.

Significant changes to the land cover include the stark rise of sparsely vegetated areas (mostly agriculturally used areas) on the Seno Plains, up from 59.8% in 1967 to 73.2% in 2011. The change on the Dogon Plateau is not as great, primarily due to the rough morphology and difficulty of expanding agriculturally used areas. Although degraded areas could not be mapped for 1967, this land cover class makes up 9.9% of the total area of the Dogon Plateau, signifying a worrying proportion of land free of vegetation.

The vegetation surveys lead to the conclusion that the vegetation composition differs depending on the land use. Because farmers favour certain species, only a specific number of tree species are found on cropland. The main species here are *Acacia albida*, *Balanites aegyptiaca* and *Guiera senegalensis*, which make up over 60% of the species found in such areas. The major difference of the bush fallow areas is the dominant presence of *Combretum glutinosum*, which constitutes 25% of the vegetation species. Information gained from interviews held with locals suggests that many species have become rare or have disappeared altogether. *Butyrospermumparkii*, *Crataevaadansonii*, *Combretummicranthum*, *Piliostigmareticulatum* are among the vegetation species often mentioned.

The mean density of woody vegetation per hectare was 15.1 on the plateau and 13.4 on the plains in 1967. This corresponds to a mean vegetation cover of 10.1% for the plateau and 11.2% for the plains. In 2011, the woody vegetation density per hectare was 7.1 on the plateau and 5.9 on the plains. The mean vegetation cover for this year was 11.8% and 7.8% for the plateau and plain respectively. Differences according to land cover class can be seen, however the major distinction between sparsely vegetated and densely vegetated areas is the number of shrubs present. Whether or not these figures may be related to one another quantitatively has been discussed with the help of the two case studies in Diamnati and Diambara and one may conclude that the relative direction of change is valid.

The use of the methodology introduced in this thesis is relatively new as far as environmental research is concerned and obviously has its limitations. The quality of the results is subject to three major factors which at the same time present the framework for the limitations: underlying data quality, software capabilities, and the size of the study area. The advantages and disadvantages of the Corona and RapidEye images have been thoroughly discussed, the geometric and spectral resolution being the decisive difference in regard to the quality of the results. The 5 m (resampled from 6.5 m) resolution of the RapidEye images may be considered the maximum pixel size needed for mapping individual trees and large shrubs. A lower resolution than this would most likely hinder an accurate feature extraction, rather the number would have to be modelled in similar fashion to the way more than 20% of the polygons extracted from the RapidEye images have been modelled (polygons larger than 225m²). For this reason, the small objects successfully mapped in the Corona image are not able to be mapped in the same way in the RapidEye images. This explains the major difference of total polygons mapped in each image. ERDAS IMAGINE Objective is the tool used for the feature extraction in this thesis. The tool provides a fairly simple method for detecting the sought after objects. An improvement would be to not have to set thresholds for the entire image, as the contrast changes considerably from one area to the next. Rather, a moving window constantly adjusting to spectral differences of the image caused by such factors as morphology, soil, and vegetation species, would enable a more dynamic and effective use for identifying objects, which themselves differ greatly as far as their spectral characteristics are concerned. This leads to the next limiting element, namely the size of the study area. At a case study level, one may argue that multiple feature models could be created for dealing with the differing spectral properties of various types and species of woody vegetation (e.g. a hierarchical approach where the first feature model extracts vegetation with a particularly high NDVI, a second feature model focuses on smaller objects and shrubs and so forth), which makes the extraction of the wide range so difficult with a single feature model. Furthermore, the landscape becomes more homogeneous the smaller the study area is, which in turn increases contrast. The research here is however

limited by time and budget constraints so that a more time-consuming detailed feature extraction is not possible, even though the possibility may exist. Furthermore, a small study area would not deliver results which can be regarded as representative of the wider area and would thus be of little value to the study of the changing environment of the Sahel.

This being said, one may conclude that the changing environment in the study area is in no way a return to the pre-drought situation of the mid-1960s. Rather land use changes have been extensive in the past fifty years, the tree density change corresponds well to land use changes in that an increase is observed on historic primary fields and a decrease mapped in areas where the dense bushland areas of 1967 have been converted to secondary cropping fields. Furthermore, many areas of the plateau are now degraded, which is often indirectly, if not, directly related to the intense droughts of the 1970s and 80s. Vegetation species have decreased due to the increased need for cropland areas and the selective process of farmers in regard to which trees are favoured. As was shown in chapter 4.3, the vegetation composition in cropland areas and fallow bush areas differs greatly as the human influence on the vegetation composition in the fallow bush areas is not as excessive. On the other hand, the awareness and knowledge of the advantages gained when protecting the environment, i.e. ensuring the sustainable use of trees on farmland, has increased among local inhabitants. This has led to a strong increase of woody vegetation, particularly in the immediate surroundings of settlements, not to mention the already highlighted areas of Bankass, Dimbal and Endé.

7 Outlook

Regional-scaled studies in the African Sahel offer detailed information on the state of the environment and represent an essential monitoring tool, as explanations for change may also be found. Research on the development of the environment of the Sahel must continue to make use of advances of science and technology. This study represents an initial response to a call for more detailed studies at local level in the Sahel concerned with the desertification/greening debate. Improvements may be made by using very high resolution multi-spectral images such as World-View2 or GeoEye-2 imagery to gain greater accuracy. The cost of such imagery is however out of range of (most) environmental research projects (the cost of World-View2 images for the study area exceed US\$100,000). The processing capabilities of hardware and software must also improve for object-oriented regional scaled studies with very high resolution images to be feasible.

Many further interesting analyses could not be carried out here due to constraints relating to time and funding. However a closer look at the impact of the morphology on the vegetation cover, particularly on the Dogon Plateau, would be of great interest. So far only climatic factors (rainfall, modelled soil-moisture) and human influences have been assessed to explain the positive greening trends in the Sahel since the 1980s. However morphologic factors have so far been neglected by research groups. Observations made during the field trip show that the morphology seems to explain spatial differences to the vegetation cover and may also offer reasons for the location of degraded areas mapped in the land cover classification of 2011. It is likely that morphometric landforms can be correlated to greening trends in the Sahel and may be used to help explain spatial greening patterns.

The results show that the distance to settlements is a highly relevant factor for tree density as fields in close proximity to villages appear to be protected by farmers and of greater historical significance. A closer look at this pattern would also be of interest and could assist policy makers to determine how to improve the protection of trees in areas further away from settlements that are less favoured by farmers.

Whether or not it is possible to relate the results of the land cover and tree density and cover mapping of 2011 to Landsat images or MODIS (also a reason for the 250 m resolution of the woody vegetation cover maps) of the same year remains to be seen. This would perhaps allow an approximation of the state of the environment after the droughts in the mid-1980s and the woody vegetation could perhaps be modelled for a larger area. In this way, information on the progression of the environment since the droughts could be acquired.

8 References

- Adamo, S.B. (2008): Addressing environmentally induced population displacements: A delicate task. *Background Paper for the Population-Environment Research Network Cyberseminar "Environmentally Induced Population Displacements"*, 18-29 August 2008.
- Becek, K.&K. Ibrahim (2011): On the positional accuracy of GoogleEarth® imagery. *FIG Working Week 2011 - Bridging the Gap between Cultures*, 18-22 May 2011.
- Brandt, M., Samimi,C., Romankiewicz,C., and R. Spiekermann (2012): Detecting environmental change using time series, high resolution imagery and field work – a case study in the Sahel of Mali. *Geophysical Research Abstracts*, EGU2012-10583 ed. Available online at: <http://meetingorganizer.copernicus.org/EGU2012/EGU2012-10583.pdf> - last access Feb. 2013.
- Brandt, M., Romankiewicz, C., Spiekermann, R., & C. Samimi: Environmental change in time series and high resolution imagery - An interdisciplinary study in." *Journal of Arid Environments*, (in review).
- Chepkochi, L.C (2011).: Object-oriented image classification of individual trees using ERDAS Imagine Objective: Case-study of Wanjohi Area, Lake Naivasha Basin, Kenya. *Proceedings, Kenya Geothermal Conference 2011*, 21-22 November 2011.
- Croll, E.J. & D.J.Parkin (1992): *Bush Base, Forest Farm: Culture, Environment and Development*. Routledge, New York.
- ERDAS, Inc. (1999): *ERDAS Field Guide. 5. Edition. Atlanta, Georgia*.
- ERDAS, Inc. (2008): *Imagine Objective User's Guide*. Norcross, Georgia.
- Erikson, M.& K. Olofsson (2005): Comparison of three individual tree crown detection methods. *Machine Vision and Applications*, Vol. 16(4), pp. 258-265.
- Förster, M., Schuster,C., Sonnenschein,R., Bahls,R.& B. Kleinschmit (2011): Möglichkeiten der Erfassung von Landbedeckung und Vegetationsgesellschaften mittels RapidEye-Daten. -In *RapidEye Science Archive (RESA) - Erste Ergebnisse*, by Borg, E.&H. Daedelow, pp. 3-17. Gito, Berlin.
- Giannini, A., Biasutti,M., & M.M. Verstraete (2008): A climate model-based review of drought in the Sahel: Desertification, the re-greening and climate change. *Global and Planetary Change*, Vol. 64, pp. 119-128.

- Hermann, S.M., Anyamba, A., & C.J. Tucker (2005): Recent trends in vegetation dynamics in the African Sahel and their relationship to climate. *Global Environmental Change*, Vol. 15, pp. 394-404.
- Hermann, S.M., & C.F. Hutchinson (2005): The changing contexts of the desertification debate. *Journal of Arid Environments*, Vol. 63, pp. 538-555.
- Hermann, S.M., & G. Tappan (2013): Vegetation impoverishment despite greening: a case study from central Senegal. *Journal of Arid Environments*, Vol. 90, pp. 55-66.
- Hese, S., Grosse, G., & S. Pöcking (2010): *Object based thermokarst lake change mapping as part of the ESA Data User Element (DUE) Permafrost*. Genth, Belgium: OBIA Conference 2010.
- Hickler, T., Eklundh, L., Seaquist, J.W., Smith, B., Ardö, J., Olsson, L., Sykes, M.T., & M. Sjöström (2005): Precipitation controls Sahel greening trend. *Geophysical Research Letters*, Vol. 32.
- Huber, S., Fensholt, R., & K. Rasmussen (2011): Water availability as the driver of vegetation dynamics in the African Sahel from 1982 to 2007. *Global and Planetary Change*, Vol. 76, pp. 186-195.
- Hunt, B.G. (2000): Natural climatic variability and Sahelian rainfall trends. *Global and Planetary Change*, Vol. 24, pp. 107–131.
- Kandji, S.T., Verchot, L. & J. Mackensen (2006): *Climate Change and Variability in the Sahel Region: Impacts and Adaptation Strategies in the Agricultural Sector*. Nairobi, Kenya: World Agroforestry Centre (ICRAF), United Nations Environment Programme (UNEP).
- Ke, Y. & L. J. Quackenbush (2012): A comparison of three methods for automatic tree crown detection and delineation from high spatial resolution imagery. *International Journal of Remote Sensing*, Vol. 32(13), pp. 3625-3647.
- Lamprey, H.F. (1975): Report on the desert encroachment reconnaissance in northern Sudan. 21 Oct. to 10 Nov. 1975. *Desertification Control Bulletin*. Paris/Nairobi, Vol. 17, pp. 1-7.
- Leckie, D.G., Gougeon, F.A., Tinis, S., Nelson, T., Burnett, C.N., & D. Paradine (2005): Automated tree recognition in old growth conifer stands with high resolution digital imagery. *Remote Sensing of Environment*, Vol. 94, pp. 311-326.
- Liang, S., Lang, H. & M. Chen (2001): Atmospheric Correction of Landsat ETM+ Land Surface Imagery—Part I: Methods. *IEEE Transactions on Geoscience and Remote Sensing*, Vol. 39(11), pp. 2490-2498.

- Mering, C. & F. Chopin (2002): Granulometric maps from high resolution satellite images. *Image Anal Stereol*, Vol. 21, pp. 19-24.
- Nicholson, S.E. & H. Flohn (1980): African environmental and climatic changes and the general atmospheric circulation in late Pleistocene and Holocene. *Climatic Change*, Vol. 2, pp. 313-348.
- Nicholson, S.E., Tucker, C.J. & M.B. Ba. (1998): Desertification, drought, and surface vegetation: an example from the West African Sahel. *Bulletin of the American Meteorological Society*, Vol. 79, pp. 815-829.
- Nielsen, A.A., Hecheltjen, A., Thonfeld, F. & M.J. Canty (2010): Automatic change detection in RapidEye data using the combined MAD. *Geoscience and Remote Sensing Symposium (IGARSS)*, 2010 IEEE International ed.
- Olsson, L., Eklundh, L. & J. Ardö (2005): A recent greening of the Sahel – trends, patterns and potential causes. *Journal of Arid Environments*, Vol. 63, pp. 556–566.
- Pouliot, D.A., King, D.J., Bell, F.W. & D.G. Pitt (2002): Automated tree crown detection and delineation in high-resolution digital camera imagery of coniferous forest regeneration. *Remote Sensing of Environment*, Vol. 82, pp. 322-334.
- Reij, C.P., Tappan, G. & A. Belemvire (2005): Changing land management practices and vegetation on the Central Plateau of Burkina Faso (1968–2002). *Journal of Arid Environments*, Vol. 63, pp. 642-659.
- Reij, C.P. & E.M.A. Smaling (2008): Analyzing successes in agriculture and land management in Sub-Saharan Africa: Is macro-level gloom obscuring positive micro-level change? *Land Use Policy*, Vol. 25, pp. 410-420.
- Reij, C.P. (2009): Scaling up: The success of natural tree regeneration. *Farming Matters*, December 2009, pp. 32-34.
- Reij, C.P. (2011): Regreening the Sahel. *Our Planet. The magazine of the United Nations Environment Programme*, September 2011, ed.: 21-22.
- Rinaudo, T (2005a): Uncovering the Underground Forest: A Short History and Description of Farmer Managed Natural Regeneration. World Vision, Melbourne, Australia.
- Romankiewicz, C. & M. Doevenspeck (2011): Climate and mobility in the West African Sahel: conceptualizing the local imensions of the environment and migration nexus. *Conference on "Climate change: global scenarios and local experiences"* 24-25 October 2011.

- Ruelland, D., Levavasseur, F. & A. Tribotte (2010): Patterns and dynamics of land-cover changes since the 1960s over three experimental areas in Mali. *International Journal of Applied Earth Observations and Geoinformation*, Vol. 12, pp. S11-S17.
- Samimi, C., Fink, A. & H. Paeth (2012): The 2007 flood in the Sahel: Causes, characteristics and its presentation in the media and FEWS NET. *Natural Hazards and Earth System Sciences*, Vol. 12(2), pp. 313–325.
- San Emeterio, J.L., & C. Mering (2012): Climatic and human impacts on the ligneous cover in the Sahel from analysis of aerial photographs before and after the drought periods of the 70's and 80's. *Geophysical Research Abstracts*, EGU2012-3052 ed. Available online at: <http://meetingorganizer.copernicus.org/EGU2012/EGU2012-3052.pdf> - last access Feb. 2013.
- Tappan, G., Sall, M., Wood, E., & M. Cushing (2004): Ecoregions and land cover trends in Senegal. *Journal of Arid Environments*, Vol. 59, pp. 427–462.
- Tucker, C.J., Pinzon, J.E., Brown, M.E., Slayback, D., Pak, E.W., Mahoney, R., Vermote, E. & N. El Saleous (2005): An Extended AVHRR 8-km NDVI Data Set Compatible with MODIS and SPOT Vegetation NDVI Data. *International Journal of Remote Sensing*, Vol. 26(20), pp. 4485-5598.
- Tucker, C.J., Dregne, H.E. & W.W. Newcomb (2005): Expansion and contraction of the Sahara Desert from 1980 to 1990. *Science*, Vol. 263, pp. 299-301.
- United Nations Conference on Desertification (UNCOD) (1978): Round-up, plan of action and resolutions. New York: United Nations.
- Von Maydell, H.J. (1990): *Trees and shrubs of the Sahel: Their characteristics and uses*. Josef Margraf, 525 pp.
- Yossi, H. & C.H. Diakité (2008): *Etude Sahel: Dynamique de L'Occupation du Sol en Zone Guineenne Nord et Soudanienne du Mali*. Ministere de L'Agriculture, Institut D'Economie Rural.

Websites

National Aeronautics and Space Administration(NASA):Vers. 4.0.20, 14 May 2012. National A.
<http://nssdc.gsfc.nasa.gov/nmc/spacecraftDisplay.do?id=1967-122A> - last access Mar.
2013.

Sahel Eco: http://www.sahelco.net/projects/regreening_mopti_en.htm - last access Mar. 2013.

USGS:*U.S. Geological Survey - Earth Resources Observation and Science (EROS) Center.*
23.03.2011.

[http://eros.usgs.gov/#/Find_Data/Products_and_Data_Available/Declassified_Satellite_Imagery
_-_1](http://eros.usgs.gov/#/Find_Data/Products_and_Data_Available/Declassified_Satellite_Imagery_-_1) - last access Jan. 2013).

DECLARATION OF ORIGINALITY

Hereby, I declare that

- this Master thesis was written by me and that I did not use any other sources and means other than specified,
- this Master thesis has not been submitted at any other university for acquiring an academic degree,
- and that this Master thesis is fully consistent with the thesis assessed and marked by my supervisor.

EIDESSTATTLICHE ERKLÄRUNG

Hiermit versichere ich,

- dass die ich die vorliegende Masterarbeit selbstständig verfasst, andere als die angegebenen Quellen und Hilfsmittel nicht benutzt und mich auch sonst keiner unerlaubter Hilfe bedient habe,
- dass ich dieses Masterarbeitsthema bisher weder im In- noch im Ausland in irgendeiner Form als Prüfungsarbeit vorgelegt habe
- und dass diese Arbeit mit der vom Begutachter beurteilten Arbeit vollständig übereinstimmt.

April 2013, Vienna

Raphael Spiekermann



Raphael Spiekermann

Address: **4/4 Krichbaumgasse, 1120 Vienna, Austria**

Telephone: **+43-699-11009557**

Email: **spiekermann.rafael@gmail.com**

Date of birth: **20.02.1987**

Citizenship: **New Zealand, German**

EDUCATION

10/2011 – 04/2013

Master Thesis: „Change of woody vegetation and land cover using high resolution images on the Dogon-Plateau and on the Seno-Plains (Mali)“

10/2010 – 04/2013

Master Study Geography

University of Vienna

Specialisations:

- Geomorphology and risk research
- Geoecology and quaternary research
- Cartography and Geoinformation

10/2007 – 09/2010

Bachelor's degree in Geography (BSc)

University of Vienna

10/2006 – 01/2007

Environmental Engineering (undergraduate studies)

University of Natural Resources and Applied Life Sciences, Vienna

03/2005 – 07/2005

Social courses and travel in Argentina

02/2004 – 11/2004

Correspondence School of New Zealand

National Certificate of Achievement Level 3 certificate in Calculus, Geography, English, German, and Physics

PRACTICAL TRAINING

02/2012 – today
(6-week full time internship,
followed by part-time work)

Luftbilddatenbank Dr. Carls GmbH

- Digital processing of aerial photography
- Geo-coding und geo-referencing of historical aerial photos
- Archiving of data in various databanks
- Assisting the preparation of digital aerial photograph analyses

02/2012 – 03/2012

Translation work for the geotechnical company Water&Waste GmbH

- Translation of a technical report from German into English

09/2011 – today

University of Vienna: Project work within the framework of MICLE – Migration, Climate & Environment

- Image processing and geo-referencing of Corona satellite images
- Research trip to Mali (November – December 2011)
- Remote sensing and GIS-analyses
- Writing and editing of publications

09/2010
(4 weeks)

Austrian Institute of Technology (AIT)

- Quantification of the morphology in Burgenland to further understanding of spatial occurrence of soil creep
- Analysis of the relationship between proximity to tectonic lineaments and soil creep in Burgenland

07/2010 – 08/2010
(6 weeks)

GNS Science, Avalon, New Zealand

- Geo-referencing of 4000 landslide records
- Analysis of landslide records and rainfall data using GIS and statistical methods towards a probabilistic landslide hazard model for the road network of Wellington City Council

PUBLICATIONS

- Spiekermann, R., Brandt M., Samimi, C., (*submitted*): Using high resolution imagery to detect woody vegetation and land-cover change over 50 years in the Sahel of Mali. Geophysical Research Abstracts, Vol. 15, EGU2013-11937, EGU General Assembly 2013.
- Brandt, M., Samimi, C., Romankiewicz, C. & R. Spiekermann (*in review*): Detecting and explaining environmental change using time series, high resolution imagery and field work – a study in the Sahel of Mali and Senegal. Journal of Arid Environments.
- Brandt, M., Samimi, C., Romankiewicz, C. & R. Spiekermann (2012): Detecting environmental change using time series, high resolution imagery and field work – a case study in the Sahel of Mali. Geophysical Research Abstracts, Vol. 14, EGU2012-10583, EGU General Assembly 2012.

LANGUAGES

English (first language), **German** (fluent), **Spanish** (basic knowledge)

GIS –SKILLS

ArcGIS (versions 9.2 – 10.1)
ERDAS Imagine 2011 (incl. tools such as Objective, MosaicPro)
QGIS (with GRASS Applications)
Ilwis GIS Open (Version 3.6)
Saga GIS
TNTmips

IT-SKILLS

MS-Office: Word, Excel, Powerpoint, Access
Statistics: SPSS and R
Image processing: Adobe Photoshop

HOBBIES

Travelling, hiking, football, bike touring & most other sports, music

THESIS SUPERVISOR

- Univ.-Prof. Dr. Cyrus Samimi
Professor for Climatology at the Department of Geography
– University of Bayreuth
E: cyrus.samimi[at]uni-bayreuth.de T: +49-921-552266